Title
Innate Immune Signaling in Homeostatic Plasticity

Author
Harris, Nathan

Publication Date
2018

Peer reviewed|Thesis/dissertation

Innate Immune Signaling in Homeostatic Plasticity

by

Nathan Christopher Stephenson Harris

DISSERTATION

Submitted in partial satisfaction of the requirements for the degree of

DOCTOR OF PHILOSOPHY

in

Neuroscience

in the

GRADUATE DIVISION

of the

UNIVERSITY OF CALIFORNIA, SAN FRANCISCO

Acknowledgements

I would like to thank my PhD advisor, Dr. Grae Davis, for his mentorship and support during my time in graduate school. Grae has given me terrific advice on everything ranging from experimental minutiae to career decisions that will shape the next decade of my life. Grae is an expert at taking the specific data coming out of our lab and generalizing it in such a way that it becomes broadly interesting – an essential skill for anyone who wants to get a paper published or a grant funded. I have really appreciated being able to sit with Grae and learn this from him as we brainstorm and write papers in this way. I thank him for his constant reminder that, as much as our data about *Drosophila* innate immune signaling pathways and the mechanisms that control very specific subpools of synaptic vesicles are interesting to me, it's the simple connection between innate immunity and nervous system function that many more neuroscientists can appreciate.

I also thank my thesis committee members Dr. Robert Edwards, Dr. Kaveh Ashrafi, and Dr. Lily Jan for their advice and knowledge. I think Rob has been on the committees of 4 or 5 members of our lab since I've been in grad school, yet he still manages to be interested and engaged in all of our projects essentially studying the same process. At the same time, he seems to mix in a healthy amount of skepticism about our understanding of homeostatic plasticity, which I really appreciate as a foil to Grae's sometimes overwhelming optimism. Kaveh has a talent for suggesting straightforward experiments that can quickly provide evidence towards a hypothesis, while everyone else in the room is speculating about complex mechanisms that could explain data. Kaveh has also provided great advice in choosing a postdoc lab and

mentor, as I make my way into the field of *C. elegans* neurobiology. Lily has the incredible wealth of knowledge of someone who has been at the top of a field for decades. This gives her the ability to occasionally stand her ground and disagree with Grae, which I know can be difficult and I value it.

I would like to thank all the members of the Davis lab who I've overlapped with. When I was just starting in the lab, Martin Müller taught me two electrode voltage clamp and more importantly some of the theory behind the experimental approaches we use to interrogate presynaptic function. Meg Younger gave me really helpful advice about how to present my work and also how to communicate with Grae. DJ Brasier started the innate immunity project by doing some of the initial work on PGRP, and was very gracious as he passed it off to me. Cody Locke was a friendly presence when I rotated and is probably the person who first made me feel welcome in the lab. Tingting Wang joined the lab around the same time as me and is leaving as I leave. She has been a great friend and willing discusser of all things neuroscience. Kevin Ford and Mike Gaviño helped create a coffee break team that was a great place to discuss science or other things, and they welcomed me into that group as I started drinking coffee while studying for my qualifying exam. Anna Hauswirth has been a great friend and is just a really supportive person. She also deserves recognition for her many years work as "sunshine coordinator" remembering people's birthdays, baking for them, and organizing so many parties and events. Jenna Whippen, Yelena Kulik, and Jen Ortega are the other students in the lab who joined shortly after me – they are wonderful friends inside and outside of lab. Alyssa Johnson helped me learn some biochemistry and molecular biology techniques that I had thought I was just plain bad at. Brian Orr is a

super friendly presence in the lab, and he has an unbelievably broad knowledge of biology that seems to always come in handy. Özgür Genç is an expert in the mechanisms of vesicular release and short-term plasticity, and his advice in framing my data correctly on these topics has been valuable. Rick Fetter is the absolute expert when it comes to electron microscopy in invertebrates, and having access to him in the lab has been great for all of us. Amy Tong was an expert molecular biologist who made most of the transgenic flies I used in the lab. Sadly, she passed away last year. Gamaliel Ruiz has been our lab manager the entire time I've been here and is probably the most essential member of the lab, since nothing would work without him and no flies would be fed.

I would like to thank Pat Veitch and Lucita Nacionales, who have kept the neuroscience graduate program running the whole time I've been here. And I would like to thank all the program directors – Lou Reichardt, Roger Nicoll, and Anatol Kreitzer who have made the program what it is.

I have been incredibly lucky to have both a wonderful group of classmates in the program as well as terrific friends from outside of science. They created a support structure without which I am certain I would have been miserable at many times during grad school. The experiences we've had together shaped who I am as a person in a really positive way, and I wouldn't trade them for anything. I would especially like to acknowledge my friends Monica Volk, Mike Craig, Danny Spencer, Jacob Mallott, Nikki Mitchell, Will Georges, Carrie Fowler, Mihir Vohra, Peter Chisnell, Laura Devault, David Conant, Sarah Robinson, Karuna Meda, Sama Ahmed, and Jenna Sternberg. I feel like I can talk to these people anytime I need to about almost anything.

Last, I would like to thank my family – my mother Tara Stephenson, my father Crafford Harris, and my brother Gabriel Harris. My parents are responsible for the things I value most in myself – kindness to others, honesty, critical thinking, and passion for equality. In addition, my dad emphasized the importance of scholarship and academic excellence. My mom sets a terrific example for doing the kind of work it takes to make the world better – one small thing at a time. My brother is an incredibly talented, funny, and kind person. Having grown up together, we understand things about each other that no one else does, and I really appreciate having him as a family member and friend.

Abstract

Brain function is remarkably stable throughout the many years of adult life even in the face of continuous internal and external change. Homeostatic plasticity is hypothesized to support this stability by constraining neuronal activity within a range appropriate for a neuron's participation in neural circuits and meaningful information transfer. Presynaptic homeostatic potentiation (PHP) is one form of homeostatic plasticity acting in both peripheral and central synapses and is conserved from insects to humans. Here we describe the function of an innate immune receptor, PGRP-LC, and its downstream signaling pathway in controlling PHP. Innate immunity is known to function in the brain where it modifies the structure of synapses and circuits during development, as well responding to and controlling neuronal activity during adulthood. This is the first evidence implicating innate immunity in presynaptic function. First, we show that PGRP-LC functions as a presynaptic receptor during the induction and expression of PHP, through modulation of the readily releasable pool of synaptic vesicles. Next, we interrogate the canonical innate immune signaling pathway downstream of PGRP-LC, testing four downstream genes for function in PHP. In so doing, we find evidence that this pathway is reorganized to support the specialized structure and function of neurons, and the needs of PHP. Last, we characterize in detail the function of a kinase in the pathway, Tak1, in controlling synaptic vesicle release probability. Our data lead us to propose a model where Tak1 acts to stabilize synaptic vesicles close to the active zone by inhibiting a de-priming or de-docking process. Therefore, we have implicated a novel kinase in regulation of neurotransmitter release. We expect that innate immune signaling through PGRP-LC then modulates the function

of Tak1 during PHP to achieve potentiation of vesicle release. Overall, our data speak to the importance of innate immune signaling in neurons specifically, as they undergo changes during their otherwise normal day-to-day activity.

Table of Contents

List of Figures

1. Introduction

1.1 Homeostatic control

Homeostatic control is used to hold the output of a system constant in the face of perturbation of its inputs. An obvious example is control of room temperature by a thermostat. Even as the surrounding temperature changes, a thermostat is able to maintain the set room temperature by adjusting variables within the system.

The term homeostasis has also been used in biology to describe the many internal processes that display this constancy. These include control of body temperature, blood glucose, and extracellular salt balance, and their stability results from homeostatic regulation at the level of single cells, biological circuits, and even whole organs. Thus, these individual homeostatic systems ultimately cooperate to generate a macroscopic homeostatic controller of organismal biology, enabling the remarkably stable overall bodily function of complex organisms. But, to what extent the properties of single cells are controlled through cell-autonomous, homeostatic mechanisms is relatively unknown.

We can use modified feedback control theory to create a simple model for a control system that could conceivably be used in biology to achieve homeostasis. The essential components of such a system are a sensor, a set point, an error signal, and effectors. The sensor is some molecular machinery that converts input to the system into a type of information that can be read by the rest of the system. The set point is some biological variable that needs to be held constant. Input to the system is continually compared to the set point. Any difference between the input and the set

point is fed back as an error signal, and this error signal modifies the activity of effectors that ultimately correct the output. If inputs are continually monitored and the system operates with relatively high gain and speed, the output can be robustly maintained at set point. As we characterize putative homeostatic phenomena in the nervous system, we can ask to what extent they reflect the predictions of negative feedback control.

1.2 Homeostatic plasticity in neurons

Neurons are a fascinating cell type for consideration in the context of homeostasis. Many neurons display marked short and long-term plasticity in response to all kinds of stimuli, including external experience (emotional state, time of day, visual information, learning) and developmental critical periods. Yet, for the most part, neurons continue to serve their proper role in computation within the extremely complex circuitry of the brain, and brain function is stable over the many years of life. Additionally, in the face of genetic mutations or disease brain function typically remains normal, due in part to the stability of neuronal activity.

At the level of single cells or synapses, many different forms of homeostatic regulation of neuronal activity have now been described. Presumably they function in concert to maintain the overall stability of neural circuits. What role can each play in stabilizing brain function, and what molecular mechanisms might be necessary for each type of homeostasis? The majority of research on neuronal homeostatic plasticity can be divided into three categories: homeostatic control of excitability or firing rate, synaptic scaling, and presynaptic homeostatic potentiation.

1.2.1 Homeostatic control of neuronal firing properties

The action potential firing properties of neurons are essential to their function within circuits and can also be used to define cell type (Markram et al., 2004). There are now many examples in which a neuron whose activity pattern is perturbed will, given enough time, return to its baseline level of excitability or activity (Nerbonne et al., 2008; Pratt and Aizenmann, 2009; Hengen et al., 2013). One example of explicit evidence is this: acute pharmacological blockade of a potassium conductance essential to action potential repolarization results in extreme hyperexcitability. But, genetic deletion of that same conductance results in little or no difference in excitability compared to wild type (Nerbonne et al., 2008; Kulik, Y., unpublished). Homeostatic rebalancing of ion channels and currents has been hypothesized to underlie this compensation, and in a few cases this has been shown experimentally (Marder and Prinz, 2002; Nerbonne et al., 2008; Pratt and Aizenmann, 2009).

Two general paradigms have been used to characterize this phenomenon. In the first, single neurons are patch clamped, and their biophysical responses to various current injection protocols measured (Nerbonne et al., 2008; Kulik, Y., unpublished). Firing properties are then described by the number and shape of action potentials characteristic of the neuron in that paradigm. This approach gives detailed insights into the biophysical and molecular mechanisms underlying homeostatic plasticity. Specifically, genetically defined neuron types can be identified and specific ion channel currents can be isolated using voltage clamp and pharmacology. This approach is just beginning to yield molecular insights into homeostatic signaling (Kulik, Y., unpublished).

In the second approach, the firing properties of neurons are measured in the context of their function within a neural circuit (Hengen et al., 2013). This approach has the advantage of measuring the true firing properties of neurons as determined in part by synaptic input, rather than relying on artificial stimulation protocols. Additionally, this experiment can be conducted in vivo in combination with behaviorally relevant perturbations of a living animal. This approach lacks the ability to describe the molecular and biophysical mechanisms of such compensation, however.

The overall findings in this field provide strong evidence for the existence of set point in neuronal firing properties. First, when extremely homogeneous genetically defined cells are sampled, they display nearly invariant excitability from cell to cell (Kulik, Y. unpublished; Wolfram et al., 2012). Furthermore, when these neurons are electrically perturbed by mutation of certain ion channels, they are able to return precisely to this set point excitability, again with very little variation. Additionally, when extremely heterogeneous neurons in visual cortex (firing rates range from 0.01 – 10 Hz) are recorded chronically in behaving animals, their firing rates are relatively stable over time. When their firing rates are impaired by monocular deprivation, many of the neurons eventually return to their original set point firing rate (Hengen et al., 2016). This also reinforces the idea that set point must be defined and maintained as part of any neuron's molecular identity (Davis, 2013). Unfortunately, this approach lacks the ability to discern cell types based on activity pattern, rather than average firing rate over minutes to hours.

1.2.2 Synaptic scaling

Many neurons respond to chronic perturbations of their activity by broadly scaling up or down synaptic strengths at the level of postsynaptic neurotransmitter receptors (Turrigiano et al., 1998; Thiagarajan et al., 2005). The standard experimental paradigm is as follows: An acute brain slice or slice culture is subjected to chronic inhibition (often using TTX to inhibit action potential firing) or chronic hyperexcitability (often using a $GABA_A$ receptor antagonist to disinhibit neurons). Electrophysiological recordings are made from these neurons, and their miniature excitatory postsynaptic currents (mEPSC) amplitudes are measured and compared to those of unperturbed neurons. When neuronal firing is inhibited, average mEPSC amplitude increases, and when firing frequency is increased, mEPSC amplitude decreases. This is expected to reflect changes in postsynaptic receptor abundance and/or function. Synaptic scaling is sometimes called anti-Hebbian plasticity, because it has the same target as classic Hebbian LTP – the postsynaptic fast neurotransmitter receptor, but it seems to operate with the opposite logic (increased firing leads to synaptic potentiation during LTP, but results in decreased synaptic strength during synaptic scaling). This difference probably reflects the rapid, input specific induction of LTP (where simultaneous postsynaptic depolarization and presynaptic neurotransmitter release are required) versus the slower, cell-wide nature of synaptic scaling (Bliss and Collingridge, 1993). Consequently, scaling has been theorized to support Hebbian potentiation by dampening cellular excitability after LTP, thereby increasing signal to noise and preventing “runaway potentiation” (Turrigiano, 2008). Synaptic scaling probably

contributes to the homeostatic control of intrinsic excitability in vivo, but how the two are linked to achieve precision is unknown.

A few molecules have been implicated in synaptic scaling. Calcium/calmodulin-dependent protein kinase type IV (CaMKIV) activity is correlated with changes in firing rate that induce synaptic scaling, and manipulation of CaMKIV function induces a change in mEPSC amplitude that appears synonymous with synaptic scaling (Ibata et al., 2008). Because CaMKIV is responsive to calcium, it has been proposed that intracellular calcium is the homeostatic signal measured in synaptic scaling (Turrigiano, 2008). In the context of control theory, CaMKIV would be part of the molecular sensor, and intracellular calcium concentration would be the variable by which set point is defined. CaMKIV is then hypothesized to mediate a downstream transcriptional program underlying the scaling response (Ibata et al., 2008). One of the essential transcriptional targets of homeostatic scaling signaling is the immediate early gene Arc (Shepherd et al., 2006), although how Arc gene expression is controlled is completely unknown in the context of synaptic scaling. The cytokine TNF-alpha is required specifically for scaling up, but not down, and its requirement is in glia, not neurons, adding another cell type and signal source to the model for synaptic scaling (Stellwagen and Malenka, 2006). These findings describe a homeostatic process that requires calcium-dependent transcription and possibly intercellular signaling. One important question relevant to all forms of activity-dependent plasticity is how altered neuronal physiology is transfigured into a transcriptional signal that directs changes in gene expression with enough precision to preserve neuronal function.

1.3 Presynaptic homeostatic potentiation

Presynaptic homeostatic potentiation (PHP) owes its name to the fact that it is undeniably expressed presynaptically, seen as an increase in the number of neurotransmitter vesicles released in response to an action potential. Therefore, it gives the brain the ability to stabilize synaptic strength at the presynaptic release site. In the complex synaptic circuitry of the central nervous system, the input specificity resulting from a presynaptic locus of action is probably essential to maintain logical information transfer. Forms of PHP have been characterized at the neuromuscular junctions (NMJs) of insects and mammals and also in the central nervous system (Frank et al., 2006; Plomp et al., 1992; Cull-Candy et al., 1980; Kazama and Wilson, 2008; Burrone and Murthy et al., 2002; Kim and Ryan, 2010; Krahe and Guido, 2011). The physiological and molecular mechanisms of PHP have been best characterized at the *Drosophila melanogaster* NMJ, reviewed below.

1.3.1 PHP – the phenomenon

PHP appears to be optimized to maintain synaptic strength in the face of reduced postsynaptic excitability by increasing presynaptic neurotransmitter release. The phenomenon is best described in terms of electrophysiological recordings from a postsynaptic cell, after impairment of postsynaptic excitability by receptor blockade or deletion. Impairment of postsynaptic sensitivity is interpreted from a decrease in average miniature excitatory postsynaptic potential (mEPSP or “mini”) amplitude. According to the simple equation derived from the binomial distribution: synaptic strength = n*p*q (where n = the number of release ready presynaptic neurotransmitter

vesicles, p = probability of release of one of those vesicles, and q = the postsynaptic response to one of those vesicles), the observed drop in q should result in reduced synaptic strength if n and p remain constant (Del Castillo and Katz, 1954). Instead, synaptic strength (the EPSP amplitude) remains constant. The interpretation is that n and/or p is indeed increased, and because n*p = quantal content (the total number of vesicles released during an action potential), we can say that PHP involves an increase in presynaptic neurotransmitter release. The presynaptic locus of expression has now been confirmed by the observation that PHP requires two parallel presynaptic changes – an increase in presynaptic action potential evoked calcium influx, and an increase in the size of the readily releasable vesicle pool (Müller et al., 2012; Müller et al., 2013). This strongly suggests a conversion of electrochemical information about postsynaptic strength into a protein-mediated transsynaptic retrograde signal – a fascinating mechanism that is the subject of intense research.

An additional feature of PHP is that it can be induced rapidly, in minutes, but also sustained for as long as years (Cull-Candy et al., 1980). No other form of homeostatic synaptic plasticity has been observed to act so quickly, so a mechanistic understanding of how PHP achieves its temporal characteristics is desired.

1.3.2 PHP in control theory

We commonly use our model for homeostatic feedback control to inform our understanding of signaling in PHP. Here I will highlight its predictions for PHP at the NMJ, and our progress towards filling in that molecular knowledge.

Set Point:

To review, set point is the target output of the system, to which all input is compared. The goal of homeostatic signaling is to correct errors in input by bringing it back to set point. In PHP, we expect that set point resides in the postsynaptic cell, because postsynaptic excitability (the EPSP) is the output that seems to be homeostatically maintained, whereas presynaptic function is modulated to achieve this. Theoretically, the set point could alternatively be simply defined as the amount of mEPSP excitation integrated over time, which is attractive because evoked synaptic activity does not appear to be required for the induction of PHP (Frank et al., 2006). We expect that set point is genetically encoded and then defined by gene expression, likely as part of the selection of terminal cell type (Davis, 2013). Importantly, the set point for PHP appears to be capable of changing over time in a consistent way, further suggesting the influence of gene expression that is plastic over the life of an animal (Mahoney et al., 2014). The genetic mechanisms defining set point in PHP are unknown, but it would be fascinating to address them by finding a postsynaptic genetic manipulation that we can use to reset set point. Towards this goal, it will be important and likely difficult to find an approach that can disentangle mechanisms that control set point specifically from those that simply affect synaptic strength.

Sensor:

Synaptic input must be sensed by a signaling system capable of comparison to set point and calculation of error. Though we measure postsynaptic excitation electrically, the physiological information of neurotransmitter receptor opening and ion influx must

somehow be converted to biochemical signaling. It seems unlikely that the difference between on average 1 mV of ionic influx and 0.5 mV during a spontaneous release event could be sensed reliably enough to generate a precise homeostatic response. An alternative proposal would be that a postsynaptic membrane proximal signaling complex monitors the opening/closing of neurotransmitter receptors over time. A protein signal would then accumulate over time and inform the postsynaptic cell of its excitation state. This would be a fascinating ability of biochemical signaling, but thus far no clear mechanism has emerged (but see Hauswirth et al., 2018). Approaches to more directly test this hypothesis would be to biochemically profile the intracellular binding partners of postsynaptic receptors and test them in PHP, or to mutate active regions of the receptor intracellular tail.

Error Signal:

Ultimately, the error sensed by the postsynaptic cell must be communicated to the presynaptic cell so that it can be corrected with precision. This is the basis for the search for a retrograde signal. Significant progress has been made in this area, as two strong candidates for transsynaptic homeostatic signaling, Endostatin and Semaphorin 2A, are required for the execution of PHP (Wang et al., 2014; Orr et al., 2017b). Still lacking is a demonstration that any retrograde signal truly communicates error in a quantitative manner sufficient for the precision of PHP. One possibility is that modulation of postsynaptic vesicle trafficking and secretion allows measured feedback (Hauswirth et al., 2018). Another possibility is that the dynamics of translation control the amount of error signal during long-term forms of PHP (Penney et al., 2012).

Effectors:

The result of these actions is the potentiation of presynaptic neurotransmitter release (synaptic input) observed in PHP. The majority of molecular progress has been made in understanding this aspect, as we have identified a set of presynaptic proteins that directly potentiate neurotransmitter release in PHP (Younger et al., 2013; Müller et al., 2012b; Müller et al., 2015). These proteins control either potentiation of presynaptic calcium influx or an increase in the number of readily releasable synaptic vesicles. Both changes are required, as disruption of either one blocks PHP. They correspond nicely to the determinants of quantal content (quantal content = n*p, where n = number of release ready vesicles and p = probability of release), as the RRP roughly corresponds to n, and increased calcium influx is expected to dramatically increase p, according to the power 3-4 relationship between calcium concentration and release rate (Wu et al., 1999). The increased RRP is amazing, because it involves a doubling of vesicular release at a synapse that is already very high release probability and therefore is already releasing vesicles from the majority of its active zones. One outstanding question is – by what physiological mechanisms are vesicles so potently engaged?

1.4 Control of vesicle release in synaptic transmission and PHP

The events that determine the number and characteristics of release ready vesicles upstream of calcium influx have been a topic of intense research for the last ~50 years. Their physiological signatures, biochemical mechanisms, genetic requirements, and experimental approaches to describe them have been reviewed extensively elsewhere

(Neher, 2015; Kaeser and Regehr, 2017). But some general concepts relevant to our system are important to review here.

The first step in making a vesicle release ready is physically bringing it extremely close to the presynaptic terminal membrane, termed docking. The majority of presynaptic genes that completely abolish release when deleted are required for vesicle docking, as measured by EM reconstruction of nerve terminals (Imig et al., 2014). The second step, called priming, is much more ambiguous, and is basically defined as an event downstream of docking that prevents release when disrupted. Priming probably involves executing the proper biochemical interactions between proteins on the vesicle surface and active zone proteins (molecular priming) as well as positioning the vesicle near enough to the presynaptic calcium channel for its exposure to sufficient calcium for release (positional priming) (Neher and Sakaba, 2008). The best evidence of genes involved in vesicle priming are Rab3, Rab3 Interacting Molecule (RIM), Munc13, and Munc18. Rab3's function appears to be specific to priming or possibly "superpriming", as its deletion has only a moderate effect on the amplitude of evoked release but a more obvious effect on the dynamics of release and the dynamics of replenishment of high release probability vesicles after pool depletion (Schlüter et al., 2006). RIM appears to have both docking and priming functions – it acts as an essential scaffold for the creation of a mature active zone with a full cohort of docked vesicles, and its dynamic biochemical interaction with Munc13 determines the priming state of vesicles at baseline and during high frequency stimulation (Deng et al., 2011; Camacho et al., 2017). Munc13's priming function has been difficult to disentangle from its requirement for vesicle docking, but it appears that Munc13 cooperates with RIM to prime synaptic

vesicles (Deng et al., 2011; Kaeser and Regeher, 2017). Deletion of Munc18 completely abolishes release, but does not greatly affect vesicle docking, suggesting that the deficit is based on the absence of priming and SNARE complex formation (Genç et al., 2014; Verhage et al., 2000). Additionally, Munc18 is a primary target of the priming action of phorbol esters (Genç et al., 2014). Impaired priming can sometimes be interpreted in electrophysiological data from a decrease in release probability during the first few responses during a stimulus train and a defect in the slow phase of recovery from synaptic depletion (Schlüter et al., 2006). We expect that homeostatic signaling interfaces with these physiological and molecular mechanisms to achieve the well characterized increase in neurotransmitter release during PHP. Defining the nature of this interface is essential to understanding PHP.

As mentioned previously, one of the required physiological events in PHP is an expansion of the RRP. Through genetic analysis, we have begun to identify active zone proteins that orchestrate this process. These molecules appear to be converging on a priming mechanism underlying RRP expansion that may be focused on high release probability vesicles in particular. Rab3 interacting molecule (RIM) was the first player implicated in RRP expansion (Müller et al., 2012). RIM is required both to generate a normal vesicle at baseline and also to modulate it during PHP. As mentioned above, RIM scaffolds together many of these essential active zone proteins. This led to the characterization of RIM binding protein (RBP), which is also required for expansion of the RRP in PHP. RBP has an additional role in stabilizing high release probability vesicles, based on a dramatic slowing of their recovery in an RBP mutant (Müller et al., 2015). This may mean that high release probability vesicles are the primary target in

RRP expansion. RBP is also known to control vesicle-calcium channel coupling, which may indicate that positional priming – driving vesicles closer to the calcium channel – is a required step in PHP (Müller et al., 2015). Lastly, we are gathering evidence of a role for Munc18, described above as a priming factor, in controlling PHP (Ortega, J., unpublished). So, we are describing an active zone complex that acts powerfully on high release probability vesicles, coupling them tightly to sites of calcium influx, and apparently controlling calcium-dependent vesicle priming. These are exactly the vesicles that would dramatically potentiate release, if recruited to the active zone during PHP. Consequently, mutations in these genes reliably disrupt PHP, often genetically interact with other known PHP genes, and even suppress PHP as heterozygous mutations (Müller et al., 2012b; Müller et al., 2015; Wang et al., 2016; Ortega, J., unpublished).

However, PHP is not merely an active zone proximal event. Rather, it requires transsynaptic signaling from a postsynaptic muscle to a presynaptic nerve terminal, and subsequent signaling from presynaptic membrane to the active zone. Furthermore, long-term perturbations on the scale of days or even years can be indefinitely compensated, and this must require signaling to the nucleus and transcriptional plasticity (Cull-candy et al., 1980). Molecular pathways that biochemically or functionally link retrograde signaling to release dynamics at the active zone are unknown, as are pathways that could consolidate rapid and sustained forms of homeostatic plasticity. The work presented here represents significant progress towards these goals, through a relatively surprising discovery of neuronal innate immune signaling in controlling PHP.

1.5 Innate immunity

Two molecularly separate immune responses exist in mammals, called innate and adaptive immunity. Innate immunity is a mostly nonspecific, rapid reaction to invasion by any pathogen, whereas adaptive immunity is slower (days) but extremely specific and effective, primarily due to the production of antibodies against the invading pathogen. These antibodies persist forever, providing lifelong protection against that pathogen. Although there is significant crosstalk between innate and adaptive immunity in mammals, insects have no adaptive immunity, relying entirely on innate immunity for pathogen defense. Therefore, adaptive immunity is not relevant to this thesis, and will not be discussed further in any great detail.

Essential to the innate immune response and this thesis is the concept of a pattern recognition receptor (PRR). PRRs are a diverse group of proteins united by their unique ability to detect pathogens and initiate an innate immune response (Janeway et al., 2001). PRRs detect pathogens by binding pathogen associated molecular patterns (PAMPs), which are often structural components of the cell wall or cytoskeleton specific to bacteria or other invaders. PRRs can influence the immune response by transducing an extracellular signal to intracellular innate immune pathways or by presenting the bound PAMP to a nearby immune cell for immune stimulation or phagocytosis. Toll-like receptor 4 (TLR4) is a good example of an essential mammalian PRR.

After pattern recognition, the innate immune response proceeds in two distinct phases. The first is extremely rapid, largely transcription-independent, and is comprised of direct pathogen attack by immune cells. The essential cell type of initial innate immune activation is the macrophage, which phagocytoses pathogens detected by its

PRRs. Upon pathogen detection, macrophages also begin to secrete cytokines and chemokines which recruit additional immune cells from the bloodstream, catalyzing a broader inflammatory response. Neutrophils are an additional phagocytic cell type present in greater number than macrophages, which are rapidly recruited during this first phase. Proteins of the complement cascade can also recognize and bind to pathogen surfaces, where they either recruit cells expressing complement receptor, stimulating phagocytosis, or instead themselves form a membrane attack complex that ruptures the bacterial cell wall. Cytokine and chemokine secretion by macrophages and neutrophils recruit additional immune cell types, beginning the second phase of the innate immune response.

The second phase is slower, transcription-dependent, and consists of a broad inflammatory response that reflects full blown innate immune activity. Here, cytokines and chemokines and their receptors are essential. Innate immune cells begin to transcribe these proteins in great number and release them into the bloodstream. Additional innate immune cells expressing cytokine receptors become activated and migrate rapidly to the site of infection where they too produce chemokines and cytokines, generating a positive feedback loop responsible for the maximal innate immune response.

Virtually all cytokine transcription, production, and detection is mediated by PRRs and cytokine receptors that feed into a well conserved signaling pathway leading to the activation of the transcription actor NF-kB (Bonizzi and Karin, 2004) (see below for detailed description of NF-kB signaling). Many PRRs and the downstream pathways to NF-kB are well conserved in the fly innate immune response, and their surprising

activity in neurons is the topic of this thesis (Myllymäki et al., 2014; Valanne et al., 2011).

1.6 PGRPs and innate immune signaling in *Drosophila melanogaster*

Two signaling pathways mediate all immune recognition in flies. The first recognizes all gram-negative bacteria (the IMD pathway, Figure 7A) and is initiated by the transmembrane PRR peptidoglycan recognition protein (PGRP)-LC (Gottar et al., 2002; Choe et al., 2002). Peptide components of bacteria cell walls bind the ligand sensing domain of PGRP-LC, inducing receptor dimerization and activation of intracellular signaling. The adaptor protein Imd (Immune Deficient) binds the intracellular region of PGRP-LC and helps to assemble a large signaling complex (Choe et al., 2005; Georgel et al., 2001). The exact protein composition and signaling logic of this complex remain unclear, and are probably cell-type specific, but three players – the kinases Tak1 and IKKβ, and the caspase Dredd – are definitely required (Vidal et al., 2001; Silverman et al., 2000; Stöven et al., 2000). Finally, the NF-kB homologue transcription factor Relish is activated by two convergent events – cleavage by Dredd, freeing the Relish DNA binding domain from an inhibitory domain, and phosphorylation by IKKβ (Hedengren et al., 1999; Ertürk-Hasdemir, 2009). Tak1 also diverges and stimulates signaling through the JNK pathway, leading to additional transcriptional activity of AP-1. These two transcriptional pathways cooperate to achieve an appropriate immune response, although exactly how they interact is unclear (Kim et al., 2005). The immune effectors transcribed in the *Drosophila* immune response are

antimicrobial peptides, which accumulate and circulate in the hemolymph (Hoffmann and Hoffmann, 1990). They directly digest different types of bacteria enzymatically.

Aside from the identity of the initiating receptor, innate immune signaling to NF-kB follows essentially the same logic in mammals. An intracellular scaffolding complex stimulates kinase activity, usually that of Tak1, which phosphorylates and activates IKK, which then phosphorylates NF-kB, degrading an inhibitory subunit and activating transcription (Häcker and Karin, 2006). A wide array of receptors can activate similar pathways, including tumor necrosis factor receptors, interleukin receptors, and toll-like receptors (Janeway et al., 2001). So we can think of a great deal of immune and inflammatory recognition being mediated by a diverse set of PRRs and cytokine receptors, most of which feed into similar intracellular signaling cascades to NF-kB.

There are an additional 12 PGRP-domain containing genes encoded in the *Drosophila* genome (Dziarski, 2004). They perform a diverse set of functions, including direct enzymatic destruction of bacteria, negative regulation by binding and inactivating PGRP-LC, and positive regulation by presenting PAMPs and stimulating other immune pathways, including the Toll pathway (Dziarski and Gupta, 2006). In this way PGRP family proteins can be considered to mediate nearly all pattern recognition and immunity in insects. We tested an additional set of PGRPs for functionality in neurons (see Section 4 – unpublished results).

The second *Drosophila* innate immune pathway is the Toll pathway, named after its initiating receptor (Valanne et al., 2011). This pathway recognizes all gram-positive bacteria. Toll does not directly recognize pathogen invasion, instead two small PGRPs, PGRP-SA and SD, bind bacterial peptides and then initiate a proteolytic cascade,

ultimately activating Spaetzle and the transmembrane receptor Toll (Steiner, 2004). The signaling downstream of Toll is similar to other NF-kB pathways, utilizing kinase signaling through IKK homologues and ultimately activating the NF-kB homologues Dif and Dorsal (Valanne et al., 2011).

1.7 Innate immunity in the brain

Classically, the brain was thought to be “immune-privileged”, largely because immune responses had never been observed in the healthy brain. Such privilege was thought to result from the blood brain barrier preventing entry of immune cells and molecules, and the absence of expression of immune system genes by cells in the brain (Lampson and Siegel, 1988). Any immune response detected in the brain was associated with pathology. This theory was challenged by the finding that class I major histocompatibility complex (MHC) genes are expressed in some regions of the brain and regulated by neuronal activity, opening a new subfield in neuroscience that has exploded in the years since (Corriveau et al., 1998). It is now clear that many, if not most innate immune genes are expressed and active in the developing and often adult brain (Cahoy et al., 2008). This includes cytokines and their cognate receptors, pattern recognition receptors, cell surface signaling proteins, immune transcription factors, and intracellular signaling cascades. Except for a few examples in a few contexts, their role in neurobiology is unknown. One essential question is – do these molecules act in their well-known immune roles, simply in different cell types (neurons and glia), or do they assume entirely new functions that serve the highly specialized cells and functions of the brain?

One avenue of research has been the function of cell surface proteins that “tag” cells and cell compartments, and the receptors on effector cells that recognize their presence. The most compelling findings concern the function of proteins in the classical complement cascade. Complement protein C1q and its receptor are present at high density in some brain regions during critical periods of circuit development (Stevens et al., 2007; Schafer et al., 2012). C1q appears to mark some developing synapses for removal so that remaining synapses can strengthen during normal circuit refinement. Loss of complement then results in unrefined connectivity, seen by incomplete segregation between contralateral and ipsilateral projections into the lateral geniculate nucleus. Complement receptor is expressed by microglia, directing them to engulf and eliminate the appropriate synapses. This falls directly in line with the concept of microglia as the resident immune cells of the brain (Kreutzberg, 1996). This is entirely reminiscent of the immune role of complement in recognizing PAMPs and also damage associated molecular patterns (DAMPs) (Janeway et al., 2001). Expression and presentation of C1q by a neuron would in effect be a DAMP that directs relatively specific synapse removal. How specific synapses are chosen to present complement is a fascinating question and remains entirely unknown.

Just as in the immune system, negative regulation of innate immunity in the brain is as important as activation of the response. Chronic or inappropriate innate immune activation leads to neurodegeneration, and increased neuroinflammation contributes to aging-associated cognitive decline (Hong et al., 2016; Cao et al., 2013). In the case of complement, its role in regulated synapse elimination during development can become

inappropriately reactivated in an Alzheimer's disease model, leading to dramatic degenerative synapse loss, again mediated by microglia (Hong et al., 2016).

These examples restrict the activity of innate immune signaling to a few relatively small windows of lifetime – early circuit development and neurodegeneration associated with old age. But, very many innate immune genes are expressed in the healthy, adult brain (Cahoy et al., 2008; Allen Brain Atlas). What might they be doing in neural tissue whose circuitry is mostly stable and in the absence of pathological neuroinflammation? Additionally, while glia and particularly microglia are clear mediators of the restructuring and engulfment of synapses, many innate immune signaling and effector proteins are present in neurons themselves (Meffert et al., 2003; Cahoy et al., 2008; König et al., 2017; our lab, unpublished RNAseq data). What cell-autonomous, neuron-specific functions do they serve, if any?

A second, relatively unappreciated line of research describes a very different function of innate immune signaling in the brain – responding to and controlling neuronal activity. Most of these findings converge on NF-kB type transcription factors, the essential transcriptional mediators of innate immune responses. First, using electrophoretic mobility shift assays and live imaging of GFP tagged NF-kB, two groups found that in response to depolarization, NF-kB translocates from the cytoplasm to the nucleus and binds DNA (Meffert et al., 2003; Wellmann et al., 2001). Further studies demonstrated a requirement for NF-kB in synaptic plasticity and learning (Boersma et al., 2011; Ahn et al., 2008). Now, in the era of genomics and sequencing, the activity-dependent function of NF-kB is again being examined. Strikingly, promoter regions of activity regulated genes are highly enriched for NF-kB binding sites, and optogenetic

stimulation rapidly activates NF-kB-dependent transcription, suggesting that it is part of a latent system primed to rapidly activate transcription in response to neural activity (Chen et al., 2016).

These findings fit very nicely with the function of NF-kB in innate immune responses, as a rapid responder and transcriptional activator. However, neurons exhibit morphological and functional specializations very different from immune cells. A linear pathway from plasma membrane to nucleus, analogous to canonical innate immune signaling, is probably insufficient to coordinate signaling along the spatial requirements of elaborate neuronal processes and within the temporal constraints of neuronal activity. No innate immune signaling pathway has been explored in any great detail in the brain, but there are a few hints towards interesting neuron-specific functions. First, subunits of the IKK complex and NF-kB appear to colocalize with ankyrin-G in the axon initial segment, and the IKK complex also accumulates in nodes of Ranvier (König et al., 2017). Additionally, there is evidence for a physical interaction between the IKK complex subunit IkBalpha and ELKS/CAST – an active zone protein known to bind RIM and regulate presynaptic vesicle release with moderate homology to *Drosophila* Bruchpilot (Wagh et al., 2006). ELKS/CAST is required for efficient IKK complex activation and NF-kB mediated transcription, and it also mediates the response of the innate immune kinase Tak1 to DNA damage (Ducut Segala et al., 2004; Wu et al., 2010). There is a tremendous opportunity to delineate the role of these proteins in neuronal activity.

Using the identification of peptidoglycan recognition protein (PGRP)-LC in a screen for genetic mechanisms of PHP as an entry point, we have in the years since

characterized the entire canonical downstream pathway from membrane to nucleus in the context of homeostatic plasticity and synaptic function. Our findings describe the ability of this pathway to serve the unique needs of a neuron undergoing rapidly induced, but indefinitely sustained plasticity. Additionally, we find a new locus of action for innate immune signaling – the presynaptic nerve terminal, and we uncover a surprising and novel role for the kinase Tak1 in regulating vesicular release probability.

2. The Innate Immune Receptor PGRP-LC Controls Presynaptic Homeostatic Potentiation

Introduction

The homeostatic modulation of presynaptic neurotransmitter release has been observed at mammalian central synapses and at neuromuscular synapses in species ranging from *Drosophila* to mouse and human (for review see Davis and Müller, 2015). The homeostatic enhancement of presynaptic release following inhibition of postsynaptic glutamate receptors is achieved by an increase in presynaptic calcium influx through presynaptic CaV2.1 calcium channels and the simultaneous expansion of the readily releasable pool (RRP) of synaptic vesicles. To date, the retrograde, trans-synaptic signaling system that initiates these presynaptic changes following disruption of postsynaptic glutamate receptors remains largely unknown (but see Wang et al., 2014).

A large-scale forward genetic screen for homeostatic plasticity genes, using synaptic electrophysiology at the NMJ as the primary assay (Dickman and Davis, 2009; Younger et al., 2013), identified mutations in the *PGRP-LC* locus that block presynaptic homeostasis. In Drosophila, PGRP-LC is the primary receptor that initiates an innate immune response through the immune deficiency (IMD) pathway (Figure 1; Royet and Dziarski, 2007). In mammals, there are four PGRPs including a 'long' isoform (PGRP-L or PGlyRP2) that appears to have both secreted and membrane-associated activity (Royet and Dziarski, 2007). In mice, the PGlyRP2 protein has two functions in the innate immune response: a well-documented extracellular enzymatic (amidase) activity (Royet and Dziarski, 2007) and a pro-inflammatory signaling function that is

independent of its extracellular enzymatic activity (Saha et al., 2009). As yet, there are no known functions for PGRPs in the nervous system of any organism.

Results

PGRP is Required for the Robust Expression of Presynaptic Homeostatic Potentiation

Two major isoforms of *PGRP-LC* are transcribed, *PGRP-LCx* and *PGRP-LCa* (Figure 1B), both of which are known to participate in the innate immune response (Choe et al., 2002). Presynaptic homeostasis was quantified (0.4mM $[Ca^{2+}]_e$) in two independent loss of function alleles, a deletion of the *PGRP-LC* gene locus ($PGRP^{del}$; Gottar et al., 2002) that removes both *PGRP* isoforms and a nonsense mutation in the PGRP domain of the *PGRP-LCx* isoform that results in an isoform-specific, loss of function allele ($PGRP^{2}$; Choe et al., 2002) (see Figure 1B). We demonstrate that application of the glutamate receptor antagonist PhTx (10-20μM) decreases mEPSP amplitudes by ~50% in all genotypes (Figure 1C-F; compare light and dark bars for each genotype, representing the absence [-] and presence [+] of PhTx; $p<0.01$). In wild type, we observe a significant homeostatic increase in quantal content ($p<0.01$) that brings EPSP amplitudes back toward the levels observed in the absence of PhTx (Figure 1D-F). We then show, in both *PGRP-LC* mutant alleles as well as the trans-heterozygous allelic combination, that there is no homeostatic enhancement of quantal content following PhTx application (Figure 1F; $p>0.5$ compare dark and light bars for each genotype) and EPSP amplitudes are dramatically decreased compared to each genotype in the absence of PhTx (Figure 1E; $p<0.01$). Thus, *PGRP-LC* is essential for the rapid induction of presynaptic

homeostasis.

Examination of baseline synaptic transmission reveals that loss of PGRP-LC has a small, but measurable, effect on baseline parameters, but completely blocks the rapid induction of presynaptic homeostasis measured at 0.4mM $[Ca^{2+}]_e$. In both *PGRP^{del}* and *PGRP^{2}* we observe small, but statistically significant, decreases in spontaneous miniature excitatory postsynaptic potential (mEPSP) amplitude and excitatory postsynaptic potential (EPSP) amplitude, but no significant change in quantal content (Figure 1 D-F). When *PGRP^{2}* is placed in trans to *PGRP^{del}*, mEPSP amplitudes remain decreased ($p<0.05$), EPSP amplitude is unchanged compared to wild type ($p>0.05$) and there is a small, but statistically significant, increase in quantal content compared to wild type ($p<0.05$). Finally, we observed that wild type and *PGRP^{2}* NMJs show statistically similar sensitivity to application of EGTA-AM (25μM for 10 min) ($p>0.5$; data not shown).

We then tested whether loss of PGRP-LC blocks presynaptic homeostasis induced by a mutation in the *GluRIIA* subunit of the postsynaptic glutamate receptor. This mutation is present throughout the life of the organism and, therefore, tests for the sustained expression of presynaptic homeostasis. The homeostatic potentiation of quantal content normally observed in the *GluRIIA* mutant background ($p<0.01$) is completely blocked in the *GluRIIA; PGRP^{del}* double mutant (Figure 1J,K; $p>0.5$). Thus, *PGRP-LC* is also necessary for the sustained expression of presynaptic homeostasis.

We next repeated our assays of presynaptic homeostasis at $[Ca^{2+}]_e$ ranging from 0.3-3mM, a 10-fold range of $[Ca^{2+}]_e$ that encompasses what is believed to be physiological $[Ca^{2+}]_e$ at this synapse. In *PGRP^{2}*, we find that homeostatic plasticity is blocked at 0.4mM (Figure 1F) as well as at 3.0mM $[Ca^{2+}]_e$ (Figure 1G and H),

demonstrating that homeostatic plasticity is blocked in the *PGRP*^{2} mutant at all $[Ca^{2+}]_e$. However, we observe a statistically significant ($p<0.01$), homeostatic response in the *PGRP-LC* deletion allele at 3mM $[Ca^{2+}]_e$ (Figure 1H), although the magnitude of this homeostatic response is significantly less that that observed in wild type ($p<0.05$), indicating that homeostatic plasticity is not normal in this allele, even at this elevated extracellular calcium concentration. When we examined two intervening calcium concentrations, specifically testing the *PGRP*^{del} allele, we find no homeostatic increase in quantal content at 0.7mM extracellular calcium (Figure 1I; $p>0.1$) and statistically significant ($p<0.01$) homeostatic plasticity at 1.5mM extracellular calcium. While it remains unclear why the *PGRP*^{2} allele is more severe than *PGRP*^{del}, we considered several issues. We tested the heterozygous *PGRP*^{2}/+ allele and find no evidence of a dominant interfering effect since both baseline release and homeostatic plasticity are normal (data not shown). It remains possible that enhanced transcription of another, related innate immune receptor could partially restore signaling in the *PGRP*^{del} gene deletion background, but not when a mutant receptor isoform is transcribed, as in *PGRP*^{2}. There are several PGRP receptors including modulatory and inhibitory receptors that could mediate this effect (Dziarski, 2004). Regardless, two conclusions are possible based upon our existing data. First, deletion of the *PGRP* gene clearly impairs presynaptic homeostasis and renders it less robust to changes in extracellular calcium, with an unequivocal blockade of homeostatic plasticity in the range of 0.3-0.7mM $[Ca^{2+}]_e$. Second, a mutation that specifically disrupts the *PGRP-LCx* isoform causes a complete failure of presynaptic homeostatic potentiation.

PGRP-LCx Functions Neuronally During Presynaptic Homeostasis

To determine the cell type in which PGRP-LC functions during homeostatic plasticity, we pursued rescue experiments with a Venus-tagged *PGRP-LCx* isoform under *UAS*-control (Figure 2A, E-G). Presynaptic expression of *UAS-PGRP-LCx-Venus* fully restores homeostatic potentiation to the $PGRP^{del}$ mutant (0.4mM $[Ca^{2+}]_e$), whereas postsynaptic muscle expression does not (Figure 2G). We note that muscle-specific *PGRP-LCx* expression in the *PGRP* mutant background causes a substantial reduction in both mEPSP and EPSP amplitudes. To control for the possibility that muscle-specific expression might dominantly interfere with presynaptic homeostasis we overexpressed *PGRP-LCx-Venus* in wild type muscle. We document a similar decrease in baseline mEPSP and EPSP amplitudes compared to wild type (Figure 2H,I) that can be attributed, in part, to diminished input resistance and a depolarized resting potential (Figure 2K,L). Importantly, homeostatic plasticity is fully expressed (Figure 2J). Thus, we can conclude that muscle-specific expression of *PGRP-LCx* fails to rescue homeostatic plasticity. We also note that motoneuron-specific expression of *PGRP-LCx* induces a modest increase in EPSP amplitude ($p<0.01$) and a trend toward increased mEPSP amplitude ($p=0.08$). This activity could reasonably contribute to the rescue of baseline defects in mEPSP and EPSP amplitudes when *PGRP-LCx-Venus* is expressed neuronally in the *PGRP* mutant background (compare Figure 2E,F with Figure 1D,E). But, the observed rescue of homeostatic plasticity when *PGRP-LCx-Venus* is expressed in motoneurons (Figure 2G) clearly occurs over and above any minor effects on baseline transmission. Therefore, we conclude that *PGRP-LCx* isoform expression in motoneurons supports robust homeostatic plasticity. This complements

the observed necessity of the PGRP-LCx isoform, demonstrated by the elimination of presynaptic homeostasis in the *PGRP*^{2} mutant.

Next, we perform the converse experiment using RNAi to deplete PGRP expression specifically in neurons or muscle (Figure 2). We demonstrate that expression of *UAS-PGRP-LC* RNAi in neurons blocks homeostatic plasticity, while expression in muscle does not (Figure 2A-D). Finally, we find that PGRP-LC mRNA is weakly, but endogenously expressed in motoneurons, determined by custom micro-array analysis of mRNA expression in FACS isolated, GFP-expressing motoneurons (Parrish et al., 2014; data not shown). Taken together, these data are consistent with the conclusion that PGRP-LC, and PGRP-LCx in particular, functions presynaptically to enable homeostatic plasticity. These experiments also demonstrate that failed presynaptic homeostasis following loss of PGRP-LC cannot be attributed to the systemic effects associated with impaired innate immunity. More specifically, neuronal expression of *PGRP-LC-RNAi* blocks homeostatic plasticity even though innate immune signaling throughout the rest of the organism is unaltered. And, conversely, in our rescue experiments, innate immune signaling should be compromised everywhere except the nervous system and homeostatic plasticity is fully functional.

PGRP-LC trafficks to the nerve terminal and does not alter synaptic growth.

We next addressed where PGRP-LC resides within motoneurons. Analysis of PGRP-LCx-Venus distribution in motoneurons demonstrates that the Venus-tagged receptor trafficks to the presynaptic nerve terminal. We observe PGRP-LCx-Venus puncta distributed throughout the presynaptic terminal (Figure 3A). Co-staining with the active

zone marker Bruchpilot (BRP) reveals that the receptors are not present at the active zone. These data suggest that PGRP-LCx is a presynaptic receptor, consistent with a required function during the rapid induction of presynaptic homeostasis, which occurs locally at the isolated NMJ.

An analysis of synapse morphology reveals a grossly normal NMJ anatomy. There are no significant changes in synaptic bouton number or active zone number that could account for the change in homeostatic plasticity (Figure 3B). Active zone number is quantified as the number of Bruchpilot (Brp) puncta at the NMJ, consistent with previous studies (Müller et al., 2012). Similarly, there are no major deficits in the abundance of essential synaptic vesicle proteins. Indeed, there is a slight increase in the abundance of Cysteine String Protein (CSP) and Synaptotagmin1 (Syt1) (Figure 5). Thus, the growth and general organization of the NMJ are not adversely affected by the absence of an essential innate immune receptor.

Finally, we examined synaptic ultrastructure. Active zones were identified by the presence of a presynaptic 'T-bar' within a zone of pre- and postsynaptic electron dense membrane. For each active zone, we identified those synaptic vesicles that reside within 150nm of the center of the pedestal of the T-bar (centroid), where presynaptic voltage gated calcium channels reside. For this population of vesicles, at each active zone, we quantified average vesicle diameter, average vesicle number, average vesicle distance from the T-bar centroid and, finally, the two-dimensional length of the active zone, defined as the continuous electron density on either side of the T-bar. There is no significant difference in any of these parameters comparing wild type with the $PGRP^{del}$ or the $PGRP^{2}$ mutants. We conclude that loss of PGRP does not impair the integrity or

organization of the active zone. By extension, the failure of presynaptic homeostatic potentiation is not a secondary consequence of impaired active zone organization, vesicle number or vesicle distance from the T-bar.

PGRP Controls the Homeostatic Modulation of the Readily Releasable Vesicle Pool

The homeostatic modulation of presynaptic neurotransmitter release has been demonstrated to require potentiation of the readily releasable pool (RRP) of presynaptic vesicles (Davis and Müller, 2015). We define the RRP as the number of vesicles released during a brief (500ms) high frequency stimulus train at elevated extracellular calcium concentrations (3mM $[Ca^{2+}]_e$), according to published methods (Schneggenburger et al., 1999). For this analysis, we focused on the *PGRP*^{2} mutation because it blocks homeostatic plasticity at 3mM $[Ca^{2+}]_e$. At this $[Ca^{2+}]_e$ *PGRP*^{2} mutants show a small decrease in mEPSP and cumulative EPSC amplitudes (Figure 4A-C), but no significant difference in the baseline RRP (wt = 2370±227; *PGRP*^{2} = 2236±190; $p>0.3$), consistent with quantification of baseline neurotransmission at a ten-fold lower $[Ca^{2+}]_e$ (Figure 1D-F). Following application of PhTx there is a statistically significant, homeostatic potentiation of the RRP in wild type (Figure 4D; $p<0.01$). However, there is no significant increase of the RRP in the *PGRP*^{2} mutant ($p>0.1$). We conclude that PGRP-LC is necessary for the homeostatic expansion of the RRP. We also note that the failure to expand the RRP does not correlate with altered vesicle number or distribution (Figure 3).

We quantified two additional parameters based on delivery of stimulus trains to

the NMJ (Figure 4A): 1) short term synaptic depression during the stimulus train and 2) an estimate of release probability at the onset of the stimulus train (P_{train}; estimated by dividing the first EPSC amplitude in the stimulus train by cumulative EPSC) (Thanawala and Regehr, 2013). Short-term depression was calculated as the percent change in EPSC amplitude comparing EPSC1 and EPSC4 of a stimulus train. There was no difference comparing wild type in the presence or absence of PhTx with $PGRP^2$ in the presence or absence of PhTx ($p>0.05$; WT (-PhTx) = 59.7 ± 1.7%, WT(+PhTx) = 54.6 ± 1.5%, $PGRP^2$(-PhTx) = 57.8 ± 2.4%, $PGRP^2$ (+PhTx) = 55.0 ± 2.3%). There is a small, but significant, 2.7% increase in P_{train} comparing wild type and $PGRP^2$ ($p<0.05$). However, application of PhTx does not alter P_{train} in either genotype (wt = 0.25 ± 0.07; wt+PhTx = 0.26 ± 0.09; $PGRP^2$ = 0.27 ± .01; $PGRP^2$ + PhTx = 0.28 ± .01). These data argue that the primary consequence of the $PGRP^2$ mutation is not a change in presynaptic release probability, but rather the elimination of a homeostatic expansion of the RRP.

Finally, we sought additional genetic evidence that PGRP acts in concert with other established mechanisms that are responsible for the homeostatic potentiation of the RRP during presynaptic homeostasis. It was previously demonstrated that the homeostatic potentiation of the RRP requires the presence of the active-zone associated scaffold RIM (Rab3 Interacting Molecule) (Davis and Müller, 2015). Therefore, we tested whether $PGRP^{del}$ interacts, genetically, with a null mutation in *rim*. The heterozygous mutation in *PGRP-LC* ($PGRP^{del}$/+) shows robust homeostatic potentiation (Figure 4E). We then examined a heterozygous null mutation in *rim* (rim^{103}/+) and, again, document robust presynaptic homeostasis, although somewhat

less pronounced compared to that observed in *PGRP*^{del} alone (Figure 4E). But, when we examine the double heterozygous mutant combination we find a block of presynaptic homeostasis ($p>0.05$; Figure 4E). This result underscores the likelihood PGRP is required for the RIM-dependent modulation of the RRP during presynaptic homeostasis. It is possible that RIM could be a target of signaling downstream of PGRP-LCx activation, but this remains speculative without additional information about the signaling system that acts downstream of PGRP-LC within the presynaptic terminal.

PGRP Interacts Genetically with Multiplexin/Endostatin

In innate immunity, PGRP-LCx recognizes a peptidoglycan sequence presented by invading bacteria. One interesting possibility is that PGRP-LCx might recognize molecular patterns caused by the cleavage of extracellular matrix proteins at the nerve terminal. Regulated proteolysis of synaptic proteins is becoming increasingly apparent as a mode of inter-cellular signaling (Peixoto et al., 2012). We recently demonstrated that Endostatin, a small peptide that is released following proteolytic cleavage of the Drosophila Collagen VIII homologue Multiplexin, is necessary for presynaptic homeostasis (Wang et al., 2014). Therefore, we tested whether *PGRP* interacts, genetically, with a strong loss of function mutation in *multiplexin*. The heterozygous mutation in *PGRP-LC* (*PGRP*^{2}/+) shows robust homeostatic potentiation, as does a heterozygous mutation in *multiplexin* (*dmp*^{f07253}/+) (Figure 4F). But, when we examine the double heterozygous mutant combination we find a complete block of presynaptic homeostasis ($p>0.05$) (Figure 4F). These data are consistent with a model in which Endostatin could function as a ligand for PGRP, but additional work is necessary to

prove that this interaction occurs biochemically.

If PGRP-LC functions as a receptor for intercellular signaling necessary for presynaptic homeostasis, then expression of PGRP-LC lacking the extracellular PGRP domain (termed $PGRP^{\Delta C}$) should fail to rescue presynaptic homeostasis in the $PGRP^{del}$ mutant background. We generated a Venus tagged *PGRP-LC* deletion transgene (*UAS-*$PGRP^{\Delta C}$*-Venus*), modeling it after a similarly truncated receptor that was previously used to study innate immunity (Choe et al., 2005). First, we document that neuronally expressed *UAS-*$PGRP^{\Delta C}$*-Venus* localizes to the presynaptic terminal (Figure 6). Then we show that *UAS-*$PGRP^{\Delta C}$*-Venus* fails to rescue presynaptic homeostatic potentiation (Figure 4G-K). There is no effect of *UAS-*$PGRP^{\Delta C}$*-Venus* expression on baseline transmission and homeostatic plasticity remains blocked in the $PGRP^{del}$ mutant background. Importantly, the *UAS-*$PGRP^{\Delta C}$*-Venus* transgene is similar to the predicted protein truncation caused by the $PGRP^{2}$ mutation, which resides at the start of the PGRP domain. This result, therefore, further validates the functional blockade of presynaptic homeostasis observed in the $PGRP^{2}$ mutant.

Discussion

The innate immune system is evolutionarily conserved in all animals. Innate immune signaling has been found to participate in neural development and disease including a role for the C1q component of the complement cascade regulating synapse elimination (Stevens et al., 2007), Toll-like receptor signaling in neural development (Okun et al., 2011; Ma et al., 2007) and tumor necrosis factor (TNF) signaling during degeneration and quantal scaling (Stellwagen and Malenka, 2006; Steinmetz and

Turrigiano, 2010). In these examples, however, the innate immune response is induced within microglia or astrocytes. Innate immune receptors on glia respond to pathogens or damage-induced cues and an innate immune response ensues (Stevens et al., 2007). Far less clear is the role of innate immune signaling within neurons, either centrally or peripherally, although there are clear examples of downstream signaling components such as Rel and NFκB having important functions during learning related neural plasticity (Meffert et al., 2003; Ahn et al., 2008). Here we place the innate immune receptor, PGRP-LC at the presynaptic terminal of *Drosophila* motoneurons and demonstrate that this receptor is essential for robust presynaptic homeostatic potentiation. Importantly, we provide evidence that the block of synaptic homeostasis cannot be due to failure of a systemic innate immune response throughout the organism. We speculate, based on our data, that PGRP-LC could function as a receptor for the long-sought retrograde signal that mediates homeostatic signaling from muscle to nerve.

A model for Innate Immune Signaling: PGRP-LC as a feed-forward signaling switch for homeostatic plasticity.

A distinguishing feature of presynaptic homeostatic potentiation is that it can be both rapidly induced and sustained for prolonged periods of time (Davis and Muller, 2015). At first glance, the finely tuned control of presynaptic release during presynaptic homeostasis seems quite different from the induction of innate immune signaling, which is generally a potent, highly amplified response to pathogen invasion. It is possible that innate immune signaling activity is adjusted to fit the requirements of presynaptic

homeostasis in motoneurons. This would be consistent with the established diversity of innate immune signaling functions during development such as dorso-ventral patterning (Anderson et al., 1985). But, from another perspective, the rapid and potent induction of innate immune signaling might serve a unique function during presynaptic homeostasis. Many homeostatic signaling systems incorporate feed-forward signaling elements such as the heat shock response (Davis and Müller, 2015). By analogy, PGRP-LCx could function as a feed-forward signaling receptor that acts more like a 'switch' to enable presynaptic homeostasis in the nerve terminal. The accuracy of the homeostatic response would be determined by other signaling elements. In favor of this idea, the induction of innate immune signaling is rapid, occurring in seconds to minutes (Stöven et al., 2000), a time frame that is similar to the induction of presynaptic homeostasis (Davis and Müller, 2015). In addition, innate immune signaling can be maintained for the duration of an inducing stimulus, consistent with recent evidence that presynaptic homeostasis is a process that is continually induced at synapses in the presence of a persistent postsynaptic perturbation (Younger et al., 2013). However, it remains formally possible that persistent PGRP-dependent signaling during development transcribes a permissive factor that is required for the motoneuron to express any form of presynaptic homeostasis.

Several lines of evidence are consistent with PGRP-LCx functioning locally, at the presynaptic nerve terminal. *PGRP*^{2} mutants disrupt the rapid induction of presynaptic homeostasis, which is induced and expressed locally at the nerve terminal. PGRP-LCx-Venus trafficks to the presynaptic terminal when expressed in motoneurons, and this expression is sufficient to restore presynaptic homeostasis to the *PGRP*^{del}

mutant. Finally, expression of *PGRP-LC* RNAi in motoneurons is sufficient to block synaptic homeostasis. There are no observable defects in neuromuscular anatomy or ultrastructure and baseline electrophysiology is remarkably normal, particularly quantal content and estimates of release probability and RRP size. Therefore, failure of synaptic homeostasis is unlikely to be a secondary consequence of altered neuromuscular development. Importantly, these data also demonstrate that the block of synaptic homeostasis cannot be due to failure of a systemic innate immune response throughout the organism, since RNAi specifically in motoneurons blocks presynaptic homeostasis.

How is signaling downstream of PGRP mediated? In innate immunity, the PGRP-LC receptor is believed to multimerize upon binding to peptidoglycans, leading to the recruitment of the intracellular adaptor protein IMD (Immune Deficient), which catalyzes the activation of two downstream signaling pathways. IMD leads to activation of the caspase DREDD, which cleaves Relish to enable nuclear translocation of the transcription factor. IMD also facilitates activation of a MAPKKK (TAK1), which leads to both activation of Jun Kinase (JNK) and, separately, enhanced activation of Relish via IKK (Royet and Dziarski, 2007). Since transcription is a major output of the innate immune response, it is important to consider how this might interfere with the rapid, transcription-independent form of presynaptic homeostasis. One possibility is that persistent PGRP-dependent signaling during development transcribes a permissive factor that is required for the motoneuron to express any form of presynaptic homeostasis. Alternatively, if PGRP-LC were activated at the presynaptic terminal, then it would have the capacity to mediate (or trigger) both rapid presynaptic homeostasis via the direct action of presynaptic kinase signaling as well as long-term, transcription-

dependent presynaptic homeostasis via the transcription factor relish. Whether or not these ideas prove correct, our data open a door toward understanding how immune signaling interfaces with the control of neural function during health and disease.

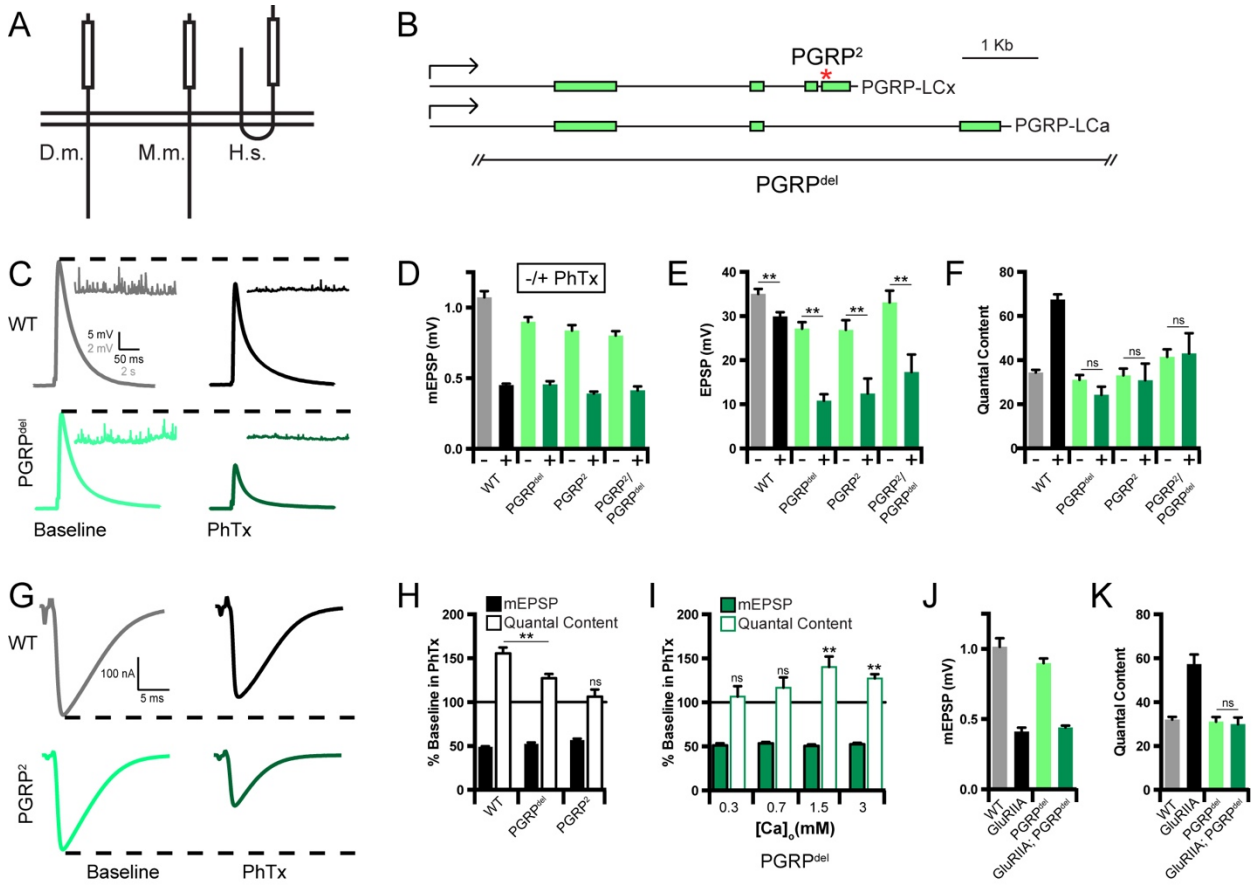

Figure 1: Identification of PGRP-LC as an innate immune receptor involved in the rapid induction and sustained expression of presynaptic homeostasis.

(A) Diagram of PGRP-LC in different species (PGLYRP 2 in mouse - M.m. and human - H.s.). Rectangles represent PGRP domains. **(B)** Schematic of the *PGRP-LC* locus showing two alternative splice variants involved in innate immune signaling (*PGRP-LCa* and *PGRP-LCx*). The entire coding region is deleted in $PGRP^{del}$. Star denotes a nonsense mutation ($PGRP^{2}$) truncating the PGRP domain of the *PGRP-LCx* isoform. **(C)** Sample data showing EPSP and mEPSP amplitudes in the absence and presence of PhTx for WT (grey/black respectively) and $PGRP^{del}$ (light green/dark green). **(D)** Average data for mEPSP amplitude for indicated genotypes in the absence (light grey/light green) and presence of PhTx (black/dark green). PhTx application reduces amplitudes in all genotypes ($p<0.01$). **(E)** Average data for EPSP amplitude as in D (**, $p<0.01$). **(F)** Average data for quantal content as in D (ns; $p>0.05$). **(G)** Sample data showing EPSC amplitudes as in C, 3mM $[Ca^{2+}]_e$. **(H)** Average data for mEPSP amplitudes and quantal content following application of PhTx expressed as percent change relative to baseline in the absence of PhTx for each genotype. Homeostasis is suppressed in $PGRP^{del}$ compared to wild type (**, $p<0.01$) and is blocked in $PGRP^{2}$ at 3mM extracellular calcium. **(I)** Analysis of $PGRP^{del}$, extracellular calcium as indicated. Homeostasis is blocked at 0.3mM $[Ca^{2+}]_e$ ($p>0.3$) and 0.7mM $[Ca^{2+}]_e$ ($p>0.1$), and is suppressed at 1.5 (see panel H) and 3mM (though statistically significant homeostasis is observed above $PGRP^{del}$ baseline, $p<0.01$). **(J-K)** Average data for mEPSP amplitude and quantal contents for indicated genotypes.

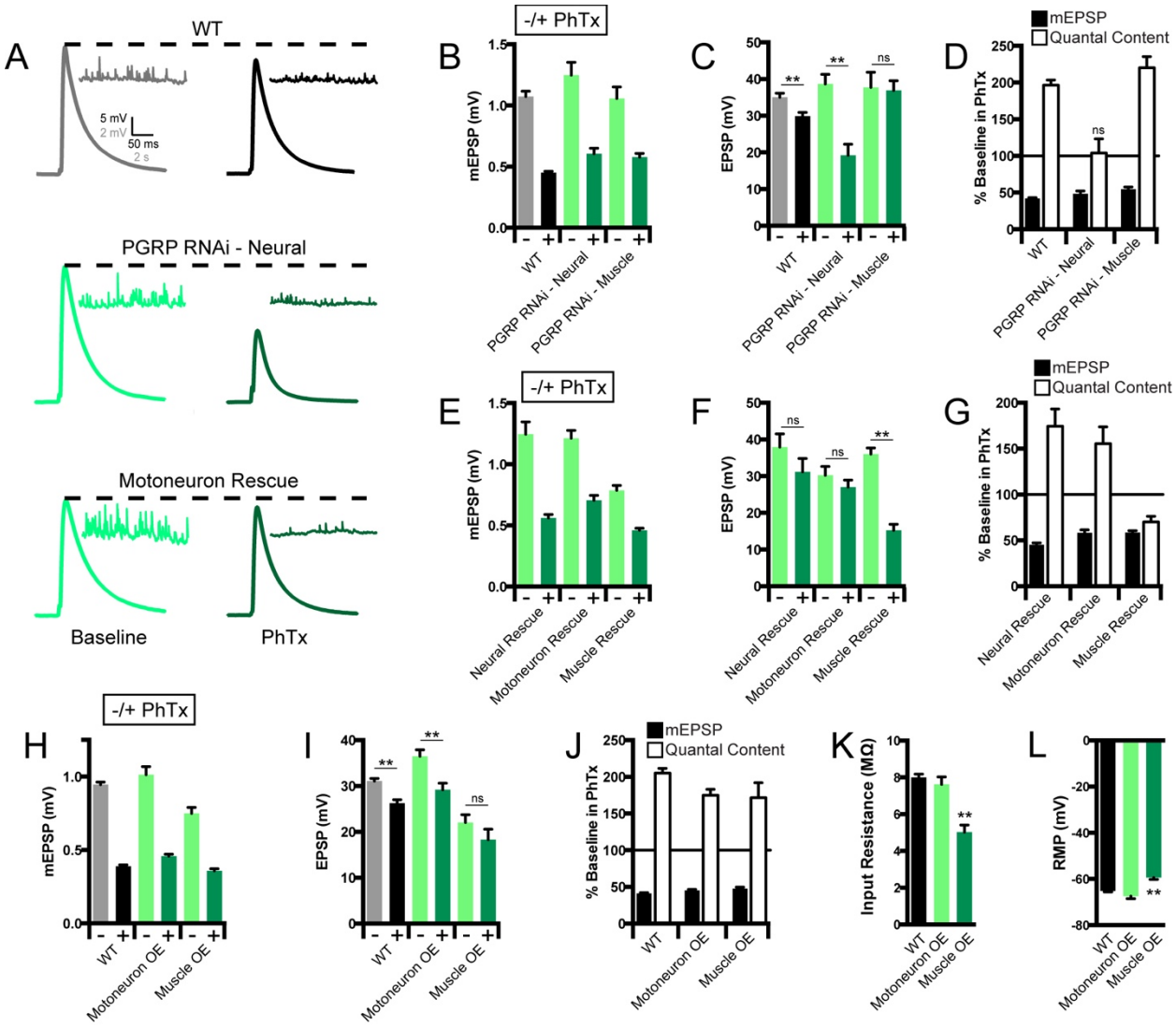

Figure 2: PGRP is required in motoneurons for presynaptic homeostasis

(A) Sample data showing EPSP and mEPSP waveforms -/+ PhTx for the indicated genotypes. **(B)** Average mEPSP amplitude when *PGRP-RNAi* is expressed neuronally (*elaV-GAL4*) or in muscle (*BG57-GAL4*), -/+ PhTx as indicated. PhTx application reduces amplitudes in all genotypes ($p<0.01$)**. (C)** Average EPSP amplitude as in B. (** $p<0.01$). **(D)** Average percent change in mEPSP amplitude and quantal content in PhTx compared to baseline for the indicated conditions. **(E)** Average mEPSP amplitude for indicated rescue experiments as follows: Neural rescue = *elaV-GAL4* expression of *UAS-PGRP-LCx* in the $PGRP^{del}$ mutant; motoneuron rescue = *OK371-GAL4*; muscle rescue = *MHC-GAL4*. PhTx application reduces amplitudes in all genotypes ($p<0.01$)**. (F)** Average EPSP amplitude as in E. **(G)** Average percent change in mEPSP amplitude and quantal content as in D. When *UAS-PGRP-LCx* is expressed presynaptically, homeostasis is rescued ($p<0.05$). Expression in muscle does not ($p>0.05$). **(H)** Average mEPSP amplitude for expression of *UAS-PGRP-LCx* in a wild type background, drivers as indicated in E. **(I)** Average EPSP amplitudes for genotypes as in H. **(J)** Average percent change in mEPSP amplitude and quantal content for genotypes as in H. Significant

homeostasis is observed in all conditions ($p<0.01$).**(K)** Muscle input resistance for the indicated genotypes. (** $p<0.01$). **(L)** Muscle resting membrane potential. Average RMP (** $p<0.01$).

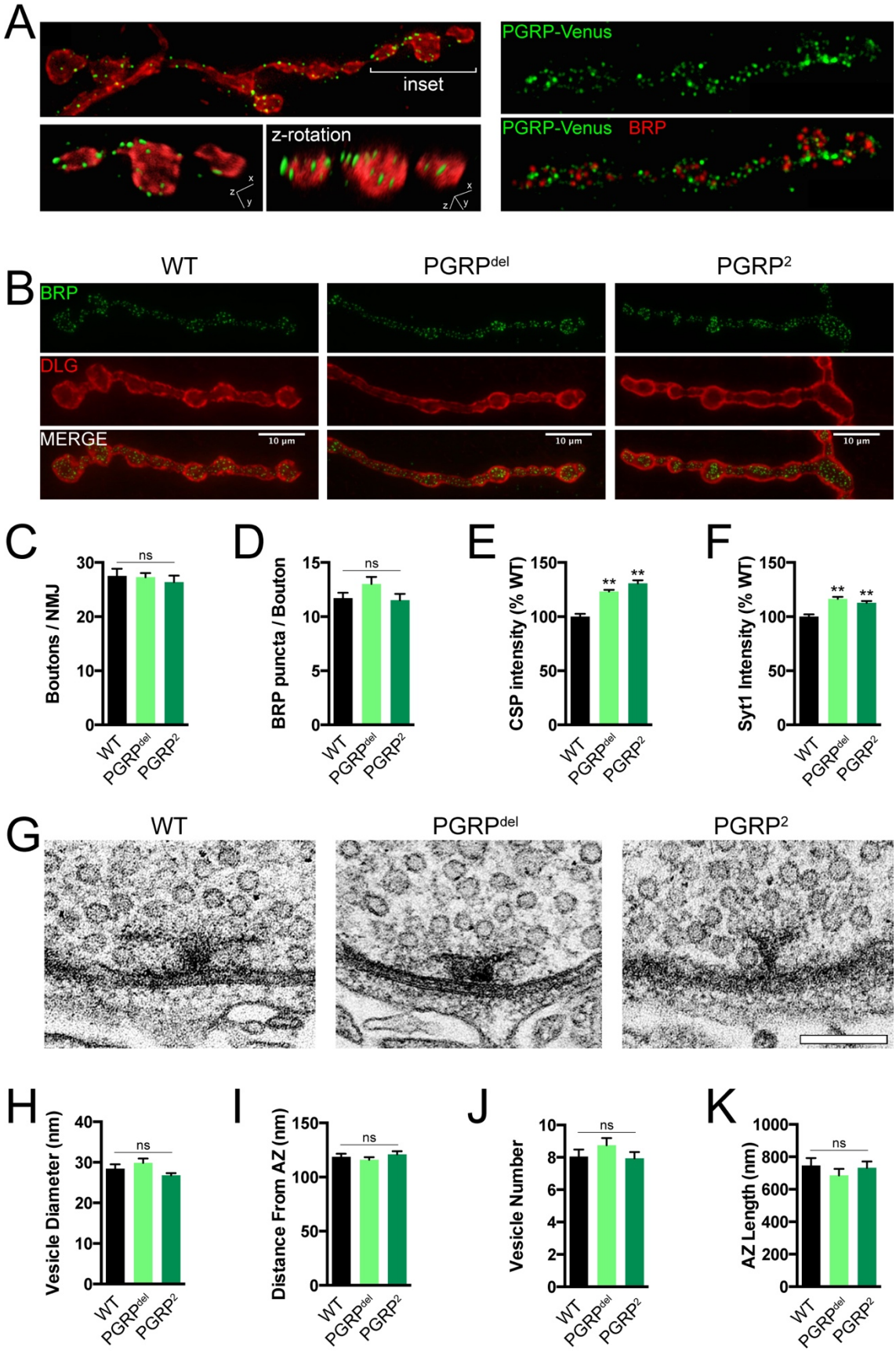
A
inset
z-rotation
PGRP-Venus
PGRP-Venus BRP
B
WT
PGRPdel
PGRP2
BRP
DLG
MERGE
10 µm
C
Boutons / NMJ
ns
D
BRP puncta / Bouton
ns
E
CSP intensity (% WT)
**
F
Syt1 Intensity (% WT)
**
G
WT
PGRPdel
PGRP2
H
Vesicle Diameter (nm)
ns
I
Distance From AZ (nm)
ns
J
Vesicle Number
ns
K
AZ Length (nm)
ns

Figure 3: PGRP-LC-Venus localizes to the presynaptic terminal

(A) (Left panels) Image in of an NMJ in which *UAS-PGRP-LCx-Venus* was expressed using *Ok371-Gal4*. The NMJ was co-stained with HRP (red) and anti-GFP (green). Magnified and rotated images (below) indicate the membrane-proximal localization of PGRP-LCx-Venus. (Right Panels) NMJ expressing *UAS-PGRP-LCx*-Venus as in A. The NMJ was co-stained with the presynaptic active zone marker Brp (left, red) and anti-Venus (middle, green). **(B)** WT NMJ at muscle 4 (left) co-stained with the presynaptic active zone marker Brp (top, green) and the postsynaptic marker Dlg (middle, red). Merge at bottom. **(C)** Quantification of bouton number per NMJ at muscle 4. **(D)** Brp puncta per bouton at muscle 4. **(E, F)** Quantification of average staining intensities for anti-Syt1 and anti-CSP (** $p<0.01$). **(G)** Representative active zone images. Scale=150nm. **(H-K)** Quantification of vesicle diameter per active zone (AZ) (H), average vesicle distance from T-bar base (see text) (I), average vesicle number per active zone within a 150nm radius of T-bar base (J), average AZ length (K).

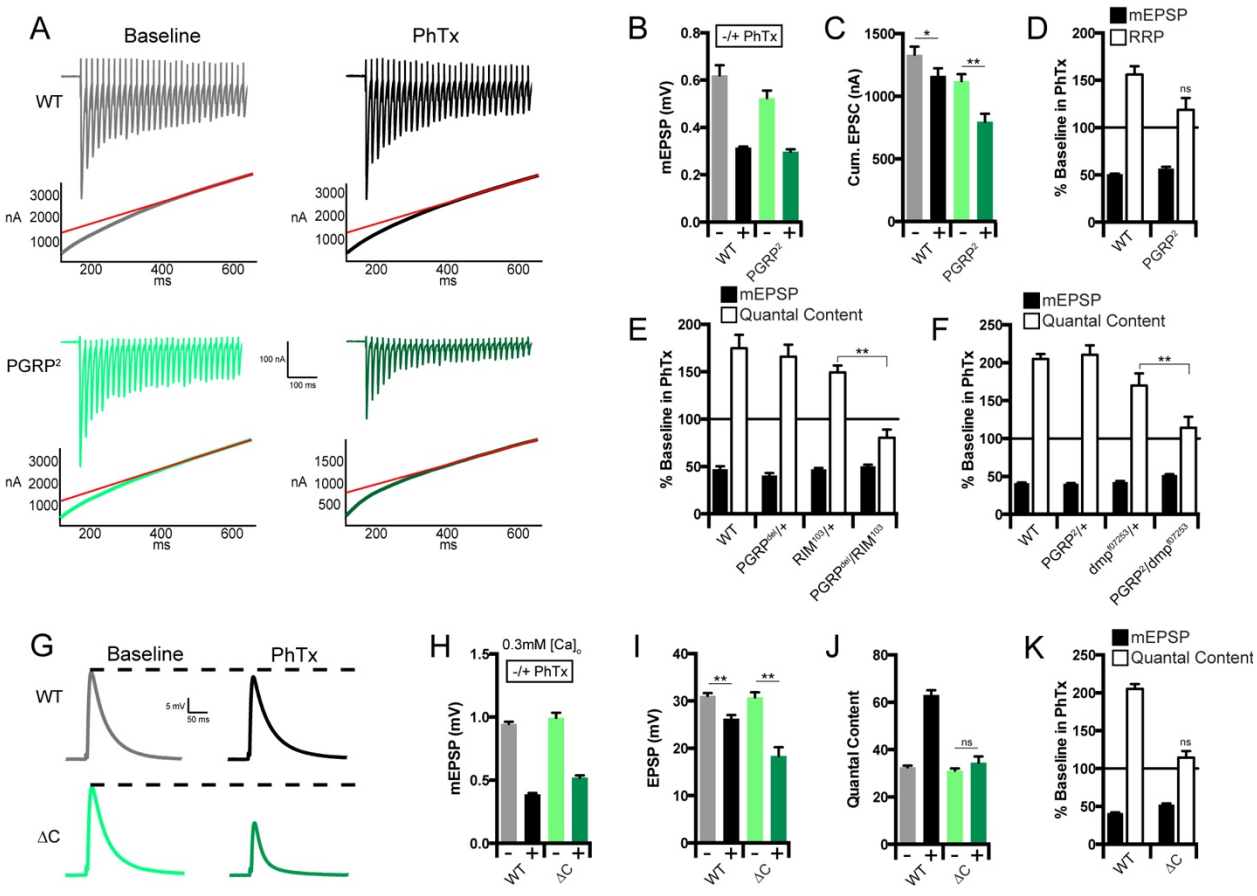

Figure 4: Loss of PGRP-LC blocks the homeostatic expansion of the readily releasable vesicle pool

(A) Example EPSC traces (top) and cumulative EPSC amplitudes (bottom) minus and plus PhTx for WT and *PGRP*^{2}. Experiment used 60-Hz stimulation (30 stimuli) in 3mM $[Ca^{2+}]_e$. The line fit to cumulative EPSC data that was back-extrapolated to time 0 is shown in red. **(B)** Average data for mEPSP amplitudes for the indicated experiments. PhTx application reduces amplitudes in all genotypes (p<0.01). **(C)** Cumulative EPSC amplitudes as in B (* p<0.05; ** p<0.01). **(D)** Average percent change in mEPSP amplitude and RRP size in PhTx. There is not a significant PhTx-dependent increase in RRP in the *PGRP*^{2} mutant (p>0.05). The % change comparing WT and *PGRP*^{2} is significantly different (p<0.05).**(E)** Average percent change in mEPSP and quantal content caused by PhTx application to the indicated genotypes. *PGRP*^{del}/+ heterozygous mutants have normal presynaptic homeostasis compared to wild type (p>0.2). There is significant presynaptic homeostasis in *rim*/+ (-/+ PhTx, p<0.01) but a slight suppression of presynaptic homeostasis in *rim*/+ compared to wild type (p<0.05). The double heterozygous condition *PGRP*^{del}/+ ; *rim*/+ completely blocks homeostatic plasticity (p>0.5). **(F)** Average changes as in E. Significant presynaptic homeostasis is observed in *PGRP*^{2}/+ and *dmp*/+ heterozygous animals (p<0.05). No significant homeostasis is observed in the double heterozygous condition (p>0.05). **(G)** Example EPSP traces minus and plus PhTx for WT and DC rescue at 0.3mM $[Ca^{2+}]_e$. ΔC denotes expression of *UAS-PGRP* truncated transgene, see methods. **(H)** mEPSP amplitudes as in B, all PhTx changes are significant (p<0.01). **(I)** Average

data for EPSP amplitudes in the indicated experiments (** $p<0.01$) **(J)** Average data for quantal content in the indicated genotypes. **(K)** Average changes as in E.

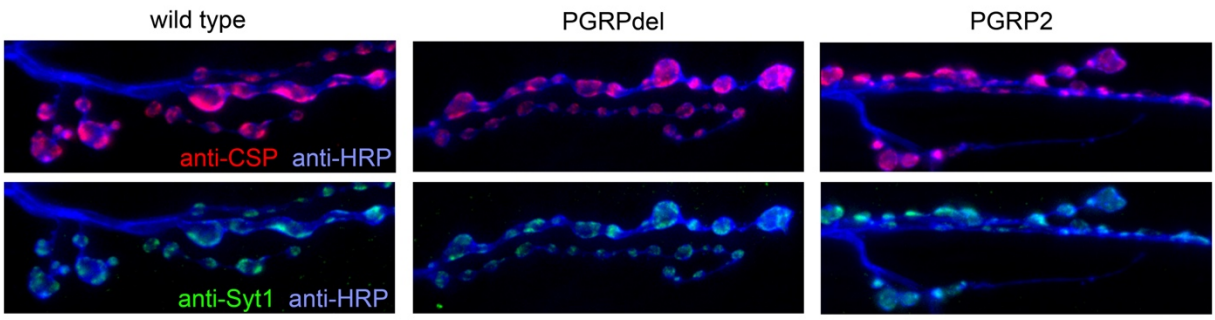

Figure 5: Representative images of Syt1 and CSP staining in wild type and PGRP.

Legend: Immunostaining of wild type, $PGRP^{del}$, and $PGRP^{2}$ NMJs, as indicated. NMJs are co-stained with anti-CSP (red), anti-Syt1 (green) and anti-HRP (blue) as indicated. Images are taken from the NMJ at muscles 6/7.

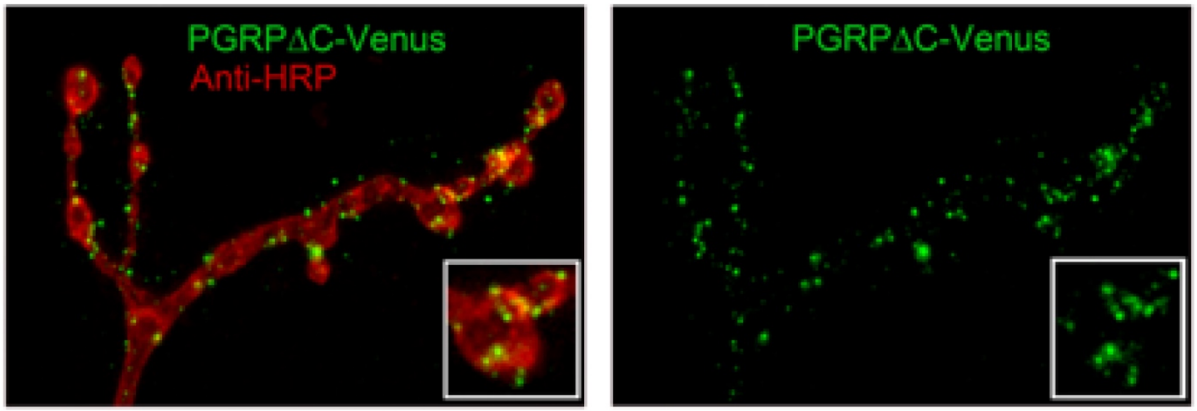

Figure 6: PGRP$^{\Delta C}$ localizes to synaptic terminals.

Legend: Expression of *UAS-PGRP$^{\Delta C}$-Venus* (green) in motoneurons trafficks to the presynaptic terminal and is distributed throughout the terminal area. The NMJ is co-labeled with anti-Brp (red) to identify presynaptic active zones.

3. Molecular Interface of Neuronal Innate Immunity, Synaptic Vesicle Stabilization and Presynaptic Homeostatic Potentiation

INTRODUCTION

Emerging models for innate immune signaling within the nervous system are consistent with an emergency surveillance system that is primarily mediated by astrocytes and microglia (Stevens et al., 2007; Schafer et al., 2012; Hong et al., 2016). Molecular patterns that are either presented by invading pathogens or that exist on cellular debris derived from damaged cells are recognized by innate immune receptors, expressed by astrocytes and microglia. Subsequent activation of innate immune signaling within astrocytes and microglia leads to the release of cytokines and antimicrobial peptides and/or the engulfment of cellular debris. Innate immunity is also hypothesized to participate in the developmental refinement of neural circuitry. Here, synapses destined for elimination are thought to expose molecular patterns on their surface to trigger immune signaling and subsequent engulfment by microglia (Schafer and Stevens, 2015). Recent evidence suggests that this process could become maladaptive in the context of neurodegenerative disease (Hong et al., 2016).

Essential components of both the adaptive and innate immune signaling systems are also present within neurons. For example, with regard to adaptive immunity, the major histocompatibility complex class I (MHC-I) proteins are neuronally expressed, regulated by neural activity and participate in the anatomical refinement of neural circuitry during development (Corriveau et al., 1998; Huh et al., 2000; Lee et al., 2014). MHC-1 may also contribute to degeneration within the diseased brain (Rivera-Quinones

et al., 1998; Adelson et al., 2012). Likewise, genes that encode innate immune receptors (Harris et al., 2015) and downstream intracellular signaling proteins are also expressed by neurons throughout the invertebrate and mammalian nervous systems (Harris et al., 2015; Cahoy et al., 2008). More specifically, in both *Drosophila* and mammals, the Rel/NFkB family transcription factors, a downstream target of innate immune signaling receptors, have been shown to be neuronally expressed and participate in learning related or circadian plasticity (Ahn et al., 2008, Meffert et al., 2003; Chen et al., 2016). Thus, while it is well-established that neurons can respond to glial-derived cytokines such as TNF-alpha (Stellwagen & Malenka, 2006; Lewitus et al., 2016), the presence of innate immune signaling systems within neurons implies that neurons are also primary mediators of innate immune signaling, the purpose of which remains virtually unknown.

Another mystery concerns the function of neuronal innate immunity throughout the health-span of an organism. It is well established that components of the innate immune signaling system are persistently expressed in neurons throughout the adult nervous system (Cahoy et al., 2008). What is the function of innate immune signaling within mature, healthy neurons? Does neuronal innate immune signaling represent a latent system, ready to engage injury and infection, or does it perform additional functions that are relevant to the day-to-day activity within the adult brain? A role for the cytokine TNF-alpha, secreted by astrocytes, has been established during the homeostatic regulation of glutamate receptor abundance (Stellwagen and Malenka, 2006). Could neuronal innate immune signaling activated within neurons also function

as a mediator of homeostatic plasticity, controlling the function of neurons, circuitry and behavior throughout life?

Recently, in *Drosophila*, an innate immune receptor was shown to be essential for the rapid induction and sustained expression of presynaptic homeostatic potentiation (PHP) (Harris et al., 2015). PHP is a highly conserved form of homeostatic plasticity being similarly expressed at the NMJ of fly, mouse and human (Frank et al., 2006; Wang et al., 2016; Cull-Candy et al., 1980), and being expressed at central synapses in both flies (Kazama and Wilson, 2008) and rodents (Burrone and Murthey, 2002; Kim and Ryan, 2010; Krahe and Guido, 2011). The discovery of PGRP-LC and its function during PHP implies a different framework for considering the function of innate immune signaling in neurons. Just as canonical immunity distinguishes self from non-self, neuronal innate immune signaling may help determine the difference between normal and non-normal neuronal function, thereby governing the induction or expression of homeostatic plasticity.

Currently, nothing is known about how neuronal PGRP receptors signal within the cell. Most of what we understand about innate immune signaling in the nervous system revolves around either signaling at the cell surface, communicated to astrocytes and microglia, or the transcription of immune effectors produced as a consequence of innate immune activation. Within neurons, very little is known about the function of the intracellular signaling pathways that link receptor activation to nuclear transcription. For example, does intracellular signaling represent a direct line of communication from receptor to nucleus, or does signaling diverge to achieve multiple, coordinated effects throughout the extended architecture of a neuron?

Here we address the function of neuronal innate immunity by exploring the function of the canonical innate immune signaling system that acts downstream of the PGRP-LC receptor during presynaptic homeostatic potentiation in *Drosophila* motoneurons. In so doing, we define a novel organization of innate immune signaling within these neurons that is uniquely suited to the rapid induction and sustained expression of PHP. First, signaling downstream of the PGRP-LC receptor bifurcates into local synaptic versus cell-wide, nuclear signaling pathways. We demonstrate that the adaptor protein Imd (immune deficiency), the kinase encoded by *IKK*β and the transcription factor encoded by *Rel* (Relish) are all essential for the long-term maintenance of PHP. However, only IKKβ and the Map3K Tak1 participate in the rapid induction of PHP, and represent a point of signaling bifurcation. We then demonstrate that Tak1 is a resident presynaptic protein and a novel synaptic vesicle priming factor that is essential for the rapid induction of PHP. As such, Tak1 represents the first known interface of intracellular innate immune signaling with the molecular mechanisms that control synaptic vesicle fusion at the active zone. Furthermore, Tak1 defines a new molecular mechanism for the persistent modulation of presynaptic release, at baseline and following the induction of PHP.

Based on our findings, we propose a general model for innate immune signaling during homeostatic plasticity in motoneurons. Activation of innate immunity provides a rapid, feed-forward potentiation of presynaptic release, via activation of Tak1, followed by a delayed activation of Rel-mediated transcription that either sustains the homeostatic response, or transforms the motoneuron in such a way that it can sustain the expression of homeostatic plasticity for prolonged periods of time. As such, innate

immune signaling may represent an emergency response, feed-forward signaling system that both induces homeostatic plasticity and sets the stage for the prolonged stability of neural function in the presence of a persistent perturbation.

RESULTS

The innate immune signaling cascade, termed the ***Im***mune ***D***eficient (IMD) signaling cascade, is initiated by ligand induced dimerization of the PGRP-LC receptor and assembly of a protein complex (IKK complex) that includes the adaptor protein Imd (**Im**mune **d**eficiency), the serine threonine kinase Tak1 (TGF-β activated kinase 1, a Map3K) and the serine threonine kinase IKKβ (note: there is only a single IKK encoded in the *Drosophila* genome, termed IKKβ). Once initiated, IMD signaling drives nuclear translocation and activation of the NFkB-type transcription factor Relish (Silverman et al., 2000; Stöven et al., 2000; Choe et al., 2002; Myllymäki et al., 2014). While additional signaling complexity exists, the signaling constituents including Imd, IKKβ, Tak1 and Rel represent several principal stages of signal transduction from receptor activation at the plasma membrane to transcription in the nucleus (Figure 7A). Therefore, we assayed whether each of these genes is necessary for presynaptic homeostatic potentiation (PHP) (Figure 7).

First, we assembled loss of function mutations that specifically disrupt the genes encoding Imd, IKKβ, Tak1 and Rel (Figure 7B). The Imd^{NP} mutation is a transposon insertion residing within the first coding exon and is predicted to be a functional null. We acquired two independently derived mutations in the *Tak1* gene. The $Tak1^{2}$ mutation is

an early stop codon and also considered a functional null mutation (Vidal et al., 2001). The *Tak1*^{179} mutation is a missense mutation in a conserved regulatory domain and is a functional null mutation (Delaney et al., 2006). We also acquired a deficiency that uncovers the *Tak1* gene locus. We generated a mutation in *IKKβ* (*IKKβ*^{CR}) using CRISPR/Cas9 technology, an indel mutation within the *IKKβ* coding sequence. This mutation causes a frame shift that results in a stop codon in the 5' region of the kinase domain, predicted to be a functional null mutation (see methods). We also acquired a deficiency that uncovers the *IKKβ* gene locus. Finally, the *Rel*^{E20} mutation is a large deletion removing all possible transcription start sites and is a molecular null mutation (Hedengren et al., 1999).

Tak1 and IKKβ are necessary for the rapid induction of PHP

Presynaptic homeostatic potentiation (PHP) can be rapidly induced by application of the glutamate receptor antagonist Philanthotoxin-433 (PhTx; 10-20μM) (Frank et al., 2006; Dickman and Davis, 2009; Younger et al., 2013; Wang et al., 2014). PhTx inhibits muscle specific glutamate receptors harboring the GluRIIA subunit, causing a decrease in postsynaptic mEPSP amplitudes. Within 10 minutes of PhTx application, retrograde signaling induces a potentiation of presynaptic neurotransmitter release (quantal content; see methods) that offsets the decrease in mEPSP amplitude and restores EPSP amplitudes toward baseline levels (Figure 7G-I, black traces and bars; Frank et al., 2006).

We began our pathway interrogation with *Imd*. The *Imd* gene encodes an adaptor protein that can directly bind the intracellular domain of PGRP-LC and is essential for

the induction of the innate immune response following a challenge with bacteria or lipopolysaccharide (LPS) stimulation (Lemaitre et al., 1995; Choe et al., 2005). Here we demonstrate that baseline neurotransmission is normal in the *Imd*^{NP} mutant (Figure 7G-I). When PhTx is applied, mEPSP amplitudes are decreased by ~50%. In response to this PhTx perturbation, we observe a robust homeostatic response as demonstrated by a significant increase in quantal content (Figure 7I, J) that restores EPSP amplitude to toward baseline levels (Figure 7H). Thus, Imd is not required for the rapid induction of PHP, despite the fact that the PGRP-LC receptor is essential (Harris et al., 2015).

We subsequently repeated our assays of baseline transmission in the *Tak1* and *IKK*β mutant backgrounds. First, we demonstrate that the *Tak1* mutations have a mild defect in baseline transmission (0.3mM extracellular calcium – $[Ca^{2+}]_e$). Specifically, mEPSP amplitudes are significantly decreased in both *Tak1* alleles and EPSP amplitudes are also diminished (Figure 7G, H). There is a significant decrease in baseline quantal content in *Tak1*^{179} ($p<0.005$), but no significant decrease in quantal content in *Tak1*^{2} ($p>0.05$). When we assay the *IKK*β mutant, we find it behaves in a similar manner, revealing a mild decreases in both mEPSP and EPSP amplitudes and no change in quantal content relative to WT.

Next, we assayed PHP in the *Tak1* and *IKK*β mutants. When we applied PhTx to the *Tak1* and *IKK*β mutants, we find that PHP is completely blocked (Figure 7H, I). For both alleles of *Tak1* as well as the *IKK*β mutant, mEPSP amplitudes are decreased by ~50% in the presence of PhTx. However, there is no statistically significant increase in quantal content, and EPSP amplitudes remain dramatically reduced compared to each mutant in the absence of PhTx. Additionally, we placed a heterozygous *Tak1*^{2} mutant

chromosome in trans to a deficiency that uncovers its locus, and we also placed the heterozygous *IKKβ^{CR}* mutant in trans to a deficiency that uncovers its locus. In each case, PHP was blocked (Figure 15A-E). We conclude that both *Tak1* and *IKKβ* are essential for the rapid induction of PHP.

Finally, we repeated our assays for baseline transmission and PHP in the *Rel* mutant background. Note that the rapid induction of PHP is independent of both transcription and translation (Frank et al., 2006), suggesting that *Rel* should not be required. At baseline, the *Rel* mutant revealed a slight, but significant increase in mEPSP amplitudes, no change in EPSP amplitude and a significant decrease in quantal content compared to wild type. When PhTx is applied to the *Rel* mutant, we find that PHP is robustly expressed, as predicted. We observe a large decrease in mEPSP amplitude and a statistically significant, homeostatic increase in presynaptic release. We note, however, that the magnitude of the increase in presynaptic release is significantly less than that observed in wild type, indicating a suppression of the homeostatic response (Figure 7I, J). From these data we conclude *Rel* is dispensable for the rapid initiation of PHP, but may contribute to the capacity of a motoneuron to fully express PHP, perhaps by participating in the steady state integrity of the IMD signaling cascade, or influencing the capacity of a motoneuron to respond to a perturbation.

Imd, IKKβ, and Relish are necessary for the sustained expression of PHP.

PHP can also be induced by genetic deletion of the *GluRIIA* subunit of the postsynaptic glutamate receptors (Petersen et al., 1997). Since this perturbation is present throughout the four days of larval life, PHP in the *GluRIIA* mutation has been considered

to reflect the long-term, sustained expression of PHP (Frank et al., 2009). We generated double mutant combinations of the *GluRIIA* mutation with the *Imd, IKK*β, *Tak1* and *Rel* mutations. Each double mutant combination was compared to the baseline functionality of the single *Imd, IKK*β, *Tak1* and *Rel* mutations alone, thereby accounting for the slight differences in baseline release in each individual mutant background. As shown previously, the *GluRIIA* mutation causes a decrease in mEPSP amplitude and a homeostatic increase in quantal content that returns EPSP amplitudes toward wild type levels, diagnostic of PHP (Figure 8A, B, C). When we examine the *GluRIIA, Imd*^{NP} double mutant, we find a complete block of PHP (Figure 8A, E, F, G). The mEPSP amplitudes are significantly decreased, but there is no homeostatic increase in quantal content. We then demonstrate that PHP is blocked in both the *GluRIIA; IKK*β and the *GluRIIA; Rel*^{E20} double mutants, arguing that this IMD signaling system is necessary for the long-term maintenance of PHP (Figure 8A, E, F, G). However, when we examine the *Tak1*^{2}*; GluRIIA* double mutants, we find that PHP is completely normal (Figure 8A, B, C; Figure 16A-D). This was true for both alleles of *Tak1* when placed in the *GluRIIA* mutant background. Thus, Tak1 appears to be selectively required for the rapid induction of PHP.

To this point, our data argue for a bifurcation in the IMD signaling cascade during PHP. The PGRP-LC receptor is necessary for both the rapid and long-term expression of PHP. Downstream of PGRP-LC, IKKβ and Tak1 are necessary for the rapid induction process, but Tak1 is dispensable for the long-term maintenance process. Conversely, Imd and Rel are selectively required for the long-term maintenance of PHP, consistent with the prior demonstration that the rapid induction of PHP is independent of

transcription and translation (Frank et al., 2006). Only IKKβ is necessary for both the rapid and long-term form of PHP, suggesting that it represents a point of signaling bifurcation (see discussion).

Normal synapse morphology.

One formal possibility is that differences in synapse growth could account for the genotype-specific effects on homeostatic plasticity. We assessed synaptic growth by quantifying synaptic bouton number and the number of presynaptic active zones. Active zones were identified by immunostaining with anti-Bruchpilot, which labels the presynaptic T-bar that resides at the active zone center and is coincident with presynaptic calcium channels (Marie et al., 2004; Kittel et al., 2006). We find that the *Tak1*^{2} mutation has a moderate reduction in bouton number and a corresponding increase in active zone density, compared to wild type (Figure 17A-D). Conversely, the *Tak1*^{179} mutants have a small, but significant increase in bouton number. We also observe a small, but statistically significant reduction in active zone density in *Imd* as well as an increase in both active zone number and density in *IKKβ*. However, across all of these mutations, these effects are small and could reasonably reflect differences in genetic backgrounds. Ultimately, there is no consistent change in bouton number or active zone number that could account for altered synaptic transmission or PHP, considering both the short and long-term expression of PHP.

Tak1 is required presynaptically for the rapid induction of PHP.

Tak1 and IKKβ represent a branch of the IMD signaling cascade that is necessary for the rapid induction of PHP. As such, these proteins could define the first known functional interface of presynaptic innate immune signaling and the mechanisms of neurotransmitter release. Therefore, we chose to define how Tak1 mediates this interface by examining the role of Tak1 during baseline release and PHP in greater detail. First, we attained genetic evidence linking *Tak1* to the function of PGRP-LC during PHP. A heterozygous deficiency that uncovers the *Tak1* locus has no effect on the rapid induction of PHP (Figure 9A-E). As shown previously (Harris et al., 2015), a heterozygous mutation in PGRP-LC is also without effect (Figure 9A-E). However, when these two heterozygous mutations are placed in trans to each other, PHP is completely blocked. Taken together with biochemical and genetic evidence in both flies and mammals (Gottar et al., 2002; Sato et al., 2005; Shim et al., 2005), these data are consistent with Tak1 acting downstream of PGRP-LC during PHP (Figure 9A-E).

The over-expression of Tak1 is cell lethal, consistent with a role in apoptosis (Takatsu et al., 2000), obviating genetic rescue experiments based on GAL4/UAS-dependent transgene overexpression. Therefore, we assessed the tissue specificity of Tak1 during PHP by generating a kinase dead transgene and expressing this protein pre- versus postsynaptically. We generated an epitope tagged, kinase dead transgene (*UAS-Tak1-K46R-FLAG*; referred to as *Tak1-DN*) based on a previously published kinase dead transgene (Takatsu et al., 2000). When this transgene is expressed presynaptically, PHP is strongly suppressed (Figure 9F-I; $p<0.005$). Next, we demonstrate that muscle-specific over-expression of *UAS-Tak1-DN* does not impair PHP, compared to wild type (Figure 9F-I). Finally, we demonstrate that the Tak1-DN

protein traffics to the presynaptic terminal, based on immunolabeling for the FLAG epitope tag (Figure 18A). From these data, combined with evidence of a strong genetic interaction with the PGRP-LC receptor and the previously published evidence that PGRP-LC is present at the presynaptic terminal (Harris et al., 2015), we conclude that Tak1 is an essential presynaptic kinase that is required for the rapid induction of PHP.

Tak1 is not required for normal synaptic anatomy

To further characterize the effects of Tak1 on synapse organization, we pursued immunostaining of key synaptic proteins. We quantified the staining intensities of the presynaptic proteins Synaptotagmin 1 (Syt1), Cysteine String Protein (CSP), and Complexin (Cpx). The abundance and distribution of all three proteins were similar comparing wild type to *Tak1* (Figure 18B, E, F, G). We also examined immunolabeling for the microtubule associated protein Futsch (Map1b-like) and observe qualitatively normal organization and appearance of the presynaptic microtubule cytoskeleton (data not shown). Finally, we quantified the abundance of the post-synaptic glutamate receptor subunits GluRIIA and GluRIIC by immunolabeling. Glutamate receptor staining in $Tak1^{179}$ was quantitatively normal. We observe a trend towards a reduction in GluRIIA staining in the $Tak1^{2}$ mutation compared to WT, (Figure 18B-D), an effect that is consistent with the modest decrease in mEPSP amplitude observed in this allele (Figure 7E). However, since PHP is blocked in both alleles of *Tak1* as well as when *UAS-Tak1DN* is overexpressed presynaptically, altered GluRIIA levels cannot account for impaired PHP. Furthermore, the long-term maintenance of PHP, induced by complete loss of GluRIIA, is fully intact in *Tak1* mutants.

Loss of Tak1 strongly impairs evoked and spontaneous neurotransmitter release. To further investigate the role of Tak1 during baseline transmission and PHP, we measured release and PHP across a range of extracellular calcium concentrations using the two-electrode voltage clamp to quantify synaptic currents. At 1.5mM external calcium ($[Ca^{2+}]_e$), there is a strong defect in baseline EPSC amplitude in *Tak1* mutants compared to wild type (Figure 10A, C, E). Indeed, baseline EPSC amplitude in the *Tak1*^{2} mutant is decreased by more than ~70% compared to wild type (Figure 10A, C, E). We observe a ~30% decrease in mEPSP amplitude that accounts for a fraction of the observed defect in average evoked release. The change in mEPSP amplitude at elevated $[Ca^{2+}]_e$ (compare to Figure 7) could reflect small differences in postsynaptic receptor subunit composition that were not resolved in our immunostaining assays (Figure 18). However, the defect in presynaptic release is pronounced. It was observed in both *Tak1* alleles and it is consistent across a nearly 10-fold range of extracellular calcium (0.4 to 3mM $[Ca^{2+}]_e$) (Figure 10E). This remarkable defect in baseline presynaptic release could reflect a major decrease in either action potential-induced presynaptic calcium influx or the calcium sensitivity of presynaptic release. Finally, we also confirm that PHP remains completely blocked at elevated (1.5mM) extracellular calcium (Figure 10A-D). Thus, Tak1 is an essential component necessary for baseline synaptic transmission and the rapid induction of PHP, both novel activities for the Tak1 protein.

During our experiments, we noted that the rate of spontaneous miniature release is dramatically reduced in the *Tak1* mutants compared to wild type (Figure 10F). This

effect is observed in both *Tak1* alleles. Spontaneous event frequency was reduced by ~90% in $Tak1^{2}$ and ~50% in $Tak1^{179}$ (Figures 10F, G). This effect was also observed when the kinase dead *Tak1* transgene is expressed presynaptically in a wild type background, confirming that this effect is due to impaired Tak1 function within the presynaptic motoneuron. The magnitude of this effect is similar to that observed in mutations that directly affect the vesicle fusion machinery, including *munc18* loss of function mutations and *complexin* overexpression (Wu et al., 1999; Weimer et al., 2003; Jorquera et al., 2012) highlighting a potentially profound action of presynaptic Tak1 on the vesicle release mechanism. The rate of spontaneous release at the *Drosophila* NMJ is largely independent of extracellular calcium (Davis and Goodman, 1998), emphasizing that Tak1 has a novel and dramatic presynaptic activity that directly affects both spontaneous and action potential evoked synaptic vesicle fusion.

Given the effects of Tak1 on spontaneous synaptic vesicle fusion rates, we took care to rule out the possibility that a change in spontaneous fusion rate is the cause of impaired PHP expression. If spontaneous synaptic vesicle fusion events are the physiological events that are monitored by the putative homeostatic sensor (Frank et al., 2006), then a large decrease in mEPSP frequency could prolong the time course of PHP induction. PHP is normally induced with a 10-minute PhTx incubation (Frank et al., 2006; Wang et al., 2014; see methods). We doubled the incubation time for the $Tak1^{2}$ allele and PHP remained blocked (see Methods). To further address this issue, we assessed the rate of spontaneous release in the other IMD signaling cascade mutations (Figure 10F, G). No significant difference was observed in the *IKKβ, Imd* or *Rel* mutants. From these data, it appears that Tak1 has a novel, constitutive, presynaptic function

that is necessary for normal spontaneous vesicle fusion and normal evoked neurotransmitter release. In addition, we show that Tak1 is essential for PHP. We hypothesize that these novel functions of Tak1 are mechanistically related.

Decreased release probability and normal calcium influx in *Tak1* mutants

To further characterize the properties of presynaptic vesicle release at the *Tak1* mutant synapse, we examined synaptic modulation during short trains of action potentials (APs) delivered at a frequency of 50 Hz. Strikingly, while the wild type synapse shows characteristic synaptic depression, all the *Tak1* mutant animals similarly displayed profound short-term facilitation (Figure 11A, B). We also performed this experiment in animals expressing dominant negative Tak1 selectively in motoneurons. Again, we observe a significant baseline defect in neurotransmitter release accompanied by strong facilitation (Figure 11A, B).

A decrease in evoked release coupled to enhanced facilitation is indicative of a decreased release probability, which could result from reduced presynaptic calcium entry. To address this possibility, we imaged spatially averaged calcium transients within individual synaptic boutons using the fluorescent calcium indicator dye Oregon Green BAPTA-1 (OGB-1). We delivered single action potentials (AP) and trains of 4 APs at 50 Hz at 1.5 mM $[Ca^{2+}]_e$. Surprisingly, we find no difference in the amplitude of calcium transients ($\Delta F/F$) in either stimulation protocol, comparing WT and *Tak1*^{179} (Figure 11C-G). Quantification of dye loading and the time constant of calcium transient decay were unchanged in *Tak1*^{179} compared to wild type (Figure 11H, I). We previously resolved a decrease in presynaptic calcium influx that was responsible for a ~30%

decrease in presynaptic release, using identical calcium imaging methodology (Gaviño et al., 2015). The *Tak1*^{179} mutation decreases release by nearly 50% and, yet, we cannot resolve a change in calcium influx. From these data, we conclude that the effects of Tak1 on presynaptic release are independent of calcium influx.

Loss of Tak1 does not influence baseline RRP.

We next asked whether Tak1 influences the readily releasable synaptic vesicle pool (RRP) under baseline conditions and following the induction of PHP. We measured the size of the RRP in response to brief trains of high frequency stimulation as previously described (Schneggenburger et al., 1999, Müller et al., 2012; Harris et al., 2015). Again, we observed pronounced facilitation in the early phase of the stimulus train in *Tak1*, compared to synaptic depression in wild type animals (Figure 12A). As a consequence of the facilitation observed in *Tak1*, and despite having a smaller initial EPSC compared to wild type, the cumulative EPSC amplitude and RRP in *Tak1* are not significantly different compared to wild type. If we compare initial EPSC amplitude to the size of the RRP in *Tak1* mutants and wild type animals, an estimate of presynaptic release probability can be obtained (P_{train}). There is a dramatic decrease in P_{train} in *Tak1* compared to wild type (Figure 12C). From these data, we conclude that Tak1 does not influence the total number of vesicles that are available for release (RRP). Rather, Tak1 appears to have a major effect on the fraction of vesicles that can be released in response to calcium influx that occurs following a single action potential.

Loss of Tak1 prevents the homeostatic modulation of the RRP

The expression of PHP has been linked to a near doubling of the RRP and mutations that prevent the expansion of the RRP have been shown to block PHP, including mutations that delete the PGRP-LC innate immune receptor (Müller et al., 2012; Harris et al., 2015). Therefore, we repeated our measurements of cumulative EPSC and RRP in the presence of PhTx to induce PHP. In wild type, as shown previously (Müller et al., 2012; Harris et al., 2015), the cumulative EPSC amplitude is restored to near wild type levels in the presence of PhTx due to a significant expansion of the RRP (Figure 12A, B). However, in the *Tak1*^{179} mutant, the homeostatic expansion of the RRP is completely blocked, an observation that mirrors the effects of the PGRP-LC receptor mutation (Harris et al., 2015). In the *Tak1*^{2} mutant we do observe a very small, but significant increase in the size of the RRP. This could reflect a small rescue of the RRP by high calcium concentration and substantial calcium influx during repetitive stimulation. Clearly, these rescued vesicles are not available on the first EPSC and therefore cannot contribute to PHP of this parameter (Figure 10). From these data, we conclude that Tak1 is essential for the homeostatic expansion of the RRP in PHP.

Tak1 stabilizes the pool of high release probability synaptic vesicles.

Loss of *Tak1* impairs the rate of spontaneous miniature release, impairs evoked release in response to a single action potential, enhances short-term facilitation, diminishes P_{train}, and blocks PHP. Yet, Tak1 has no effect on action-potential evoked calcium influx, nor the size of baseline RRP. One possibility, consistent with all of these separate observations, is that Tak1 controls the existence or stability of a pool of primed, high-release probability synaptic vesicles. By studying the recovery of synaptic vesicle

release after strong stimulus-dependent depletion of the synaptic vesicle pool, we are able to assay the replenishment of high versus low-release probability vesicle pools. By doing so, we have gained further insight into how Tak1 influences the behavior of discrete synaptic vesicle pools.

We investigated recovery from strong synaptic depression at elevated extracellular calcium (3mM), consistent with previously published methods (Müller et al., 2015). The recovery from synaptic depression occurs with two time constants at the *Drosophila* NMJ, just as it does at mammalian central synapses (Müller et al, 2015; Sakaba & Neher, 2001). An initial phase of fast recovery is associated with the replenishment of a low-release probability vesicle pool that is thought to reside at a distance from sites of presynaptic calcium influx. A second, slower phase of recovery is associated with the replenishment of a high release probability vesicle pool, tightly coupled to sites of calcium entry (Müller et al., 2015; Sakaba & Neher, 2001). We delivered high frequency stimulus trains to deplete the RRP (30 APs at 60 Hz). We then delivered paired-pulse stimuli at varying intervals following cessation of the stimulus train, allowing us to quantify the rate of EPSC recovery (Figures 13A, B). First, we plot the rate of recovery as a percent of the initial EPSC amplitude (specific to each genotype since *Tak1* reduces initial EPSC amplitudes). As expected, we observe two time constants of recovery in wild type, a fast time constant (tau_{fast} = 53ms) and a slow time constant (tau_{slow} = 6.25s). These values are quantitatively similar to previous measurements made in this system (Hallermann et al., 2010, Müller et al., 2015). By contrast, recovery in the *Tak1* mutants is highly unusual, becoming tri-phasic and preventing estimation of recovery time constants. The initial phase of EPSC recovery in

the *Tak1* mutants is significantly enhanced compared to wild type (Figure 13B). Indeed, EPSC amplitude is fully recovered within the first 200ms, a time point when wild type remains 40% depressed. However, the initial recovery of EPSC amplitude is not sustained in *Tak1*. The EPSC amplitude subsequently decays between 200ms and 5s, before finally entering a new, slow phase of recovery to a steady state that is significantly smaller than that observed in wild type. This unusual recovery profile has never been previously observed at a synapse, to our knowledge.

Next, we assessed EPSC recovery with paired-pulse stimulation, quantifying the paired-pulse ratio (EPSC2/EPSC1) at each time point in the recovery phase. In wild type, PPR is unchanged throughout the recovery phase, always resembling the pre-stimulus PPR, showing synaptic depression. By contrast, PPR in *Tak1* changes dramatically. Prior to the stimulus train, *Tak1* shows pronounced facilitation. Immediately following the stimulus train, at the 50-200ms time point, the time at which EPSC amplitudes have fully recovered to baseline levels, we find that PPR converts from facilitation to depression, resembling wild type (Figure 13C). Then, during the 200ms-5s post-train interval, initial EPSC amplitude decays and PPR reverts to strong facilitation (exceeding that observed at baseline). Finally, in the last phase of recovery (20s-90s), PPR reverts to levels of facilitation observed prior to the stimulus train. Thus, during an initial recovery phase, *Tak1* mutants revert to 'wild type' release in terms of release probability. However, this 'wild type' state cannot be sustained in *Tak1*, and it rapidly decays (between 200ms and 5s after cessation of the stimulus train).

Finally, we re-analyzed the EPSC recovery kinetics without normalization to the initial EPSC amplitude. In this analysis, EPSC amplitudes prior to the stimulus train are

significantly smaller in *Tak1* compared wild type. During the stimulus train, EPSC amplitudes depress to a similar amplitude in *Tak1* compared wild type. During the first 200ms of recovery, the EPSC in $Tak1^{179}$ becomes identical to that observed in wild type (Figure 13D), while the EPSC in $Tak1^{2}$ is strongly rescued, but remains depressed relative to wild type (Figure 13F). But, the *Tak1* mutants cannot sustain this rescued level of release, and EPSC amplitudes decay over the next 5s. To further characterize this effect, we subtracted the *Tak1* recovery curves from the wild type recovery curve, yielding a subtracted curve that represents the fraction of recovery that is dependent upon Tak1 (Figure 13D-G). The subtracted curves (blue line in E and purple line in G) make it clear that *Tak1* mutants recover normally during the first 200 ms. Then, the recovery fails and *Tak1* not only falls below the wild type curve, it never fully reaches wild type levels.

One interpretation of these data, taking into account all of our observations, is that the initial phase of recovery (50-200ms) is largely independent of Tak1 function. As such, wild type and *Tak1* begin to recover from the same depressed EPSC amplitude, recover with initially identical kinetics, and PPR is identical during this time interval. The activity of the Tak1 kinase is revealed only after the first 200ms of recovery. During this time interval, Tak1 appears to be necessary to stabilize the newly recovered, high release probability vesicle pool. Therefore, in the absence of Tak1, the rate of de-priming (or undocking) exceeds the rate of vesicle replenishment causing a decay in EPSC amplitude and transition from depression to paired-pulse facilitation. Ultimately, after a prolonged period of rest, a new steady state is reached in the *Tak1* mutant, one in which there is a reduction in the number of primed/docked vesicles that can be

released in response to a single action potential. The conversion of short-term dynamics to facilitation can be understood if the stabilizing effects of Tak1 differentially act upon the high-release probability vesicles in close proximity to calcium channels. If this is the case, then steady state release in *Tak1* would be prone to paired-pulse facilitation. This model can also account for the decrease in mEPSP rate observed in *Tak1*, if a population of vesicles is no longer docked and primed at the presynaptic release site. Recent evidence has linked the expression of PHP to the stabilization of the RRP via RIM Binding Protein (Müller et al., 2015). We propose that loss of Tak1 mediates this effect, again linking the stability of high release probability vesicle pool to the expression of presynaptic homeostatic potentiation. Importantly, Tak1 is a kinase, acting downstream of innate immune receptor activation, providing a novel signaling system that links receptor activation at the plasma membrane to the control of synaptic vesicle pools at the presynaptic active zone.

To address our priming and de-priming hypothesis from another angle we performed an additional experiment using phorbol esters. Phorbol esters are diacyl glycerol analogs that stimulate priming of synaptic vesicles by potentiating the activity of PKC>Munc18 and/or Munc13 (Lou et al., 2008). We hypothesized that if de-priming is in fact enhanced by the loss of Tak1, phorbol esters would potentiate release to a greater extent in *Tak1* mutants, relative to wild type. We used a high extracellular calcium concentration (3 mM) at which priming and release probability are saturated or nearly saturated in wild type, but release in *Tak1* mutants remains deficient. Indeed, when we applied phorbol ester (1 μM) to wild type synapses there was no effect on EPSC amplitudes or the rate of synaptic depression (Figure 19A,B,D). However, upon phorbol

ester application in *Tak1* mutants, EPSC amplitudes and synaptic depression were partially rescued. Additionally, mEPSP frequency was unchanged by phorbol ester application in wild type, but was increased in *Tak1* mutants (Figure 19C). These data further suggest that Tak1 is required for normal vesicle priming, and potentiation of priming can ameliorate the priming deficit in *Tak1* mutants.

Ultrastructural evidence that Tak1 stabilizes the active-zone associated synaptic vesicles

If Tak1 is necessary to stabilize synaptic vesicles at the active zone, then it should be possible to observe changes in the distribution of synaptic vesicles at the active zone in a *Tak1* mutant compared to wild type. More specifically, our model suggests that, at steady state, loss of Tak1 will result in fewer vesicles in close proximity to the calcium channels (contained within the T-bar). For each active zone, we quantified synaptic vesicles that reside within 150nm and 400nm of the center of the pedestal of the T-bar, where presynaptic voltage gated calcium channels reside (Kittel et al., 2006). We also measured the distance from each vesicle to its nearest neighboring vesicle (see Methods for details of sample acquisition and analysis). There is a striking, highly significant decrease in the density of synaptic vesicles near the T-bar (Figure 14B-D), whether this measurement is made within 150nm or 400nm of the T-bar. A similar change is also observed in the inter-vesicle distance (Figure 14E). The decrease in synaptic vesicle packing density could reasonably be a reflection of what we observe electrophysiologically, a failure to functionally stabilize a population of high release probability vesicles.

To further characterize synaptic vesicle stabilization and positioning, we made use of the slow calcium buffer EGTA. EGTA buffers calcium concentration at a distance from calcium channels, thereby limiting the size of the calcium microdomain during stimulation. We can use this approach to estimate the amount of EGTA-sensitive versus EGTA-insensitive vesicles and their positioning relative to the active zone. When we applied EGTA-AM (50 μM) to wild type synapses, release was moderately reduced (Figure 20A, B). This suggests that in wild type, a subset of vesicles available for release in response to a single stimulus are EGTA-sensitve and likely relatively far from the site of calcium influx. EGTA is also expected to buffer the increase in the calcium microdomain during high frequency stimulation, limiting the normal recruitment of additional, more distant vesicles, lower release probability vesicles resulting in increased synaptic depression. Indeed, we observe a modest increase in synaptic depression in wild type (Figure 20A, C). In *Tak1* mutants we find a substantial reduction in release at baseline, as before (Figure 20A, B). When we apply EGTA-AM, release is unchanged. This demonstrates that there is a large deficit in the high release probability vesicles that comprise release on the first EPSC, although there are enough remaining to support a small amount of release. All the other vesicles at the synapse cannot be released on the first stimulus, and are therefore not affected by EGTA. More importantly, we find that EGTA causes a striking reduction in the facilitation observed at baseline in *Tak1* mutants, reflecting a high calcium dependence of the farther away vesicles that apparently comprise the majority of the RRP of *Tak1* mutants (Figure 20A, C). We conclude that the pool of docked, primed, very high release probability vesicles in *Tak1* mutants is drastically reduced relative to wild type, and that the majority of

vesicles released during a stimulus train are very low release probability or unreleasable until positionally recruited and/or primed by high frequency stimulation and an expanded calcium microdomain. Addition and/or stabilization of these high Pr vesicles during PHP requires the function of Tak1 – hence the observed block of PHP in *Tak1* mutants.

DISCUSSION

We have tested the core signaling components of an innate immune signaling pathway (IMD signaling) for a role during presynaptic homeostatic potentiation. Our data support a model in which IMD signaling bifurcates downstream of the presynaptic innate immune receptor PGRP-LC to achieve immediate, local modulation of the presynaptic release apparatus via Tak1 and prolonged maintenance of the homeostatic response via the transcription factor Relish (Figure 14F). This model allows the innate immune signaling system to rapidly alter presynaptic release (seconds to minutes) and simultaneously initiate a Rel-dependent consolidation of PHP. PHP consolidation can persist for months in insects (Mahoney et al., 2014) and decades in humans (Cull-Candy et al., 1980). It has become clear that the molecular mechanisms responsible for the rapid induction and sustained expression are genetically separable (Davis, 2013; Frank et al., 2009; Marie et al., 2010; Brusich et al., 2015*;* Penney et al., 2012). For example, mutations exist that selectively block the long-term maintenance of PHP without altering the rapid induction (Marie et al., 2010; Brusich et al., 2015*;* Penney et al., 2012). Our findings provide an explanation for how the rapid induction and sustained expression of PHP are mechanistically coordinated.

The canonical function of innate immunity is to recognize invading pathogens or non-normal molecular patterns and induce a rapid, inflammatory reaction that is

sustained for as long as the invasion persists. During an innate immune response, Tak1-dependent signaling turns on more rapidly, and turns off more rapidly, than Rel-mediated transcription (Boutros et al., 2002; Park et al., 2004). As such, Tak1 signaling can be considered as a feed-forward activator of the cellular immune response. Based on our data, we propose that innate immune signaling in the nervous system is transfigured to detect non-normal neurophysiology, although the molecular event that reports altered neural (synaptic) function and is subsequently detected by presynaptic PGRP-LC remains a mystery. In our study, we place Tak1 at the presynaptic release site where homeostatic plasticity is rapidly induced. Thus, just as in canonical innate immunity, Tak1 is ideally situated to act as a feed-forward potentiometer that controls vesicle fusion, thereby achieving a rapid compensatory change in presynaptic release following postsynaptic glutamate receptor inhibition. Subsequent activation of Rel-mediated transcription provides a sustained response that can be maintained for the duration of the perturbation. This model illustrates how Tak1 mediates an interface of intracellular IMD signaling and vesicle release.

Tak1 stabilizes a high release probability vesicle pool during baseline release and PHP

We provide evidence that Tak1 has a potent, constitutive function to stabilize a high release probability synaptic vesicle pool. *Tak1* mutants have decreased baseline release, reduced mEPSP frequency, enhanced short-term facilitation, but no change in action potential induced presynaptic calcium influx. Our analysis of recovery from vesicle depletion pinpoints the time at which Tak1 activity becomes essential. The

recovery of synaptic transmission is completely normal in *Tak1* for the first 500ms following a stimulus train. It is only after this time point that recovery becomes defective. The defect is characterized by a decay in presynaptic release probability that is correlated with an ultrastructural defect in which vesicles reside at a greater distance from the presynaptic calcium channels, as reflected by the decrease in vesicle density. We propose that, under baseline conditions, Tak1 stabilizes vesicles that have been mobilized to the release site. One possibility is that Tak1 protein normally functions to inhibit the rate of de-priming or undocking, thereby persistently stabilizing the docked/primed vesicle pool. Immediately following a stimulus train, calcium-dependent mechanisms will actively mobilize vesicles to the active zone and drive calcium-dependent vesicle priming (Sakaba and Neher, 2001). During the 500ms window following a stimulus train, residual calcium could obscure or obviate the need for Tak1-dependent vesicle stabilization. Thus, Tak1 does not have a role in the immediate recovery of synaptic vesicles (within 500ms of a stimulus train). However, once residual calcium levels decay to baseline, Tak1 becomes essential in order to stabilizes vesicles at the release site.

Tak1 represents a mechanism that can couple innate immune signaling to the expression of PHP. Prior work has shown that the expression of PHP is achieved through the modulation of the high release probability pool of synaptic vesicles (Müller et al., 2015). More specifically, loss of Rim Binding Protein (RBP) destabilizes the high release probability vesicle pool and blocks the expression of PHP (Müller et al., 2015). The means by which RBP controls the high-P_r vesicle pool remains uncertain since RBP is a protein-scaffold. By contrast, Tak1 is a kinase, known to be activated

downstream of PGRP-LC, with substrates that could reasonably modulate synaptic vesicle stability or fusion (Levin et al., 2016).

Organization of innate immune signaling in *Drosophila* motoneurons

Most of our knowledge regarding the organization of innate immune signaling pathways in a cell are based on assays that detect the nuclear translocation of Rel/NFkB, or quantify Rel/NFkB -mediated transcription (Sato et al., 2005; Delaney et al., 2006; Rothwarf & Karin, 1999; Choe et al., 2002). Thus, the logic and spatial organization of innate immune signaling in neurons has yet to be clearly defined. Our data argue for several novel features of signaling organization, beyond the local synaptic action of Tak1. In canonical innate immune signaling receptor activation catalyzes the assembly of an intracellular complex that includes Imd, Tak1 and IKKβ. Current models suggest that signaling proceeds from Imd to Tak1 and IKKβ and is then relayed from IKKβ to activation of Rel, in concert with caspase-mediated cleavage of Rel. Here, we demonstrate that IKKβ is necessary for both rapid and sustained PHP, while the receptor associated scaffolding protein Imd is necessary only for long-term PHP. So, IKKβ represents a point of signaling bifurcation, presumably occurring at the presynaptic terminal. One possibility is that IKKβ is necessary for the assembly of the IMD signaling complex following PGRP-LC activation. As such, in the absence of IKKβ, a failure of complex assembly would prevent downstream signaling. By contrast, loss of either Imd or Tak1 can have pathway specific activities downstream of PGRP-LC (Figure 14F). We note, however, that other models for IKKβ activation should also be considered (Polley et al., 2013; Häcker & Karin, 2006). Finally, our data raise an important question

regarding how signaling is conveyed from synaptic IKKβ to nuclear Rel, a topic of future studies.

Future considerations in health and disease

We have defined a novel role for neuronal innate immune signaling; the lifelong homeostatic regulation of synaptic transmission. How might this impact our understanding of disease? On the one hand, loss of innate immune signaling could lead to a failure of homeostatic plasticity. There are numerous reviews postulating connections between failed homeostatic plasticity and the etiology of neurological and psychiatric disease (Ramocki and Zohgbi, 2008; Nelson and Valakh, 2015; Mullins et al., 2016). On the other hand, it is equally clear that aberrant or prolonged activation of innate immunity can be deleterious. In the nervous system, chronic neuroinflammation has been linked to a range of non-degenerative neurological disorders, including schizophrenia, autism, epilepsy, and neuropathic pain (Voineagu et al., 2011; Vargas et al., 2005; Vezzani & Granata, 2005; Samad et al., 2001). If our data can be generalized, it seems plausible that neuroinflammation could encompass maladaptive engagement of homeostatic plasticity. This raises a final question that is central to the function of innate immune signaling in the nervous system. If innate immune signaling is essential for non-inflammatory homeostatic plasticity and if it is also essential for a canonical neuroinflammatory response, what controls the switch between these modes of action? It could be determined by the cell-type specificity of the response, with neuroinflammation being primarily expressed in reactive glia and homeostatic activity functioning within other glial types (Stellwagen and Malenka, 2006) or within neurons

(this study). Alternatively, different receptors may be engaged to stimulate homeostatic versus neuroinflammatory responses. To date the ligands that stimulate PGRP-dependent homeostatic plasticity remain to be defined. Given the prevalence and potency of both homeostatic plasticity and the neuroinflammatory response, defining the intersection and governance of these processes may have important ramifications for how we understand the robustness and stability of neural function throughout life.

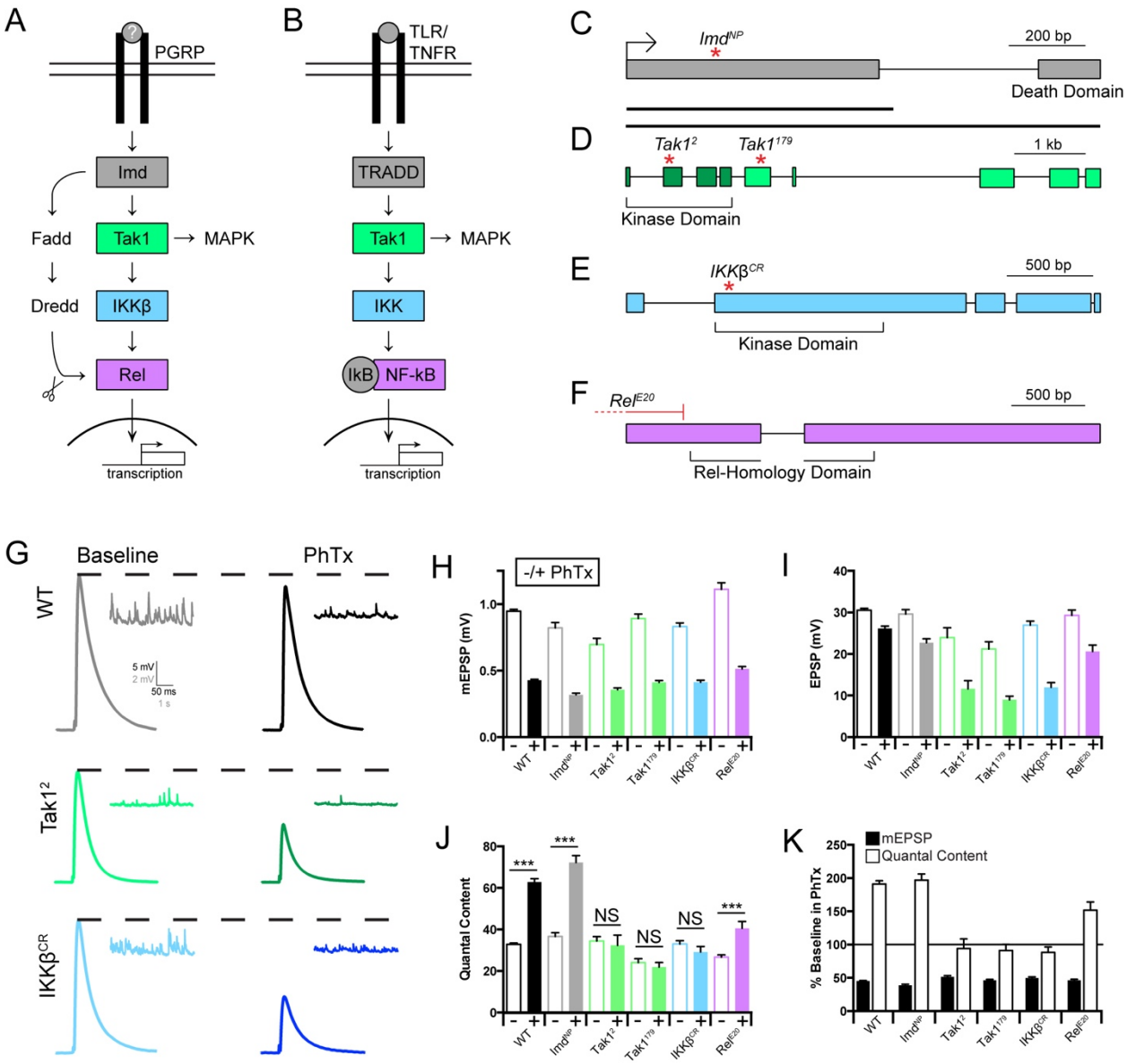

Figure 7: Innate immune signaling during the rapid induction of PHP.

(A) Diagram of the *Drosophila melanogaster* Immune Deficient (IMD) pathway and homologous mammalian innate immune signaling. (B-E) Diagrams of the gene loci for *Imd*, *Tak1*, *IKKβ*, and *Rel*, annotated with known signaling domains and with genetic reagents used in this study. (B) Imd^{NP} is a p-element insertion in a coding exon ($P\{GawB\}imd^{NP1182}$). (C) $Tak1^{2}$ is a nonsense mutation (E53>Stop) early in the kinase domain. $Tak1^{179}$ is a missense mutation (N384>T) in a conserved regulatory domain. (D) $IKK\beta^{CR}$ is a 1 bp deletion creating a frame shift and early stop codon (see Methods). (E) Rel^{E20} is a large excision that removes all transcription start sites of the gene. (F) Representative traces for EPSP (scale, 5 mV, 50 ms) and mEPSP (scale, 2 mV, 1 s) at baseline, and in the presence of philanthotoxin (PhTx) for the indicated genotypes. (G) Average mEPSP amplitude for each genotype in the absence (light bars) or presence (dark bars) of PhTx. (H) Average EPSP amplitude in the absence (light bars) or presence (dark bars) of PhTx. (I) Average quantal content in the absence (light bars) or presence (dark bars) of PhTx.

Quantal content is calculated as EPSP amplitude divided by mEPSP amplitude for each muscle recording. (J) mEPSP amplitudes (filled bars) and quantal content (open bars) for each genotype in the presence of PhTx, normalized to baseline values in the absence of PhTx. Data are presented as average (+/- SEM) and statistical significance determined by Student's t-test (unpaired, two-tailed).

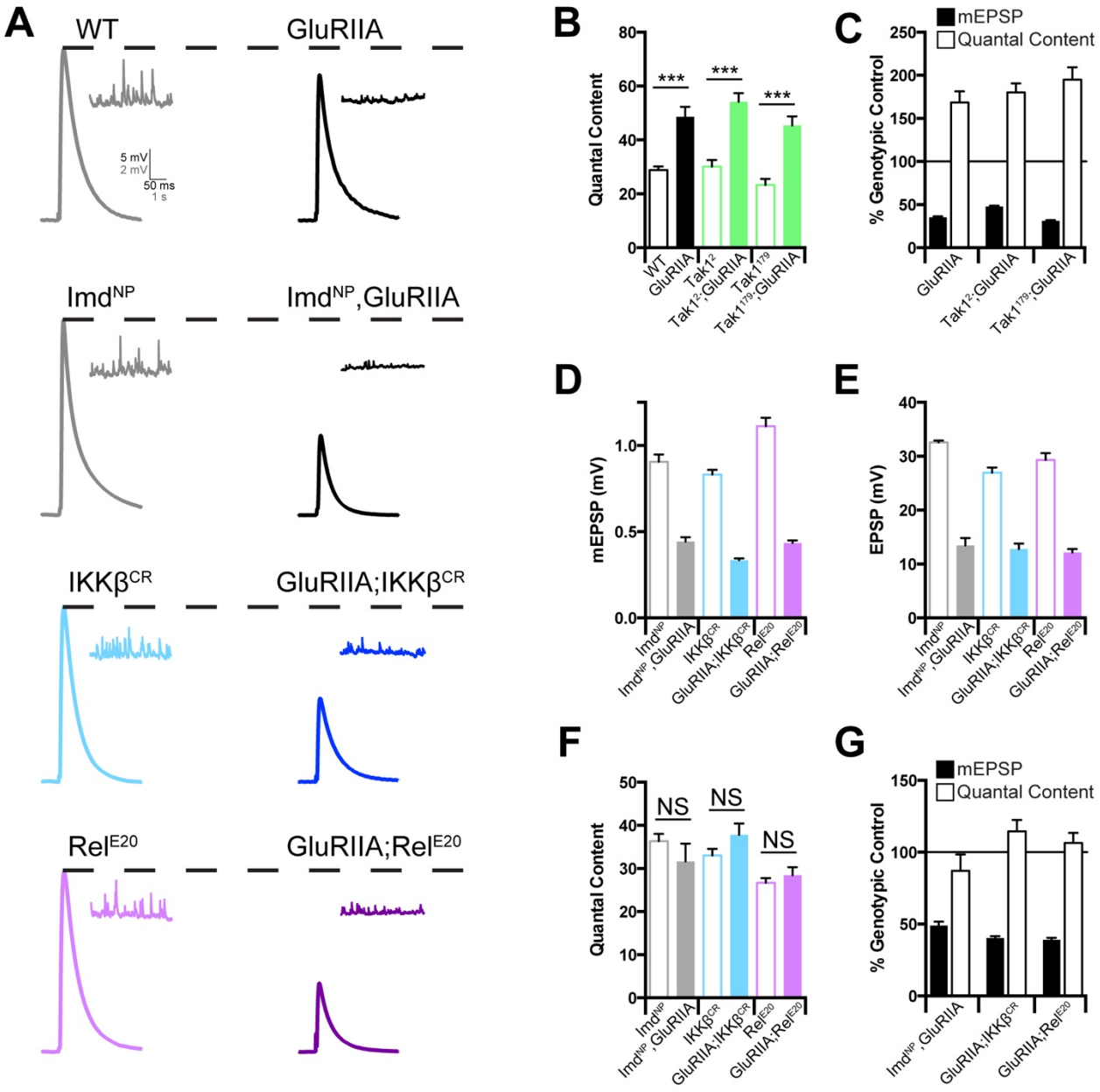

Figure 8: Innate immune signaling during the sustained expression of PHP.

(A) Representative traces for EPSP (scale, 5 mV, 50 ms) and mEPSP (scale, 2 mV, 1 s) at baseline, and in the background of the *GluRIIA*^{SP16} mutation, for the indicated genotypes. (B) Average quantal content for each genotype in the absence (light bars) or presence (dark bars) of the *GluRIIA* mutation. (C) mEPSP amplitudes (filled bars) and quantal content (open bars) for each genotype in the *GluRIIA* background, normalized to the control genotype in the absence of *GluRIIA*. (D) Average mEPSP amplitude for each genotype in the absence (light bars) or presence (dark bars) of the *GluRIIA* mutation. (E) Average EPSP amplitude for each genotype in the absence (light bars) or presence (dark bars) of the *GluRIIA* mutation. (F) Average quantal content in the absence (light bars) or presence (dark bars) of the *GluRIIA* mutation. (G) Average mEPSP and quantal content normalized to genotypic controls as in C. Data are presented as

average (+/- SEM) and statistical significance determined by Student's t-test (unpaired, two-tailed).

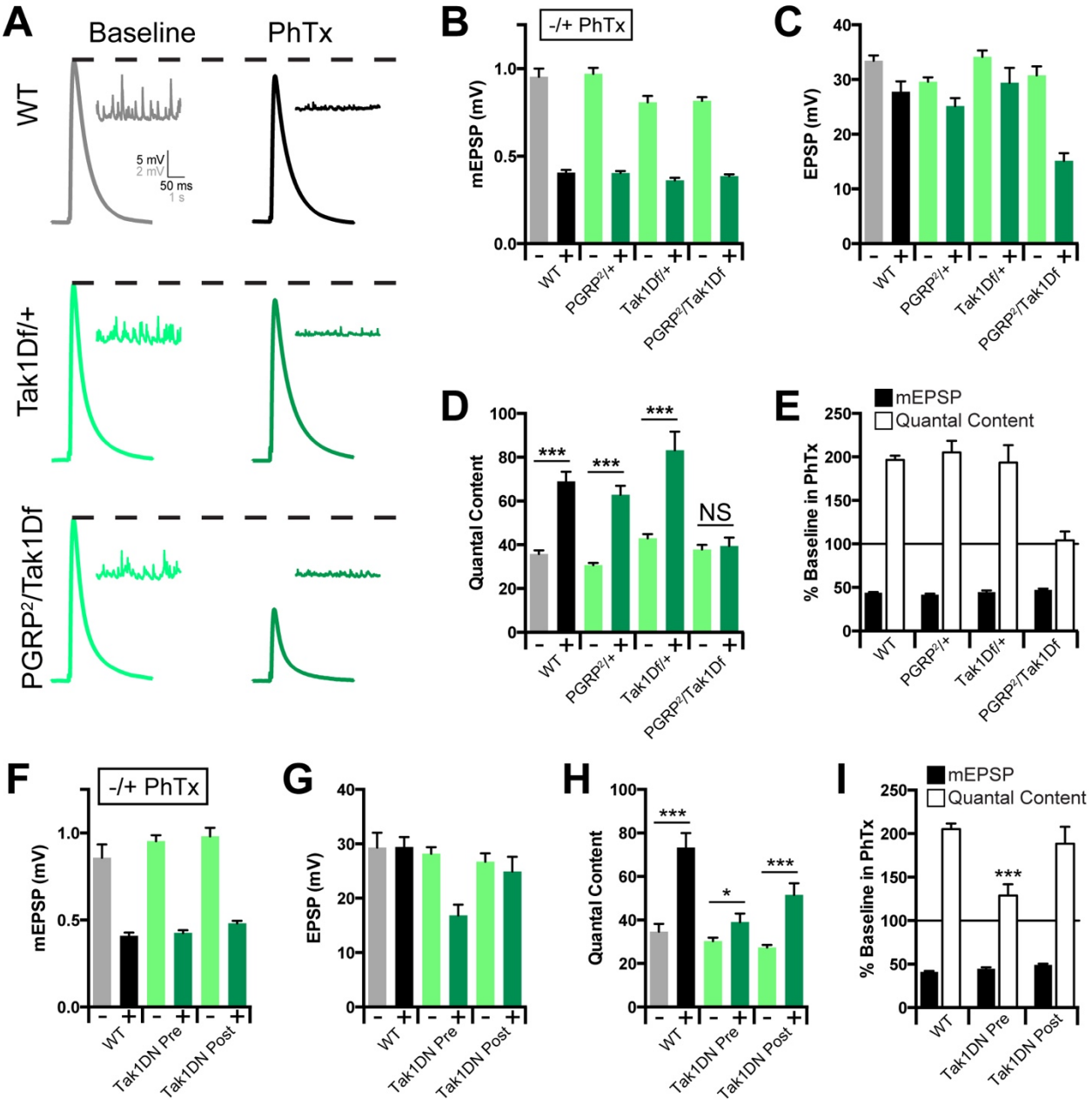

Figure 9: Tak1 Interacts genetically with PGRP-LC.

(A) Representative traces for EPSP (scale, 5 mV, 50 ms) and mEPSP (scale, 2 mV, 1 s) at baseline, and in the presence of PhTx, for the indicated genotypes. (B) Average mEPSP amplitude for each genotype in the absence (light bars) or presence (dark bars) of PhTx. (C) Average EPSP amplitude in the absence (light bars) or presence (dark bars) of PhTx. (D) Average quantal content in the absence (light bars) or presence (dark bars) of PhTx. (E) mEPSP amplitudes (filled bars) and quantal content (open bars) for each genotype in the presence of PhTx, normalized to baseline values in the absence of PhTx. (F) Average mEPSP amplitude for each genotype in the absence (light bars) or presence (dark bars) of PhTx. (G)

Average EPSP amplitude in the absence (light bars) or presence (dark bars) of PhTx. (H) Average quantal content in the absence (light bars) or presence (dark bars) of PhTx. (I) mEPSP amplitudes (filled bars) and quantal content (open bars) for each genotype in the presence of PhTx, normalized to baseline values in the absence of PhTx. Data are presented as average (+/- SEM) and statistical significance determined by Student's t-test (unpaired, two-tailed).

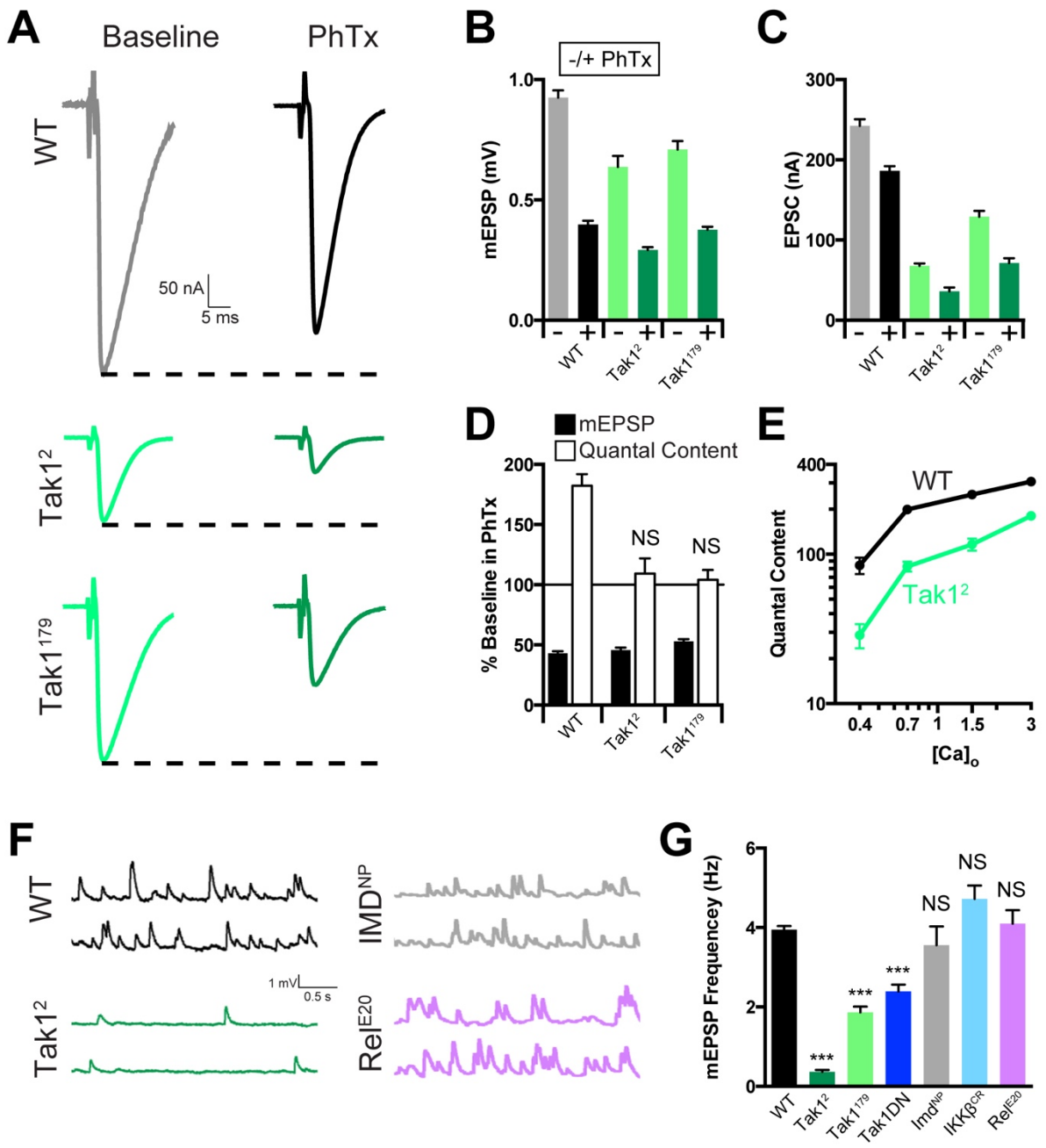

Figure 10: Tak1 is necessary for baseline vesicle fusion and PHP under physiological conditions.

(A) Representative traces for EPSC (scale, 50 nA, 5 ms) at baseline, and in the presence of PhTx, for the indicated genotypes. (B) Average mEPSP amplitude for each genotype in the absence (light bars) or presence (dark bars) of PhTx. (C) Average EPSC amplitude in the absence (light bars) or presence (dark bars) of PhTx. (D) mEPSP amplitudes (filled bars) and quantal content (open bars) for each genotype in the presence of PhTx, normalized to baseline values in the absence of PhTx. (E) Calcium cooperativity curves for the indicated genotypes. Neurotransmitter release was measured at 0.4, 0.7, 1.5, and 3 mM extracellular calcium concentration. Quantal content was calculated by dividing EPSC amplitudes by mEPSC

amplitudes. (F) Representative traces for mEPSP (scale, 1 mV, 0.5 s) for the indicated genotypes. (G) Average mEPSP frequency for the indicated genotypes. Data are presented as average (+/- SEM) and statistical significance determined by Student's t-test (unpaired, two-tailed) (C) or by one way ANOVA with Tukey's multiple comparisons test (G).

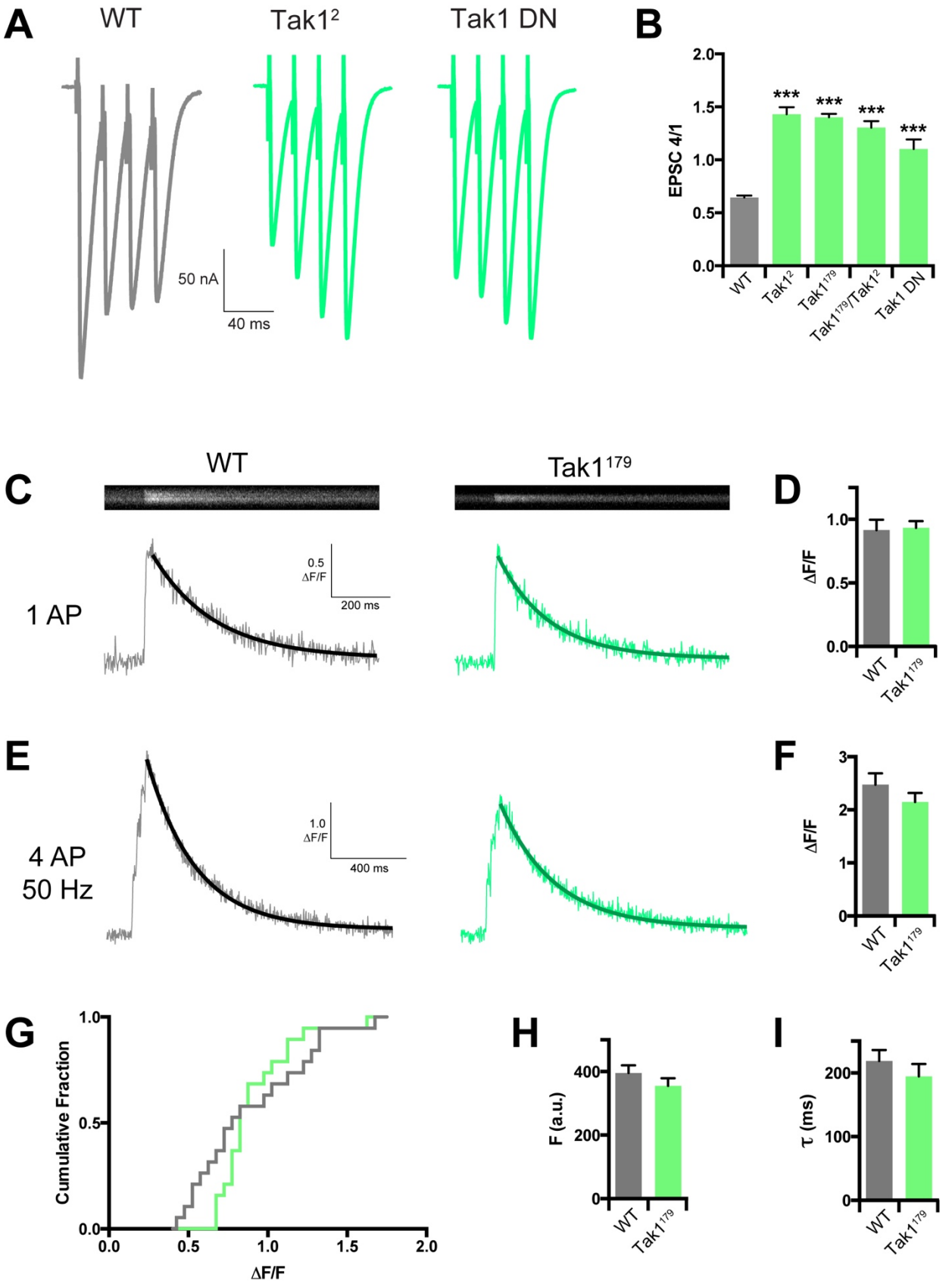
A
WT
Tak1²
Tak1 DN
50 nA
40 ms
B
EPSC 4/1
2.0
1.5
1.0
0.5
0.0
***
***
***
***
WT
Tak1²
Tak1¹⁷⁹
Tak1¹⁷⁹/Tak1²
Tak1 DN
C
WT
Tak1¹⁷⁹
1 AP
0.5
ΔF/F
200 ms
D
ΔF/F
1.0
0.5
0.0
WT
Tak1¹⁷⁹
E
4 AP
50 Hz
1.0
ΔF/F
400 ms
F
ΔF/F
3
2
1
0
WT
Tak1¹⁷⁹
G
Cumulative Fraction
1.0
0.5
0.0
0.0
0.5
1.0
1.5
2.0
ΔF/F
H
F (a.u.)
400
200
0
WT
Tak1¹⁷⁹
I
τ (ms)
200
100
0
WT
Tak1¹⁷⁹

Figure 11: Tak1 functions downstream of action-potential induced presynaptic calcium influx.

(A) Representative traces for EPSC trains (scale, 50 nA, 40 ms). Stimulation frequency was 50 Hz, and extracellular calcium concentration was 1.5 mM. *UAS-Tak1DN* was expressed presynaptically with *OK371-GAL4*. (B) Average ratio of EPSC #4 in the train divided by EPSC #1 for the indicated genotypes. (C) Representative line scans and calcium transients (scale, 0.5 ΔF/F, 200 ms) for WT (grey bar) and $Tak1^{179}$ (green bar). (D) Average ΔF/F for the indicated genotypes. (E) Representative calcium transients (scale, 1 ΔF/F, 400 ms) for the indicated genotypes. Stimulation was identical to that used in F. (F) Average ΔF/F for the indicated genotypes. (G) Cumulative frequency distributions of ΔF/F for WT (grey line) and $Tak1^{179}$ (green line). (H) Average baseline fluorescence as a measure of dye-loading for the indicated genotypes. (I) Average decay constants of the transients in H and I for the indicated genotypes. Data are presented as average (+/- SEM) and statistical significance determined by Student's t-test (unpaired, two-tailed) (D-I) or by one way ANOVA with Tukey's multiple comparisons test (B).

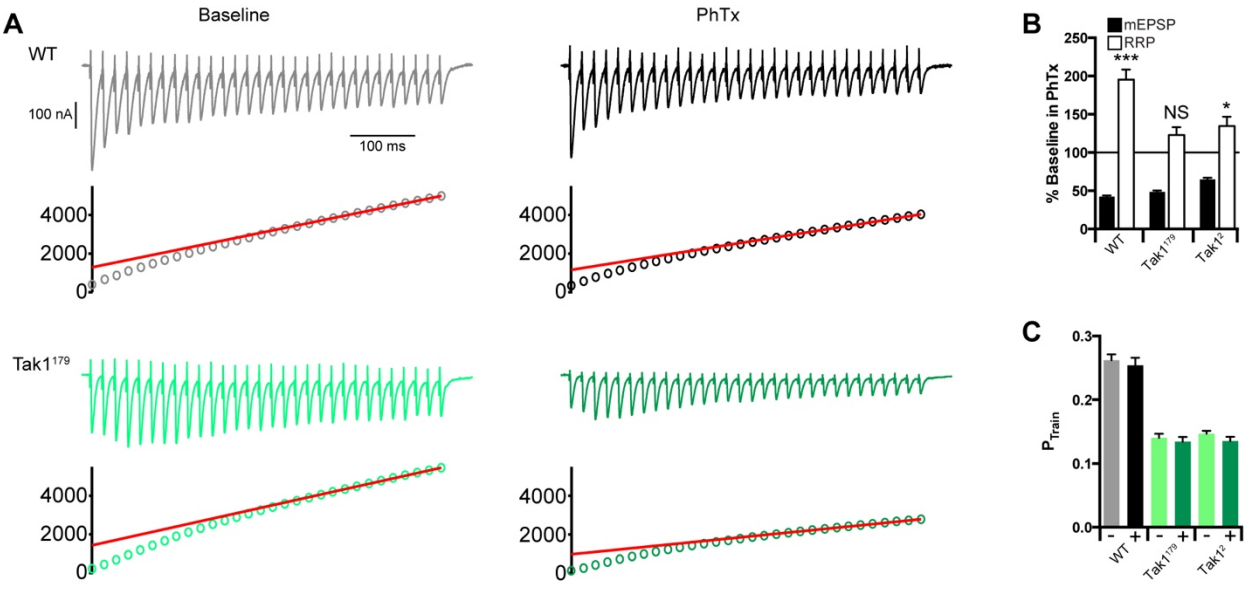

Figure 12: Tak1 is necessary for the homeostatic modulation of the RRP.

(A) Representative EPSC trains (scale, 100 nA, 100 ms) at baseline, and in the presence of PhTx, for the indicated genotypes. Trains are 30 stimuli delivered at 60 Hz. Extracellular calcium concentration is 3 mM. (B) mEPSP amplitudes (filled bars) and readily releasable pool size (open bars) in the presence of PhTx, normalized to baseline. (C) Average P_{Train} in the absence (light bars) or presence (dark bars) or PhTx, for the indicated genotypes. P_{Train} is calculated by dividing the cumulative EPSC by the amplitude of the first EPSC in the train. Data are presented as average (+/- SEM) and statistical significance determined by Student's t-test (unpaired, two-tailed).

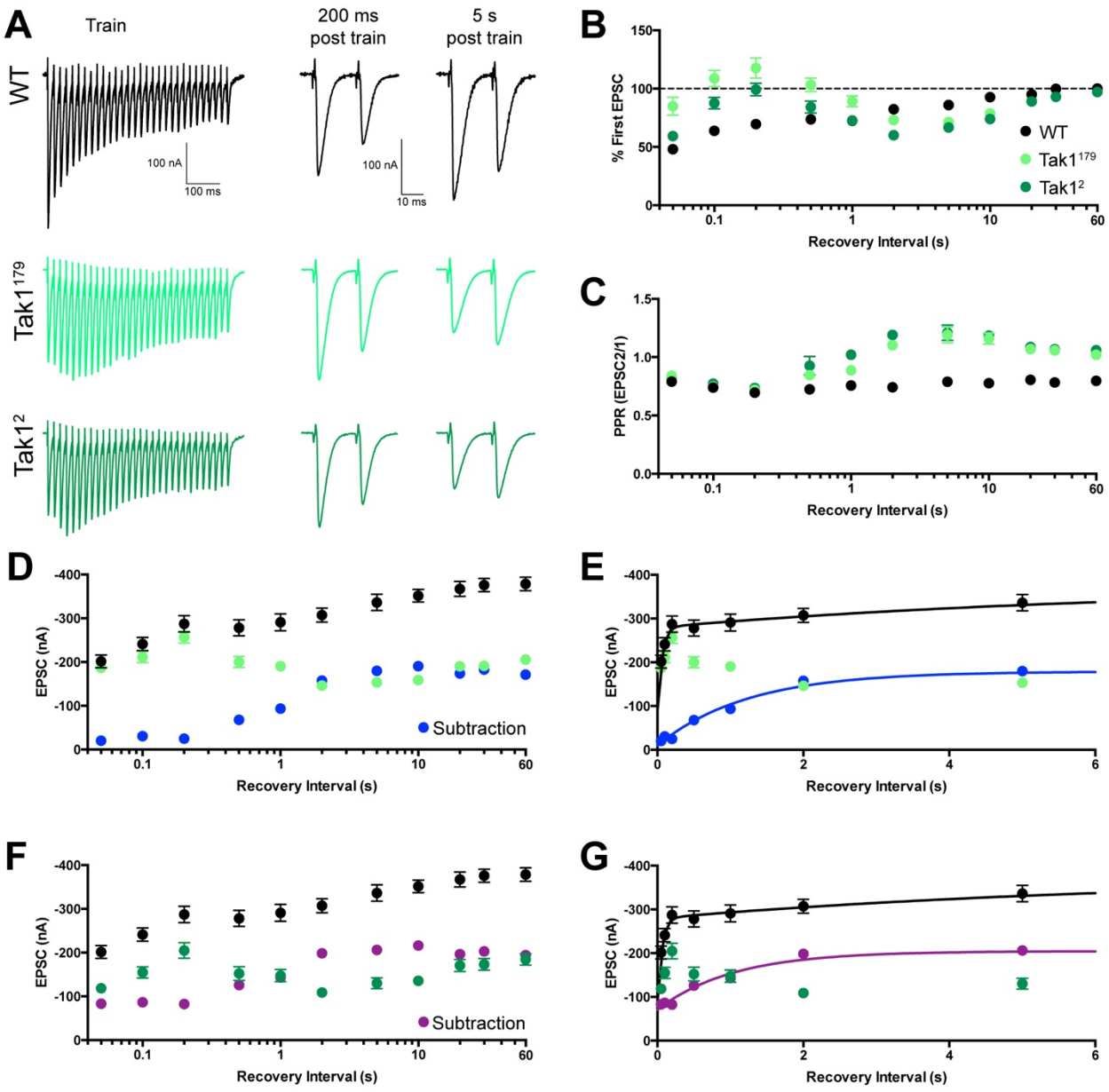

Figure 13: Tak1 stabilizes a high release probability synaptic vesicle pool.

(A) Representative traces for trains as in Figure 12, used to deplete the vesicle pool (scale, 100 nA, 100 ms), and paired EPSC pulses at recovery intervals of 200 ms and 5 s after the train (scale, 100 nA, 10 ms), for the indicated genotypes. (B) Summary data showing average recovery time courses in the indicated genotypes. (C) Average paired-pulse ratio, calculated as the amplitude of EPSC #2 divided by that of EPSC #1, at each recovery interval, for the indicated genotypes. (D) Average data for recovery time courses of raw EPSC amplitudes in the indicated genotypes. The data labelled "subtraction" result from the subtraction of the average amplitude in *Tak1*^{179} from that of WT, at each tested recovery interval. (E) View of the first 6 seconds of the data presented in D, now plotted on a linear x axis. WT data are fit with a double-exponential function (τ_{fast}=0.053 s, τ_{slow}=6.25 s). Subtraction data could not be fit with a double-exponential function and are fit with a single exponential function (τ=1.23 s). Fits were

calculated using all the data out to 90 s, but the x axis is limited to 6 s for ease of visualization. (F) Average data for recovery time courses of raw EPSC amplitudes in the indicated genotypes. The data labelled “subtraction” result from the subtraction of the average amplitude in *Tak1*^{2} from that of WT, at each tested recovery interval. (G) View of the first 6 seconds of the data presented in F, now plotted on a linear x axis. Subtraction data are fit with a single exponential function (τ=1.04 s). Data are presented as average (+/- SEM) and statistical significance determined by Student’s t-test (unpaired, two-tailed).

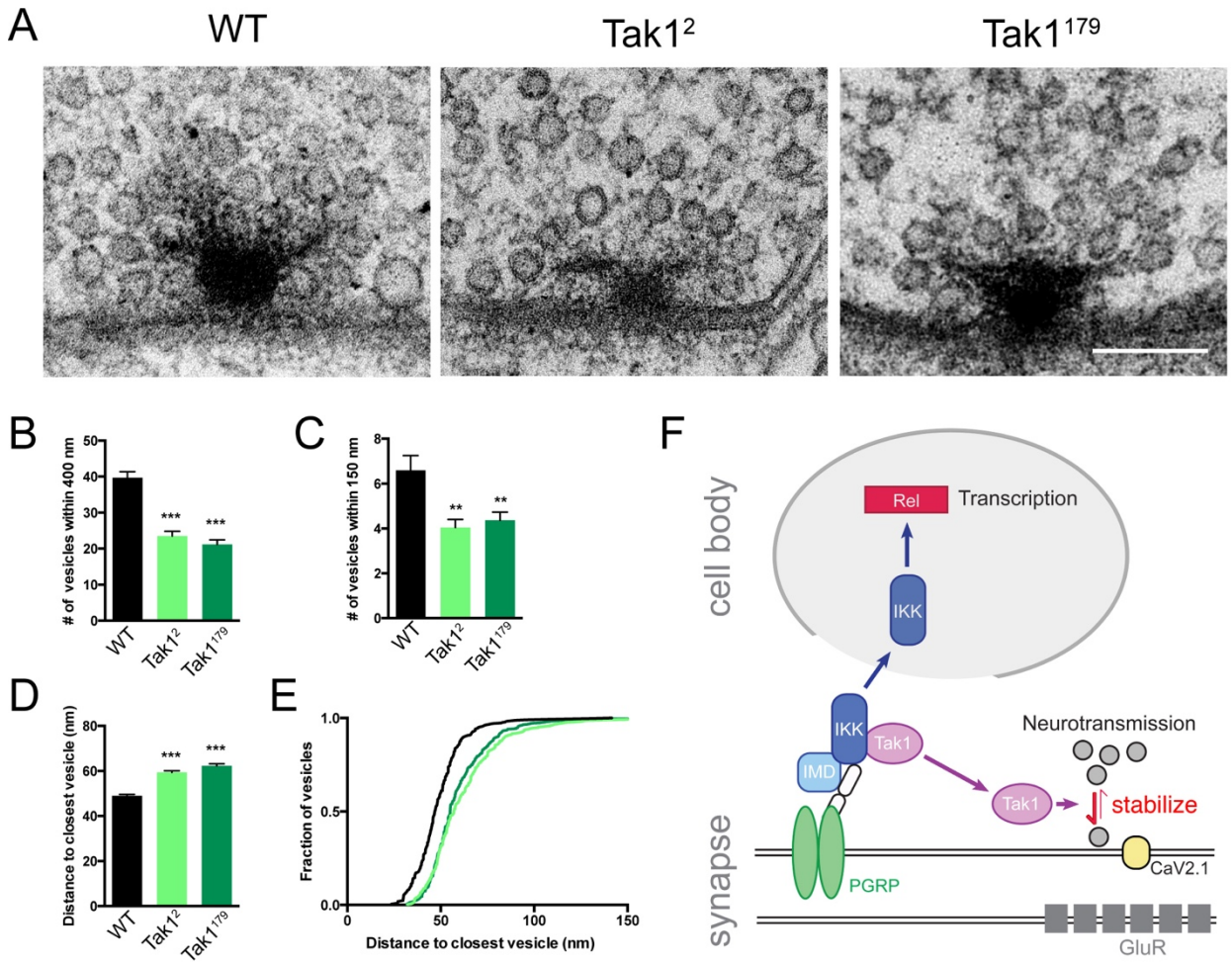

Figure 14: Impaired synaptic vesicle distribution at the active zones of Tak1 mutants.

(A) Representative electron micrographs of presynaptic active zones in the indicated genotypes. Scale bar represents 100 nm. (B) Average number of vesicles within 400 nm of the base of the T-bar for the indicated genotypes. (C) Average number of vesicles within 150 nm of the base of the T-bar for the indicated genotypes. (D) Average distance from a vesicle to its nearest neighboring vesicle for the indicated genotypes. (E) Cumulative frequency distribution of these nearest vesicle distances for the indicated genotypes. (F) Model for the organization of innate immune signaling in *Drosophila* motoneurons. Dimerization activates PGRP receptors (green), initiating signal transduction via assembly of a receptor associated complex that includes ubiquitin poly-peptide chain (white oval; Zhou et al., 2005), the adaptor protein IMD, IKK and Tak1. Rapid signaling, via Tak1 within the presynaptic terminal, leads directly or indirectly to the stabilization of high release probability vesicles residing in close proximity to presynaptic calcium channels (CaV2.1, yellow). Persistent PGRP receptor activation leads to IKK dependent signaling from the synapse to the motoneuron cell body, presumably necessitating retrograde axonal transport. Within the cell body, Rel-mediated transcription is necessary to achieve long-term persistence of PHP. Data are presented as average (+/- SEM) and statistical significance determined by one way ANOVA with Tukey's multiple comparisons test.

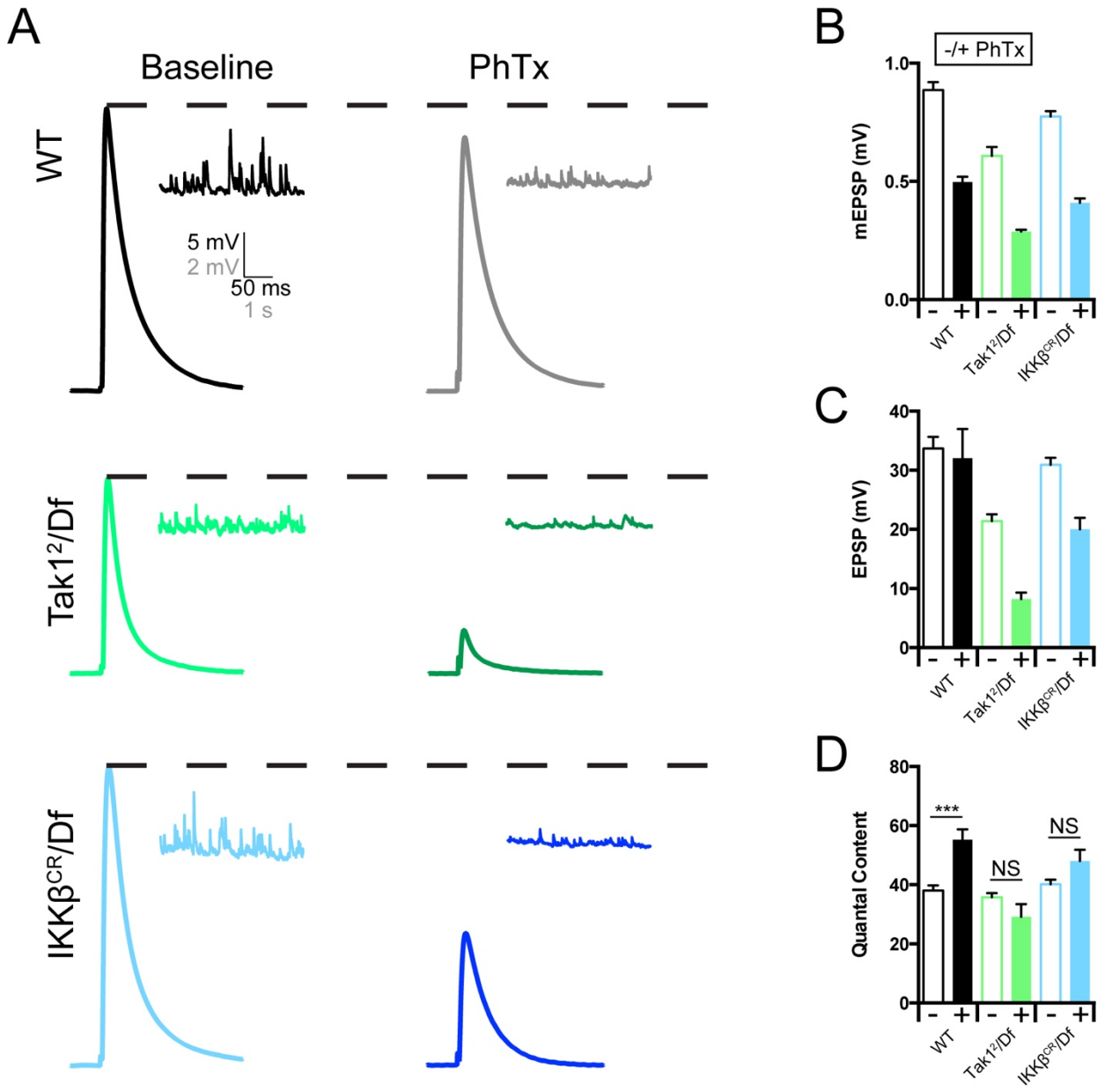

Figure 15: Additional genetic controls for Tak1 and IKK.

(A) Representative traces for heterozygous *Tak1*^{2} over deficiency and heterozygous *IKK*β^{CR} in the absence (light traces) and presence (dark traces) or PhTx. (B) Average data for mEPSP amplitude in the absence (unfilled bars) and presence (filled bars) of PhTx for the indicated genotypes. (C) Average data for EPSP amplitude as in B. (D) Average data for quantal content as in B. There is no significant increase in quantal content in the presence of PhTx in either genotype ($p>0.05$). (E) Percent change in mEPSP amplitude and quantal content in the presence of PhTx, normalized to averages in the absence of PhTx. Data are presented as average (+/- SEM) and statistical significance determined by Student's t-test (unpaired, two-tailed).

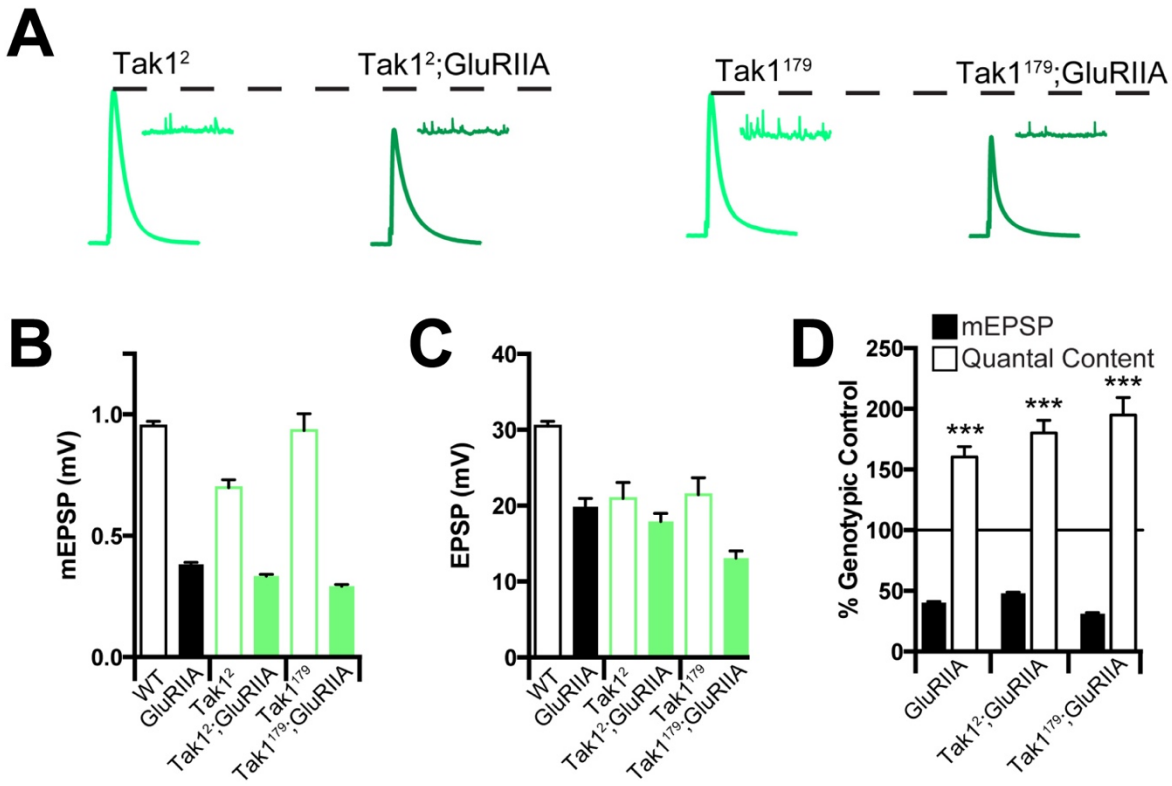

Figure 16: Tak1 is not required for the sustained expression of presynaptic homeostatic potentiation.

(A) Representative traces for EPSP (scale, 5 mV, 50 ms) and mEPSP (scale, 2 mV, 1 s) at baseline, and in the background of the *GluRIIA*^{SP16} mutation, for the indicated genotypes. (B) Average mEPSP amplitude for each genotype in the absence (light bars) or presence (dark bars) of the *GluRIIA* mutation. (C) Average EPSP amplitude for each genotype in the absence (light bars) or presence (dark bars) of the *GluRIIA* mutation. (D) Average mEPSP amplitude and quantal content relative to controls, repeated from Figure 8 for clarity. Data are presented as average (+/- SEM) and statistical significance determined by Student's t-test (unpaired, two-tailed).

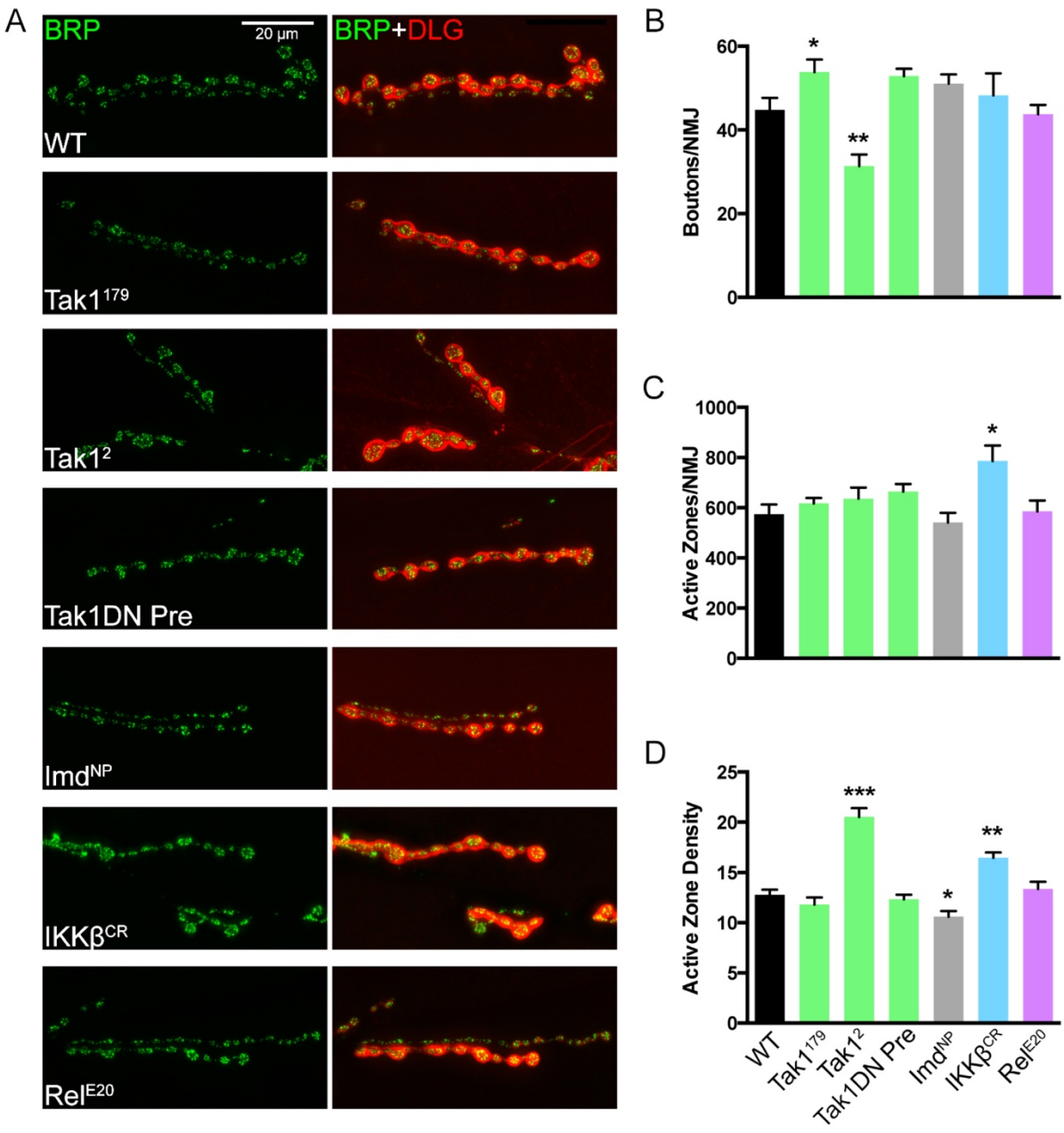

Figure 17: Effects of IMD pathway mutations on synapse morphology.

(A) Representative images of NMJs (muscle 6/7) co-stained with the presynaptic active zone marker Brp (left, green) and the postsynaptic marker Dlg (middle, red). Merge on right. (B) Average number of type 1b boutons per NMJ for the indicated genotypes. (C) Average number of active zones per NMJ for the indicated genotypes. (D) Average number of active zones per bouton for the indicated genotypes. Data are presented as average (+/- SEM) and statistical significance determined by one way ANOVA with Tukey's multiple comparisons test.

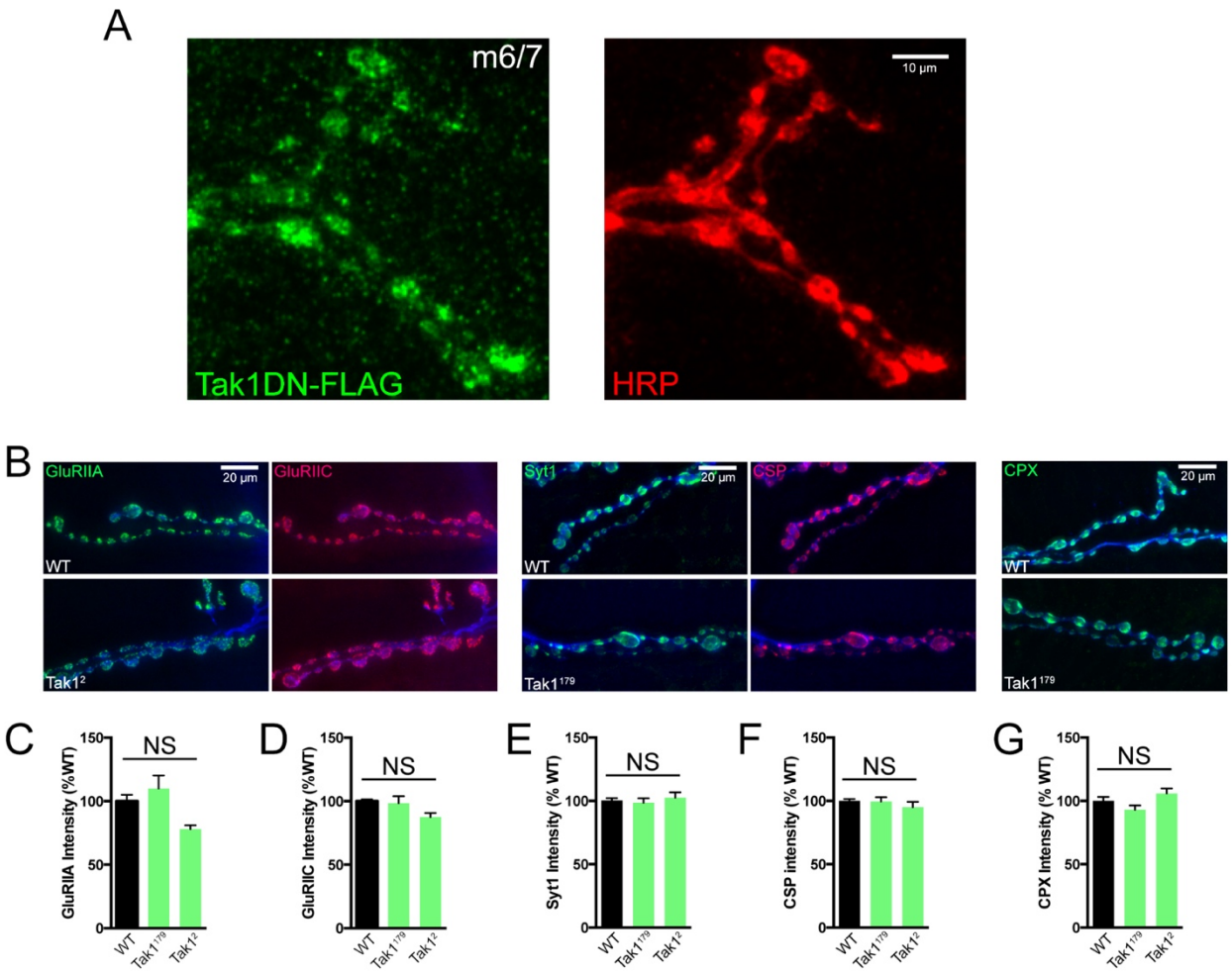

Figure 18: Tak1 localization at the presynaptic terminal.

(A) Image of an NMJ in which *UAS-Tak1-DN-FLAG* was expressed using *OK371-GAL4*. The NMJ was co-stained with HRP (red) and anti-FLAG (green). (B) Immunostaining of the synaptic proteins GluRIIA, GluRIIC, Synaptotagmin-1, Cysteine string protein, and Complexin in the indicated genotypes, all co-stained with HRP (blue). (C-G) Average intensity of each stain across the synapse for the indicated genotypes, normalized to wild type. Data are presented as average (+/- SEM) and statistical significance determined by one way ANOVA with Tukey's multiple comparisons test.

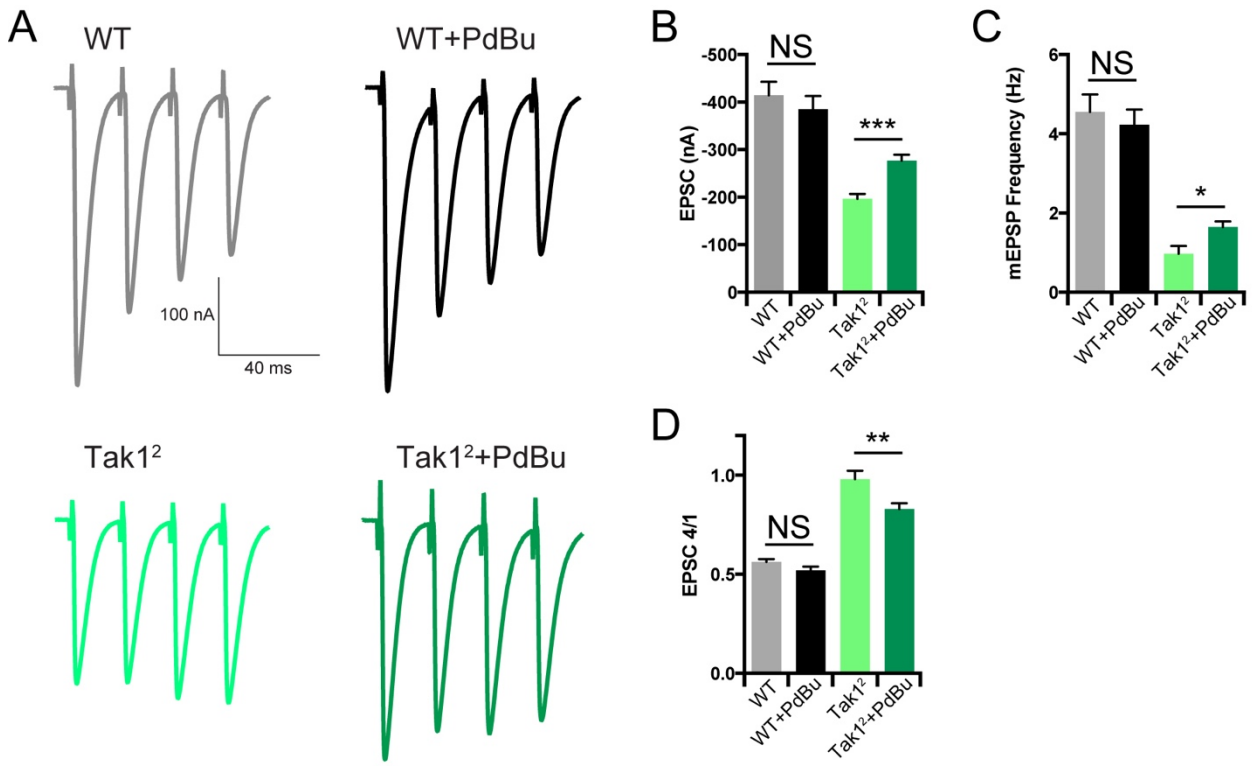

Figure 19: Potentiation of priming with phorbol esters rescues *Tak1²*.

(A) Representative traces in control (light traces) and after incubation with the phorbol ester PdBu (1 µM) (dark traces) for the indicated genotypes. (B) Average data for EPSC amplitude in control (light bars) after incubation with the phorbol ester PdBu (1 µM) (dark bars). (C) Average data for mEPSP frequency as in B. (D) Average data for the ratio of the amplitude of the 4th EPSC in a train over the 1st EPSC in a train. Data are presented as average (+/- SEM) and statistical significance determined by Student's t-test (unpaired, two-tailed).

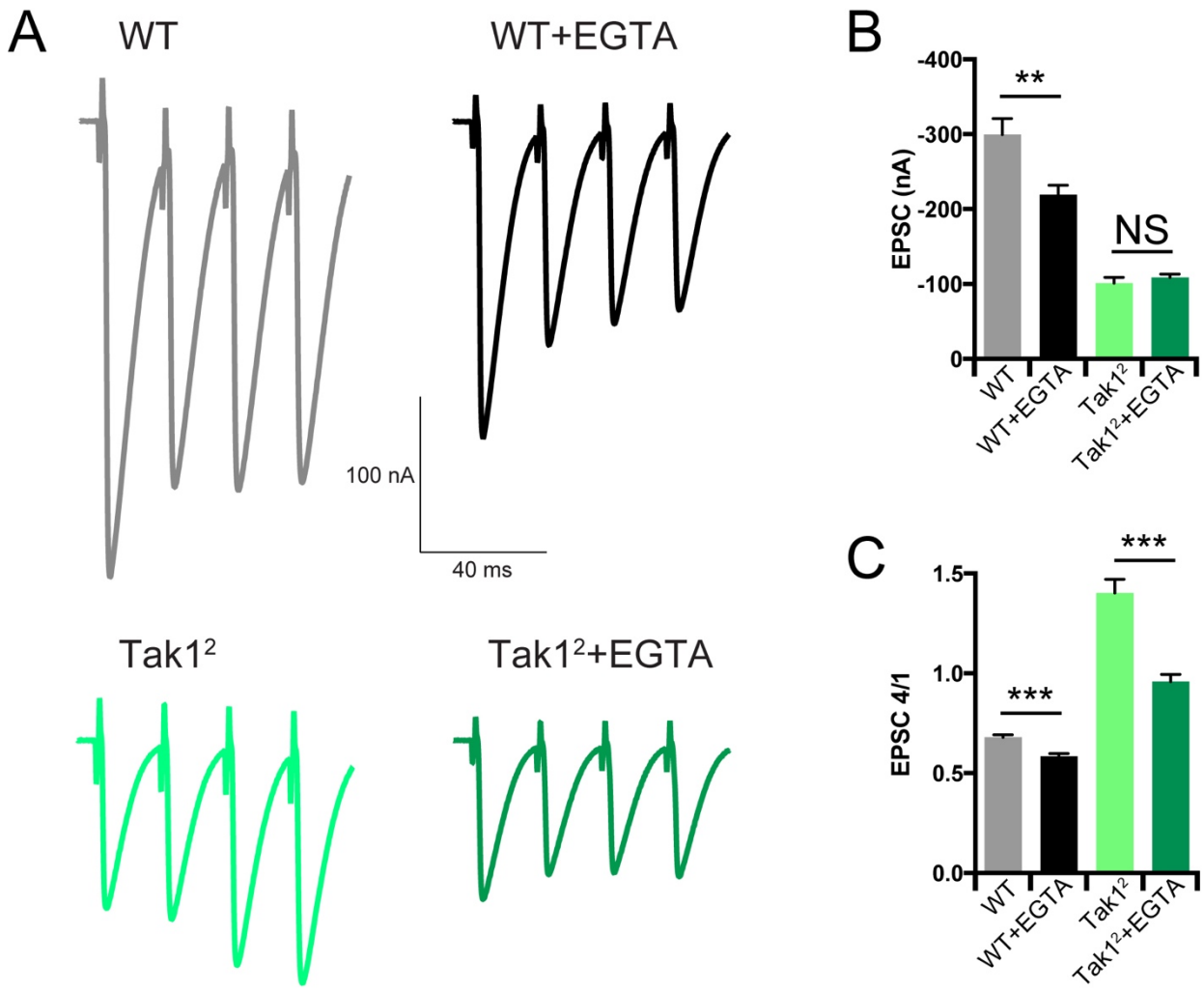

Figure 20: Facilitation in Tak1 results from recruitment of EGTA-sensitive vesicles.

(A) Representative traces in control (light traces) and after incubation with EGTA-AM (50 μM) (dark traces) for the indicated genotypes. (B) Average data for EPSC amplitude in control (light bars) and after incubation with EGTA-AM (50 μM) (dark traces) for the indicated genotypes. (C) Average data for the ratio of the 4th EPSC amplitude over the 1st EPSC amplitude in a train. Data are presented as average (+/- SEM) and statistical significance determined by Student's t-test (unpaired, two-tailed).

4. Unpublished data

4.1 Long-type PGRPs in PHP

In addition to PGRP-LC, we tested nearly all of the long PGRPs (PGRP-LA, LB, LE, and LF) for function in PHP. Only PGRP-LC is essential for the immune response. The other long PGRPs are modulators, negative regulators, or have unknown function. PGRP-LA is not predicted to be capable of binding peptidoglycan, but it may positively regulate the function of other PGRPs in some tissues (Gendrin et al., 2013). PGRP-LB functions as a negative regulator by preventing the diffusion of peptidoglycan to distant immune tissues (Charroux et al., 2018). PGRP-LE functions extracellularly to enhance PGRP-LC activity and can rescue loss of PGRP-LC in some types of infection (Kaneko et al., 2006). PGRP-LF is a negative regulator whose activity is essential in the absence of infection to prevent constitutive low levels of IMD pathway activity (Maillet et al., 2008).

We acquired molecular null alleles for PGRP-LA, LB, and LE (PGRP-LA^{2A} (Gendrin et al., 2013), PGRP-LB$^{\Delta}$ (Paredes et al., 2011), and PGRP-LE^{112} (Takehana et al., 2004), and a hypomorphic allele for PGRP-LF (PGRP-LF^{200} (Maillet et al., 2008)). We tested all four mutants for requirement in the rapid induction of PHP, induced by PhTx application (Figure 21A-D). Except for PGRP-LA, all other mutants showed a significant increase in quantal content in the presence of PhTx, indicating intact homeostatic plasticity (Figure 21C). PGRP-LA had reduced EPSP amplitudes and no significant increase in quantal content, although there was a strong trend towards one. We conclude that PGRP-LA likely somehow supports the activity of PGRP-LC in PHP. PGRP-LA is expressed in the brain, and although it is not required for the immune response, it can stimulate immune activation when overexpressed, suggesting that its

intracellular domain is active, even though it cannot bind extracellular signals (Gendrin et al., 2013). It is conceivable then that PGRP-LA could enhance the activity of PGRP-LC or downstream signaling during PHP.

4.2 TNF-alpha regulates postsynaptic strength, but not PHP

TNF-alpha has a well-characterized role in synaptic scaling in cultured pyramidal neurons. TNF-alpha derived from glia is required for scaling up in response to activity blockade with TTX, but not scaling down in response to picrotoxin (Stellwagen and Malenka, 2006). This makes TNF-alpha one of the best known extracellular ligands regulating homeostatic plasticity. TNF-alpha is also an essential cytokine in the innate immune response (Janeway et al., 2001). Therefore, we tested its function in PHP.

We used a previously published null allele of *Eiger* (*Egr*) – the *Drosophila* homologue of TNF-alpha (Keller et al., 2011). We found that mutation of *Egr* resulted in dramatically increased mEPSP amplitudes in our assay of baseline neurotransmission (Figure 22B). This could reflect either a change in postsynaptic glutamate receptor function or abundance. When we tested PHP, we found that it was entirely normal in *Egr* mutants (Figure 22B-D). We conclude that TNF-alpha is not required for this form of homeostatic potentiation. It could still be fruitful to examine the role of TNF-alpha in long-term PHP, induced by deletion of *GluRIIA*.

4.3 Target substrates of Tak1

Tak1 could either be working through its well-known function as an upstream MAP3 Kinase, activating the JNK pathway and controlling transcription, or it could be

phosphorylating targets directly, independent of a MAPK pathway. We favor the latter possibility, since the main neuronal function of *Tak1* mutants seems to be in controlling neurotransmitter release – a process operating on the timescale of milliseconds and seconds, and there are no obvious developmental abnormalities in the nervous system of *Tak1*. Recently, these direct targets of Tak1 were identified in a screen using chemical genetics (Levin et al., 2016). These are only putative targets, and they come from human cancer cell lines, so they must be validated in our model system. Within these target proteins, the specific phosphorylated amino acid residue(s) were identified as well. We noticed a few interesting targets on the list, including some proteins implicated in synaptic function. We chose first to test two of them – Rab3 and actin.

4.3.1 Rab3 is not the synaptic target of Tak1

Rab3 is a synaptic vesicle-bound protein that also binds RIM and Munc13 (Wang et al., 1997; Dulubova et al., 2005). Rab3 is a known vesicle priming factor, and it affects PHP, although its function in this context is unclear (Schlüter et al., 2006; Müller et al., 2011). Since Tak1 appears to affect vesicle priming and PHP, Rab3 seemed like a good candidate target. The Tak1 target residue – T85 in *Drosophila* Rab3 – lies in the switch II region of the protein. Previous work characterizing this Tak1 substrate in the similar protein Rab1 demonstrated that phosphorylation disrupts an interaction between Rab1 and GDP dissociation inhibitor 1 (GDI1), biasing Rab1 towards membranes and away from the cytosol (Levin et al., 2016). If this affected the cytoplasmic to vesicle-bound ratio of Rab3, it could conceivably modulate vesicle priming.

To test the function of this putative Tak1 phosphorylation substrate in Rab3, we generated a knockin phosphonull mutation (T>A) in genomic Rab3, using CRISPR-mediated homology directed repair. We simultaneously tagged endogenous wild type and mutant Rab3 with N-terminal Venus. As expected, we found that endogenously tagged Rab3 is distributed in high concentration throughout the nervous system and forms synaptic clusters in nerve terminal boutons (data not shown).

We then recorded from Rab3 wild type and Rab3 phosphonull mutant NMJs, using short high frequency stimulus trains to assess its possible function downstream of Tak1 on release probability and vesicle priming. We found that the phosphonull mutation had no discernable effect on synaptic physiology. EPSC amplitudes were unchanged relative to wild type, as was release probability as assessed by the degree of synaptic depression during a train, and mEPSP frequency (Figure 23A-D). We conclude that Rab3 is unlikely to be the target of Tak1 in synaptic transmission and PHP. Nonetheless, we have generated a fluorescently tagged endogenous Rab3, which will likely be useful as a synaptic marker and for functional imaging experiments.

4.3.2 Actin may be a synaptic target of Tak1

The screen mentioned above identified 8 potential Tak1 phosphorylation substrates in actin (Levin et al., 2016). We chose to focus on a cluster of three (T202/3/4 in *Drosophila* actin) whose phosphorylation by other kinases has been shown to modulate actin polymerization and elongation (Constantin et al., 1998; Terman and Keshina, 2013). We expected that mutation of endogenous actin would have many non-specific effects, since it has essential functions in every cell type, so we instead

generated a mutant actin overexpression construct (*UAS-GFP-Act5cT202/3/4A*) that we hoped might act as a dominant negative.

When we drove expression of the protein in motoneurons using the *OK371-Gal4* driver, we observed expression of GFP-tagged actin in the motoneuron cell body, at the nerve terminal, and in the salivary glands (data not shown). The expression pattern appeared the same when we used a GFP-tagged wild type actin. We then tested the effect of expressing mutant actin on synaptic physiology using the same stimulus train as above. There was a trend towards a moderate reduction in EPSC amplitude when mutant actin was overexpressed, as well as a significant reduction in the amount of synaptic depression, suggesting a drop in release probability (Figure 24A-C). Although the reduction in EPSC amplitude and release probability is not as dramatic as in our *Tak1* mutants, this may indicate that synaptic actin is a target of Tak1, and that loss of Tak1 phosphorylation affects actin polymerization, somehow contributing to the neurotransmitter release deficit. An obvious next step will be to test the rapid induction of PHP in these animals. We can also mutate the five remaining putative Tak1 target residues and see if that enhances the phenotype.

There are certainly caveats to this experiment. Actin has many functions within a cell, which could indirectly affect synaptic function or development. There are probably a handful of kinases that phosphorylate actin, and maybe even these same residues, in addition to Tak1. The deficit we observe could reflect a change in any of their functions. We also need to make sure that our mutant actin construct expresses at a level similar to our wild type actin, in case having too much normal actin disrupts synaptic function. Last, we would need to confirm by biochemistry that Tak1 is capable of phosphorylating

actin. Ideally, we would also show that actin phosphorylation by Tak1 is modulated during induction of PHP, but this would be an extraordinarily difficult experiment.

There is some precedent for actin function in neurotransmitter release. Actin polymerization seems to be a required step during recovery from synaptic depression, although disruption of actin polymerization has typically not affected the amplitude of initial EPSCs (Sakaba and Neher, 2003; Lee et al., 2013). Actin dynamics have recently been implicated in PHP, as overexpression of depolymerization-resistant actin disrupts the homeostatic modulation of the RRP (Orr et al., 2017b). Based on the reduced vesicle clustering in EM images from our *Tak1* mutants (Figure 14) where vesicles appear to be “floating away” from the active zone, we imagine actin functioning to tether vesicles in close proximity to the release site, dependent on phosphorylation by Tak1.

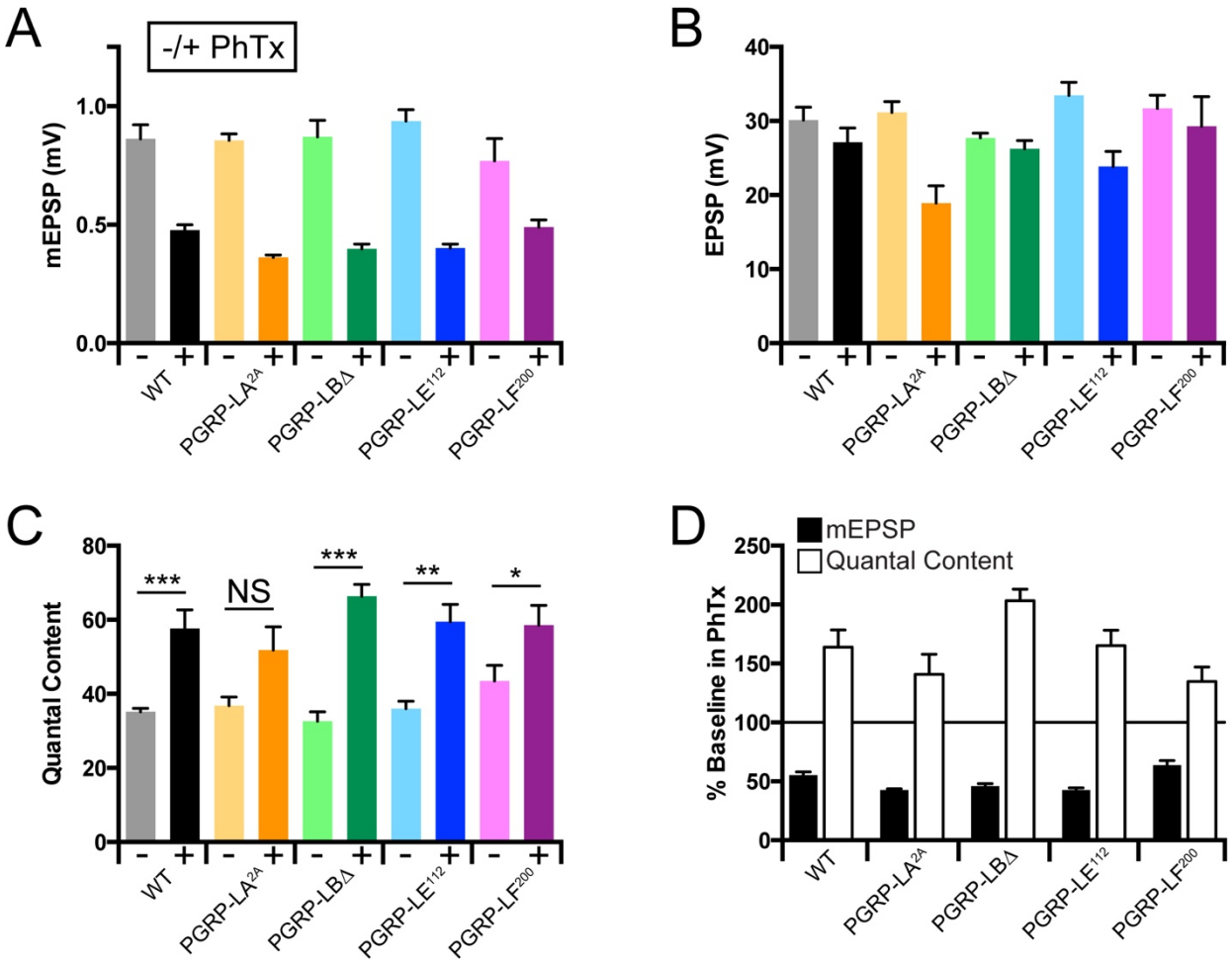

Figure 21: Additional long-type PGRPs in PHP.

(A) Average data for mEPSP amplitude in the absence (light bars) and presence (dark bars) or PhTx for the indicated genotypes. (B) Average data for EPSP amplitude as in A. (C) Average data for quantal content as in A. (D) Average percent change of mEPSP amplitude and quantal content in the presence of PhTx normalized to baseline for the indicated genotypes. Data are presented as average (+/- SEM) and statistical significance determined by Student's t-test (unpaired, two-tailed).

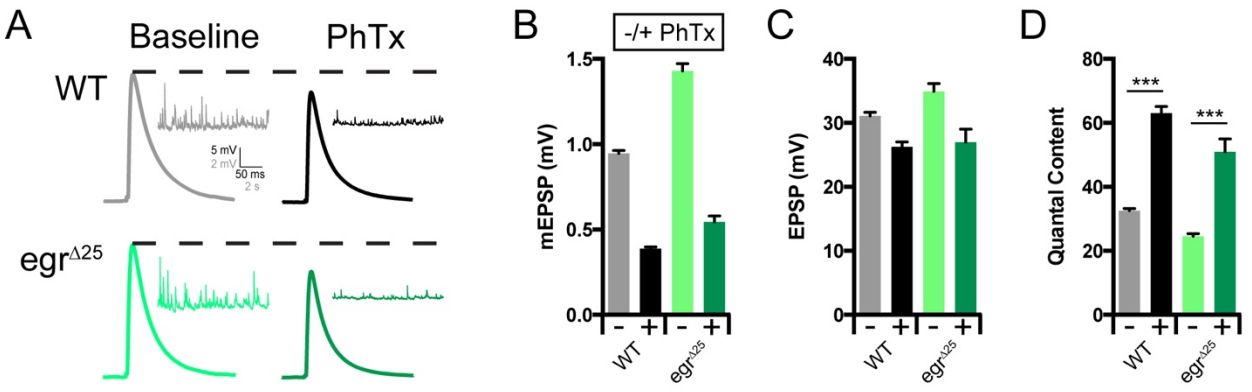

Figure 22: TNF-alpha is not required for PHP.

(A) Representative traces in the absence (light traces) and presence (dark traces) of PhTx for the indicated genotypes. (B) Average data for mEPSP amplitude in the absence (light bars) and presence (dark bars) of PhTx. (C) Average data for EPSP amplitude as in B. (D) Average data for quantal content as in B. Data are presented as average (+/- SEM) and statistical significance determined by Student's t-test (unpaired, two-tailed).

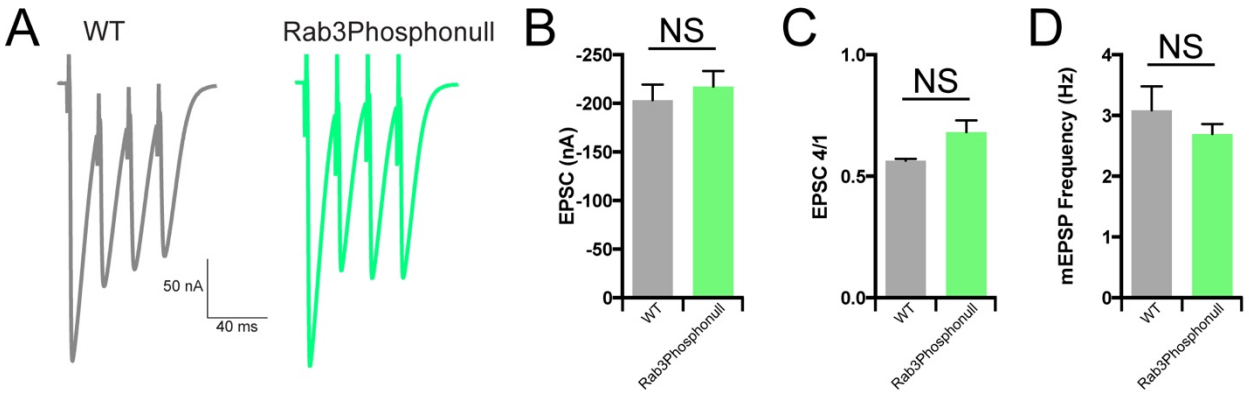

Figure 23: Rab3 is unlikely to be a synaptic target of Tak1.

(A) Representative traces for WT Rab3 animals endogenously tagged with GFP (grey trace) and mutant (T85A) Rab3 GFP tagged animals (green trace). (B) Average EPSC amplitudes for the indicated genotypes. (C) Average ratio of the amplitude of the 4th EPSC in a train to the 1st for the indicatd genotypes. (D) Average mEPSP frequency in the indicated genotypes. Data are presented as average (+/- SEM) and statistical significance determined by Student's t-test (unpaired, two-tailed).

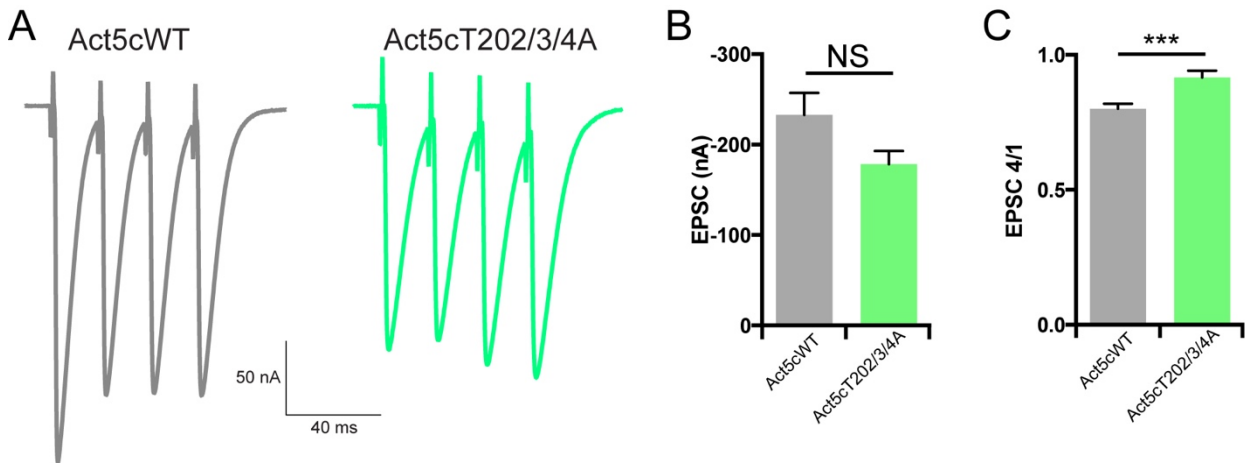

Figure 24: Actin may be a presynaptic target of Tak1.

(A) Representative traces for overexpression of GFP tagged WT Actin or GFP tagged phosphonull (T202/3/4A) Actin. (B) Average EPSC amplitude for the indicated genotypes. (C) The average ratio of the amplitude of the 4th EPSC in a train to the 1st. Data are presented as average (+/- SEM) and statistical significance determined by Student's t-test (unpaired, two-tailed).

5. Conclusions

Adoption of innate immune signaling for neuronal plasticity

From a certain point of view, innate immune signaling pathways are ideally suited to support neuronal plasticity. The first molecular responses to pathogen invasion, mediated by PRRs and cytokine signaling, occur on the time scale of seconds to minutes. They immediately evoke profound changes in the activity of innate immune cells, namely phagocytosis and rapid chemotaxis. Ultimately, these initial immune events stimulate transcription, generating a consolidated state of inflammation that transforms the activities and molecular identities of responding immune cells. Innate immune transcription factors – mostly NF-kB family proteins – have to be already present in sufficient numbers, primed for rapid transcription of immune effectors. The consolidated response is then sustained through transcription for the duration of an infection.

These events exactly mirror the temporal characteristics of many forms of activity-dependent plasticity, including PHP. PHP can be induced rapidly, in minutes, but it can also be consolidated to compensate for a perturbation indefinitely (Frank et al., 2009). Efficient cessation of immune activity is built into innate immune signaling systems through extensive negative feedback loops, because chronic inflammation is hazardous to the body, and also the brain (Park et al., 2004). PHP is also reversible, although the possible negative consequences of inappropriate homeostatic plasticity are unknown (Yeates et al., 2017). Negative innate immune regulators may also be present in neurons to limit the extent of plasticity, but their function has not been tested thus far.

The complement pathway is equally as important as PRR-based signaling in innate immune pathogen recognition and destruction. In the brain, complement undeniably participates in activity dependent circuit refinement and plasticity during development and can be detrimentally reactivated during the onset of neurodegenerative disease (Stevens et al., 2007; Schafer et al., 2012; Hong et al,. 2016). PRR and cytokine receptor signaling within neurons seems to instead regulate neuronal activity, not profoundly restructure neural tissue, and it is not strongly associated with the progression of neurodegenerative disease. It is worth pointing out that, even though they work hand in hand in the overall innate immune response, these two types of responses are fundamentally different in their design and execution. Complement operates nearly entirely in extracellular space, where it recognizes cells and cellular structures opsonized by antibodies or tagged by complement and destroys them directly. Transmembrane PRRs and cytokine receptors recognize an extracellular signal, but then rapidly transduce it into an intracellular signaling cascade that results in a broad transcriptional response and further activation of innate immunity. These differences probably account for their adoption for separate needs of the brain.

The majority of research on innate immune control of neuronal plasticity has focused on postsynaptic function, and communication between the postsynaptic compartment and the nucleus (Meffert et al., 2003; Boersma et al,. 2011). Indeed, NF-kB accumulates in the dendrites of neurons, and it regulates Hebbian synaptic plasticity and remodeling of dendritic spines, which are expressed postsynaptically. NF-kB also regulates postsynaptic glutmate receptor abundance at the *Drosophila* NMJ, a transcription-independent function (Hecksher et al., 2007). Also, cytokine signaling

through glial TNF-alpha regulates synaptic scaling, another postsynaptic phenomenon (Stellwagen and Malenka, 2006). Here we present evidence for a new site of action for these innate immune pathways – the presynaptic active zone.

We have arrived at this new understanding of an innate immune pathway in neurons through stepwise interrogation of the entire canonical IMD pathway. Our findings highlight the importance of rapid, local, transcription-independent functions of this intracellular signaling pathway. This would not have been anticipated based on the accepted understanding of PRR innate immune signaling – a linear pathway from receptor to NF-kB and transcription. Instead, we find a bifurcation of signaling requirements for rapid versus long-term forms of plasticity. We predict that this enables the conversion of local, synaptic sensing and plasticity into retrograde axonal signaling and ultimately transcription in the nucleus that consolidates PHP. This opens the door for extensive characterization of innate immune molecules in this new context.

One immediate goal should be to identify the subcellular localization of these proteins in multiple neuronal cell types and contexts, ideally through antibody staining or endogenous tagging and colocalization with presynaptic markers. Live imaging of the fluorescently tagged proteins during plasticity would then tell us how they respond to neural activity. This information could be used to generate hypotheses about which molecules directly modulate neurotransmitter release and which ones transduce signals throughout the cell.

Another aim would be a fuller characterization of the role of NF-kB-dependent transcription in neuronal activity. Description of activity regulated differential gene expression and genome wide identification of activity dependent NF-kB DNA binding

sites would contribute to our understanding of what consolidated plasticity is and how it is achieved. Some neuronal binding sites for NF-kB have already been identified (Chen et al., 2016). A more straightforward goal is to link innate immune signaling in PHP to the expression of known PHP effector genes. *Ppk1*, *11*, and *16* are the most interesting, because their expression increases during the long-term consolidation of PHP (Younger et al., 2013). *Ppk11* and *16* also carry low-confidence NF-kB binding sites within their gene locus.

Integration of innate immune signaling with known genetic mechanisms of PHP

How does the innate immune pathway we have described here interface with the known signals and effectors in PHP? First, we have identified a presynaptic innate immune receptor – PGRP-LC – that is required for the induction of PHP, but we have not found the extracellular ligand that stimulates it during PHP. We do at least have good evidence that PGRP binds a ligand during PHP – expression of a PGRP with a truncated ligand binding domain is unable to rescue deletion of PGRP (Figure 4). The only known ligands for PGRP are structural components of bacteria cell walls, the ligand in the innate immune response. This makes it difficult to know where to start when looking for an endogenous ligand stimulating its function in the nervous system. We have made some progress by genetically linking PGRP to Multiplexin, an extracellular matrix protein required for PHP and proposed to be a necessary retrograde signal (Figure 4) (Wang et al., 2014). Evidence is accumulating in the lab that synaptic glia are the source for Multiplexin during PHP, potentially adding a third cell type to our understanding of homeostatic signaling (Wang, T., unpublished). Glia are certainly

immunologically active in the brain, and glial-derived TNF-alpha is known to support homeostatic plasticity in a different context, although not in our system (Stellwagen and Malenka, 2006). It is conceivable that PGRP could be responding to Multiplexin or some other signal from glia, and we have no evidence that PGRP responds to a signal from the postsynaptic muscle as opposed to from glia. It is typically difficult to demonstrate potentiation of a biochemical interaction during PHP, because restricting tissue collection to motoneurons yields very small amounts of total protein, but it should be possible to show that PGRP and Multiplexin are at least capable of binding in a heterologous system.

Here we propose a signaling link between the presynaptic membrane and the active zone, mediated in part by IKKβ and Tak1. Our only evidence in the case of IKKβ is that it is required for the rapid induction of PHP, a process that occurs locally at the synaptic terminal within 10 minutes. *IKKβ* is also required for the indefinitely sustained form of homeostasis, suggesting that it is capable of converting a local synaptic signal to nuclear transcription. As mentioned above, an obvious approach is to tag IKKβ and characterize its subcellular localization. If the IKK complex binds Bruchpilot and perhaps RIM in neurons, as suggested in the immune literature, this approach should show localization of IKK to the active zone (Ducut Sigala et al., 2004). Additionally, the possibility that IKK complex members localize to nodes of Ranvier and the axon initial segment in *Drosophila* would be addressed by this approach (König et al., 2017). This would be a much stronger suggestion that the IKK complex transduces a synaptic signal back to the nucleus.

Lastly, we implicate Relish as a transcription factor specifically required for the long-term form of PHP. The most convincing way to link Relish to the function of other known genes in PHP will be to show that Relish is required for their transcription. As mentioned above ENaC channels are the obvious candidate. Endogenous tagging of Relish would also be helpful in this case to show its cytoplasmic versus nuclear localization during the expression of PHP. However, Relish has previously been described as a rapid response transcription factor, upstream of immediate early genes (Chen et al., 2016). It may be that Relish activates an initial set of homeostatic signaling genes and then turns back off while they consolidate PHP. It might also be possible to artificially induce PHP and the transcriptional signature of PHP by overexpressing a constitutively active Relish that lacks its inhibitory subunit.

Tak1 controls vesicular release probability

Tak1 can clearly be added to the relatively small list of kinases that affect release probability, and in particular the characteristics of a subpool of synaptic vesicles. This is the first description of its role in controlling presynaptic function or even neuronal activity in general. This is also the first evidence linking innate immune signaling to presynaptic neurotransmitter release. What exactly is Tak1 doing?

The simplest interpretation of our data is that Tak1 stabilizes a pool of synaptic vesicles with relatively high release probability. The deficit in neurotransmitter release in *Tak1* mutants is most pronounced on the first 2 or 3 responses in a high frequency stimulus train, after which marked facilitation brings neurotransmitter release back to near wild type levels. By definition, these first few responses are likely to be composed

mainly of high Pr vesicles. This is mirrored by reduced mEPSP frequency in the *Tak1* mutants, which is often associated with impaired vesicular release probability. Additionally, Tak1 is required for PHP, and evidence is accumulating that high Pr vesicles are a primary target of homeostatic signaling (Müller et al., 2015).

A drop in calcium influx could explain the change in release probability, but we find that calcium influx is normal, further suggesting that Tak1 does not target calcium channel abundance or function, but rather controls the properties of synaptic vesicles. Furthermore, increasing extracellular calcium concentration above physiological levels does not even partially rescue the release deficit.

The profile of recovery from synaptic depression in *Tak1* mutants is also consistent with an effect on high Pr vesicles. Mutation of *Tak1* disrupts primarily the late phase of recovery, from ~1 second onward, with little to no deficit in EPSC amplitude during the early time constant of recovery – 50 to 500 ms. One way of saying this is that these early recovering vesicles in *Tak1* mutants are essentially wild type vesicles – they do not depend at all on the presence or absence of Tak1. This may suggest that Tak1 targets a biophysical process that operates in seconds, but not so fast as milliseconds. The late phase of recovery has previously been associated with the positional or molecular priming of high Pr vesicles, further supporting the idea that Tak1 targets these vesicles (Schlüter et al., 2006, Sakaba and Neher, 2001). We also found that *Tak1* can be partially rescued by application of phorbol esters, at a calcium concentration where wild type release is saturated and phorbol esters have no effect. Phorbol esters are known to potently increase vesicle priming and release probability, supporting the idea that Tak1 is involved with the priming process.

Lastly, direct visualization of presynaptic active zone ultrastructure by electron microscopy reveals an obvious deficit in vesicle positioning/clustering in *Tak1* mutants. Vesicles appear to be "floating away" from the active zone and calcium channels, suggesting the existence of a process meant to tether vesicles near the active zone (although not necessarily dock them) for which Tak1 is required. This is the basis for our hypothesis that Tak1 "stabilizes" vesicles in close proximity to the active zone. One implication would be that the increased local calcium concentration during a stimulus train or in the early phase of recovery engages a process that drives these vesicles back towards the release site, possibly analogous with priming. When we apply the calcium buffer EGTA to *Tak1* mutant synapses, we find a much milder reduction in vesicle release relative to wild type. This suggests that there are still some docked, primed, EGTA insensitive vesicles in *Tak1* mutants that are responsible for all release on the first EPSC. But, the farther away vesicles seen in EM are so far away that they can never be released on the first stimulus and are therefore not revealed by EGTA application. They can be released when the calcium microdomain is expanded by a stimulus train, but not when microdomain expansion is limited by EGTA. This fits with our finding that the RRP (as far as vesicles that can be released during a stimulus train) is unaffected, as these farther away vesicles are indeed part of the releasable pool, but only when driven to the release site by increased calcium influx during facilitation.

Overall, these data lead us to propose the following model: Tak1 inhibits a process that negatively regulates vesicular release probability. This process acts on the timescale of seconds, and it gradually pushes vesicles away from the release site. We would then say that Tak inhibits the rate of "dedocking" or "depriming". This process can

be overcome by high frequency stimulation and/or increased local calcium acting to rapidly drive vesicles back towards release sites. Release probability would then be determined in part by an equilibrium reaction between docking/priming and this inhibitory process; a process that can be modulated during PHP.

This is consistent with a previously proposed framework for vesicle release and the RRP, in which RIM organizes “active” release sites (Kaeser and Regehr, 2017; Tang et al., 2016). Not all active release sites are occupied by morphologically docked vesicles, but they can become occupied during a high frequency stimulus by the calcium dependent priming activity of RIM, Munc13, and Munc18 (Kaeser and Regehr, 2017). We propose a process that moves vesicles away from these sites, resulting in fewer immediately release ready vesicles, which is normally inhibited by Tak1. In the absence of Tak1, this deficit can then be overcome by increased priming during or after high frequency stimulation. This also suggests the existence of “depriming” factors in this process, which may be the target of Tak1.

An exciting next step will be to look for the presynaptic target(s) of Tak1. This will tell us more about how Tak1 functions, and it may also help describe the “depriming” process we propose above. Putative Tak1 target residues have already been identified in cancer cell lines, using a chemical genetic strategy (Levin et al., 2016). The list contains a number of neuronally relevant proteins that could control presynaptic release. We have already tested two targets by making phosphonull mutations of the target residues (Figures 23 and 24). An additional two targets are of interest. The first, Integrin beta, has already been implicated presynaptically in PHP in our hands and is known to link the plasma membrane to cytoplasmic actin (Calderwood et al., 2000; Orr,

B., unpublished). The second, Munc13, is a well-known vesicle priming factor (Deng et al., 2011). These possible targets will be tested in the future as part of the ongoing work to understand the function of Tak1 and the mechanisms for control of vesicular release probability in PHP.

Overall, our findings speak to the importance of innate immune genes and signaling pathways in controlling neuronal function, in the day-to-day challenges experienced by an otherwise normal, fully developed nervous system. We propose that in many cases the genetic makeup of these pathways is conserved from immune cells to neurons, but the timing, signaling logic, and biochemical targets of the molecular events are modified to support the unique requirements of neuronal morphology and electrochemical communication. This is exciting because it provides a system for coordination of neuronal activity at multiple levels, namely synaptic plasticity and transcriptional plasticity, which may support PHP as well as other types of activity dependent plasticity. The door is now open to find out how it all works.

6. Methods

Fly stocks and genetics

For all experiments except electron microscopy, the w^{1118} strain was used as the wild type control. For electron microscopy the w^{-3605} strain was used as the wild type control. Animals were raised at 20-25°C. Imd^{NP1182}, Rel^{E20}, $Tak1^{2}$, $Tak1^{179}$, $PGRP\text{-}LB^{\Delta}$, $PGRP\text{-}LE^{112}$, *UAS-GFPAct5c* and the *Tak1* deficiency (*Df(1)BSC645*) were obtained from the Bloomington Drosophila Stock Center. $PGRP\text{-}LC^{del}$ and $PGRP\text{-}LF^{200}$ were provided by Julien Royet. $PGRP\text{-}LC^{2}$ was provided by Kathryn Anderson. $PGRP\text{-}LA^{2A}$ was provided by Bruno Lemaitre. *PGRP-LC* RNAi animals were obtained from the Vienna Drosophila stock center. The $GluRIIA^{SP16}$ mutation (Petersen et al., 1997), the $elav^{c155}$*-Gal4, OK371-GAL4* (Mahr and Aberle, 2006), *BG57-GAL4* (Budnik et al., 1996), and *MHC-Gal4* (Davis et al., 1998) drivers have been previously described.

The $IKK\beta^{CR}$ mutation was generated following the protocol of (Kondo and Ueda, 2013). *IKKβ* gRNA was selected using the CRISPR optimal target finder website (http://tools.flycrispr.molbio.wisc.edu/targetFinder). The gRNA sequence AAGTCAAGCTCAGCGAGCGT was cloned into the pCDF3-dU6:3gRNA vector (Addgene plasmid #49410, Simon Bullock). Flies expressing the *UAS-gRNA* were crossed with flies expressing *UAS-Cas9* in the germline (*nos-GAL4VP14, UAS-cas9*). Male offspring were used to create unique stable lines after removing the *UAS-cas9* and removing in the next generation the *UAS-gRNA*. Putative *IKKβ* mutants were sequenced to identify the nature of the Cas9 mediated mutation using the primers CTTATAGCCTTTCGGCTGAGTTAG and CCACCGTTACAGTATTCCAGC. The

resulting mutation, is a deletion of the 162nd nucleotide in *IKKβ* cDNA, creating an early stop codon shortly thereafter.

The *GFP-Rab3WT* and *GFP-Rab3Phosphonull* knockin mutations were made using "scarless" gene editing and CRISPR-mediated homology directed repair (HDR) (Gratz et al., 2015). Specifically, the genomic Rab3 locus was amplified and cloned into the 5' arm of the pHD-Scarless DsRed plasmid (*Drosophila* Genomics Resource Center), and further downstream DNA in the locus was separately cloned into the 3' arm of the plasmid. EGFP and a linker (linker aa sequence: SGLRSRGA) was cloned into the 5' arm immediately before the Rab3 N-terminal start site using Gibson assembly. The plasmid was then mutagenized to generate the T85A mutation. Guide RNAs targeted to regions upstream and downstream of Rab3 exons (sequences CCGTGCAGCACCGCTCTAAA and TTGTGTTGGGGTCGCTAATC) were cloned into the pCFD4-U6:1_U6:3tandemgRNAs plasmid (Addgene). Donor and gRNA plasmids were injected into flies expressing *vas-Cas9* and progeny screened for successful HDR (Bestgene). The resulting fly stocks were sequenced to confirm insertion.

Generation of *UAS-PGRP-LCx-Venus* constructs

The *UAS-PGRP-LCx-Venus* construct was generated by amplifying the full-length *PGRP-LCx* open reading frame from the BDGP DGC cDNA clone IP15793 and cloning into pENTR/D-TOPO (Invitrogen). The *PGRP-LCx* cDNA was then directly cloned into the UAS-C-terminal Venus (EYFP) vector, pTWV (T. Murphy, *Drosophila* Genomics Resource Center) using the Gateway recombination cloning system (Invitrogen). The

following primers were used to amplify the *PGRP-LCx* open reading frame: CACCACACATAACGCTCAGAGATCCAG and GATTTCGTGTGACCAGTGCG. The construct was confirmed by sequencing. Transgenic flies were generated by standard injection methods (BestGene). The *UAS-PGRP∆C-Venus* construct was generated similarly, except that the primers used for amplification were caccATGCCTTTTAGCAATGAAACGG and GCTATTATCGATGACATCCAAGG, thereby creating a PGRP-LCx protein lacking amino acids 333-500.

Generation of *UAS-Tak1DN-FLAG*

The *UAS-Tak1DN-FLAG* construct was generated by amplifying the full-length *Tak1* open reading frame from the BDGP DGC cDNA clone LD42274 and cloning into pENTR/D-TOPO (Invitrogen). Duplex PCR was used to simultaneously amplify the *Tak1* open reading frame and generate the dominant negative mutation. Specifically, the following three primer pairs were used: 1) caccATGGCCACAGCATCGCTGG and GAAGAACTCCcTGACGGCAA, 2) TTGCCGTCAgGGAGTTCTTC and CGCATTGTGATGCGGTGGG, 3) caccATGGCCACAGCATCGCTGG and CGCATTGTGATGCGGTGGG. Amino acid 46 was changed from K to R. The *Tak1* cDNA was then directly cloned into the *UAS-C-terminal FLAG* (3x FLAG) vector, pTWF (T. Murphy, Drosophila Genomics Resource Center) using the Gateway recombination cloning system (Invitrogen). Transgenic flies were generated by standard injection methods (BestGene).

Generation of *UAS-GFP-Act5cT202/3/4A*

The *UAS-GFP-Act5cT202/3/4A* construct was generated by amplifying the full-length *Act5c* open reading frame from the BDGP DGC cDNA clone RE02927 and cloning into pENTR/D-TOPO (Invitrogen). Amplification primers were CACCATGTGTGACGAAGAAG and TTAGAAGCACTTGCGGTG. Amino acids 202, 203, and 204 were then mutated from T to A. The *Act5c* cDNA was then directly cloned into the *UAS-N-terminal GFP* vector, pTVW (T. Murphy, Drosophila Genomics Resource Center) using the Gateway recombination cloning system (Invitrogen). Transgenic flies were generated by standard injection methods (BestGene).

Electrophysiology

Sharp-electrode recordings were performed as previously described (Davis and Goodman, 1998; Müller et al., 2012). Two-electrode voltage-clamp recordings were performed with an Axoclamp 2B amplifier. The extracellular HL3 saline contained the following (in mM): 70 NaCl, 5 KCl, 10 $MgCl_2$, 10 $NaHCO_3$, 115 sucrose, 4.2 trehalose, 5 HEPES, and 0.3 $CaCl_2$ (unless otherwise specified). For acute pharmacological homeostatic challenge, partially dissected larvae were incubated in Philanthotoxin-433 (PhTx; 10-20 μM; Sigma-Aldrich) for 10 min according to published methods (Frank et al., 2006). Quantal content was estimated by calculating the ratio of EPSP amplitude/average mEPSP amplitude and then averaging recordings across all NMJs for a given genotype. EPSC data were analyzed identically. The RRP was estimated by cumulative EPSC analysis (Schneggenburger et al., 1999; Müller et al., 2012). Muscles were clamped at −65 mV, and EPSC amplitudes during a stimulus train (60 Hz, 30 stimuli, 3 mM extracellular calcium) were calculated as the difference between peak and

baseline before stimulus onset of a given EPSC. For recovery of the vesicle pool, stimulus trains (60 Hz, 30 stimuli, 3 mM extracellular calcium) were first given to deplete the pool to steady-state. Recovery was then interrogated with paired pulses (2 pulses, 50 Hz) at varying recovery intervals post-train. EGTA-AM was applied at a concentration of 50 μM to a partially dissected prep for 10 minutes before recording. PdBu was applied at a concentration of 1 μM to a partially dissected prep for 10 minutes before recording. Electrophysiology data were analyzed with custom-written routines in Igor Pro 6.37 (Wavemetrics), MATLAB 8.5 (Mathworks), and Mini Analysis (Synaptosoft).

Calcium Imaging

Ca^{2+} imaging experiments were done as described in (Müller et al., 2012). Third instar larvae were dissected and incubated in ice-cold HL3, 0.3 mM calcium, containing 5 mM Oregon green 488 BAPTA-1 (OGB-1; hexapotassium salt, Invitrogen) and 1 mM Alexa 568 (Invitrogen). After incubation for 10 min, the preparation was washed with ice-cold HL3 for 10–15 min. Single-action-potential-evoked spatially averaged Ca^{2+} transients were measured at an extracellular $[Ca^{2+}]$ of 1.5 mM using a confocal laser scanning system (Ultima, Prairie Technologies) at room temperature. Fluorescence changes were quantified as $\Delta F/F = (F_{(t)} - F_{baseline})/(F_{baseline} - F_{background})$, where F(t) is the fluorescence in a region of interest (ROI), $F_{baseline}$ is the mean fluorescence from a 50-ms period preceding the stimulus, and $F_{background}$ is the background fluorescence from an adjacent ROI without any indicator-containing cellular structures.

Anatomical Analyses

Third-instar larvae were dissected in 0 Ca^{2+} HL3 and fixed for 1-2 min in Bouin's fixative (100%; Sigma-Aldrich), for 15 min in PFA (4% in PBS), or for 7 minutes in ice-cold ethanol, and incubated overnight at 4°C with primary antibodies. The following primary antibodies were used at the indicated dilutions: mouse anti-Bruchpilot (Brp), 1:100 (nc82; Kittel et al., 2006); mouse anti-CSP, 1:250; mouse anti-GluRIIA, 1:100; rabbit anti-synaptogamin, 1:1000; rabbit anti-complexin, 1:500; mouse anti-FLAG, 1:50; rabbit anti-GluRIIC, 1:1000; and rabbit anti-Dlg, 1:10,000. Cy5-conjugated or Cy3-conjugated anti-HRP was used at 1:50, (Invitrogen), and applied for 1 h at room temperature. Larval preparations were mounted in Vectashield (Vector Laboratories). An Axiovert 200 inverted microscope (Carl Zeiss), a 63x or 100x (1.4 NA) Plan Apochromat objective (Carl Zeiss), a cooled CCD camera (CoolSNAP HQ; Roper Scientific), and Slidebook 5.0 (3i) were used for deconvolution microscopy. Synaptic boutons were identified by anti-Dlg. Active zones were identified by anti-Brp and quantified using automated functionality in ImageJ and a watershed plug-in (http://bigwww.epfl.ch/sage/soft/watershed/). Parameters were: radius=1, 8-connected, Min/Max=0,170-210. For staining intensity quantification, a mask was made on the CSP signal (for CSP and Synaptotagmin 1), the GluRIIA signal (for GluRIIA and GluRIIC), or the Complexin signal (for Complexin). The average pixel intensity across the mask is reported. For Supplemental Figure 3A, a Nikon Ti microscope, a 60x Plan Apochromat objective, a Photometrics Evolve Delta EMCCD camera, and a Yokogawa CSU-22 spinning disk confocal were used, in the UCSF Nikon Imaging Center.

Electron Microscopy

Samples were prepared and imaged as previously described. (Harris et al., 2015). Images were analyzed using the ImageJ ROI manager and a custom-written program in Python 2.7. ROIs for all vesicles within 400 nm of an active zone (from the base of the t-bar) were acquired, and their XY coordinates were compared to the XY coordinates of the active zone and to all other vesicle ROIs. Thus, a list of distances was created and used to calculate the following parameters: number of vesicles within 400 and 150 nm of the active zone, distance to nearest neighboring vesicle.

Quantification and Statistical Analysis

Statistical details can be found in the Results, Figures, and Supplemental Table. Unpaired Student's t-test was used for comparison of two groups (typically comparison of a genotype in the presence vs absence of a manipulation). Where three or more groups were compared, one-way ANOVA was used to determine significance, and Tukey's test was used to compare individual groups. N represents number of synapses recorded from. All bar graphs display the mean plus standard error. Significance was defined as $p<0.05$ (one asterisk), with two asterisks indicating $p<0.01$ and three indicating $p<0.005$. A prior power analysis indicates samples size of 5 is sufficient given that our effect size is often 50-100% and synapse to synapse variance is low. None-the-less, our data sets greatly exceed this number with few exceptions.

7. References

Acuna, C., Liu, X., and Südhof, T.C. (2016). How to Make an Active Zone: Unexpected Universal Functional Redundancy between RIMs and RIM-BPs. Neuron *91*, 792–807.

Adelson, J.D., Barreto, G.E., Xu, L., Kim, T., Brott, B.K., Ouyang, Y.-B., Naserke, T., Djurisic, M., Xiong, X., Shatz, C.J., et al. (2012). Neuroprotection from stroke in the absence of MHCI or PirB. Neuron *73*, 1100–1107.

Ahn, H.J., Hernandez, C.M., Levenson, J.M., Lubin, F.D., Liou, H.-C., and Sweatt, J.D. (2008). c-Rel, an NF-kappaB family transcription factor, is required for hippocampal long-term synaptic plasticity and memory formation. Learn. Mem. *15*, 539–549.

Anderson, K.V., Jürgens, G., and Nüsslein-Volhard, C. (1985). Establishment of dorsal-ventral polarity in the Drosophila embryo: genetic studies on the role of the Toll gene product. Cell *42*, 779–789.

Bliss, T.V., and Collingridge, G.L. (1993). A synaptic model of memory: long-term potentiation in the hippocampus. Nature *361*, 31–39.

Bergquist, S., Dickman, D.K., and Davis, G.W. (2010). A hierarchy of cell intrinsic and target-derived homeostatic signaling. Neuron *66*, 220–234.

Boersma, M.C.H., Dresselhaus, E.C., De Biase, L.M., Mihalas, A.B., Bergles, D.E., and Meffert, M.K. (2011). A requirement for nuclear factor-kappaB in developmental and plasticity-associated synaptogenesis. J. Neurosci. *31*, 5414–5425.

Bonizzi, G., and Karin, M. (2004). The two NF-kappaB activation pathways and their role in innate and adaptive immunity. Trends Immunol. *25*, 280–288.

Boutros, M., Agaisse, H., and Perrimon, N. (2002). Sequential activation of signaling pathways during innate immune responses in Drosophila. Dev. Cell *3*, 711–722.

Brusich, D.J., Spring, A.M., and Frank, C.A. (2015). A single-cross, RNA interference-based genetic tool for examining the long-term maintenance of homeostatic plasticity. Front Cell Neurosci *9*, 107.

Budnik, V., Koh, Y.H., Guan, B., Hartmann, B., Hough, C., Woods, D., and Gorczyca, M. (1996). Regulation of synapse structure and function by the Drosophila tumor suppressor gene dlg. Neuron *17*, 627–640.

Burrone, J., O'Byrne, M., and Murthy, V.N. (2002). Multiple forms of synaptic plasticity triggered by selective suppression of activity in individual neurons. Nature *420*, 414–418.

Cahoy, J.D., Emery, B., Kaushal, A., Foo, L.C., Zamanian, J.L., Christopherson, K.S., Xing, Y., Lubischer, J.L., Krieg, P.A., Krupenko, S.A., et al. (2008). A transcriptome database for astrocytes, neurons, and oligodendrocytes: a new resource for understanding brain development and function. J. Neurosci. *28*, 264–278.

Calderwood, D.A., Shattil, S.J., and Ginsberg, M.H. (2000). Integrins and actin filaments: reciprocal regulation of cell adhesion and signaling. J. Biol. Chem. *275*, 22607–22610.

Camacho, M., Basu, J., Trimbuch, T., Chang, S., Pulido-Lozano, C., Chang, S.-S., Duluvova, I., Abo-Rady, M., Rizo, J., and Rosenmund, C. (2017). Heterodimerization of Munc13 C2A domain with RIM regulates synaptic vesicle docking and priming. Nat Commun *8*, 15293.

Cao, Y., Chtarbanova, S., Petersen, A.J., and Ganetzky, B. (2013). Dnr1 mutations cause neurodegeneration in Drosophila by activating the innate immune response in the brain. Proc. Natl. Acad. Sci. U.S.A. *110*, E1752-1760.

Charroux, B., Capo, F., Kurz, C.L., Peslier, S., Chaduli, D., Viallat-Lieutaud, A., and Royet, J. (2018). Cytosolic and Secreted Peptidoglycan-Degrading Enzymes in Drosophila Respectively Control Local and Systemic Immune Responses to Microbiota. Cell Host Microbe *23*, 215-228.e4.

Chen, X., Rahman, R., Guo, F., and Rosbash, M. (2016). Genome-wide identification of neuronal activity-regulated genes in Drosophila. Elife *5*.

Choe, K.-M., Werner, T., Stöven, S., Hultmark, D., and Anderson, K.V. (2002). Requirement for a peptidoglycan recognition protein (PGRP) in Relish activation and antibacterial immune responses in Drosophila. Science *296*, 359–362.

Choe, K.-M., Lee, H., and Anderson, K.V. (2005). Drosophila peptidoglycan recognition protein LC (PGRP-LC) acts as a signal-transducing innate immune receptor. Proc. Natl. Acad. Sci. U.S.A. *102*, 1122–1126.

Constantin, B., Meerschaert, K., Vandekerckhove, J., and Gettemans, J. (1998). Disruption of the actin cytoskeleton of mammalian cells by the capping complex actin-fragmin is inhibited by actin phosphorylation and regulated by Ca2+ ions. J. Cell. Sci. *111 (Pt 12)*, 1695–1706.

Corriveau, R.A., Huh, G.S., and Shatz, C.J. (1998). Regulation of class I MHC gene expression in the developing and mature CNS by neural activity. Neuron *21*, 505–520.

Cull-Candy, S.G., Miledi, R., Trautmann, A., and Uchitel, O.D. (1980). On the release of transmitter at normal, myasthenia gravis and myasthenic syndrome affected human end-plates. J. Physiol. (Lond.) *299*, 621–638.

Davis, G.W. (2013). Homeostatic Signaling and the Stabilization of Neural Function. Neuron *80*, 718–728.

Davis, G.W., DiAntonio, A., Petersen, S.A., and Goodman, C.S. (1998). Postsynaptic PKA controls quantal size and reveals a retrograde signal that regulates presynaptic transmitter release in Drosophila. Neuron *20*, 305–315.

Davis, G.W., and Goodman, C.S. (1998). Synapse-specific control of synaptic efficacy at the terminals of a single neuron. Nature *392*, 82–86.

Davis, G.W., and Müller, M. (2015). Homeostatic control of presynaptic neurotransmitter release. Annu. Rev. Physiol. *77*, 251–270.

Del Castillo, J., and Katz, B. (1954). Quantal components of the end-plate potential. J. Physiol. (Lond.) *124*, 560–573.

Delaney, J.R., Stöven, S., Uvell, H., Anderson, K.V., Engström, Y., and Mlodzik, M. (2006). Cooperative control of Drosophila immune responses by the JNK and NF-kappaB signaling pathways. EMBO J. *25*, 3068–3077.

Deng, L., Kaeser, P.S., Xu, W., and Südhof, T.C. (2011). RIM proteins activate vesicle priming by reversing autoinhibitory homodimerization of Munc13. Neuron *69*, 317–331.

Dickman, D.K., and Davis, G.W. (2009). The schizophrenia susceptibility gene dysbindin controls synaptic homeostasis. Science *326*, 1127–1130.

Ducut Sigala, J.L., Bottero, V., Young, D.B., Shevchenko, A., Mercurio, F., and Verma, I.M. (2004). Activation of transcription factor NF-kappaB requires ELKS, an IkappaB kinase regulatory subunit. Science *304*, 1963–1967.

Dulubova, I., Lou, X., Lu, J., Huryeva, I., Alam, A., Schneggenburger, R., Südhof, T.C., and Rizo, J. (2005). A Munc13/RIM/Rab3 tripartite complex: from priming to plasticity? EMBO J. *24*, 2839–2850.

Dziarski, R. (2004). Peptidoglycan recognition proteins (PGRPs). Mol. Immunol. *40*, 877–886.

Dziarski, R., and Gupta, D. (2006). The peptidoglycan recognition proteins (PGRPs). Genome Biol. *7*, 232.

Ertürk-Hasdemir, D., Broemer, M., Leulier, F., Lane, W.S., Paquette, N., Hwang, D., Kim, C.-H., Stöven, S., Meier, P., and Silverman, N. (2009). Two roles for the Drosophila IKK complex in the activation of Relish and the induction of antimicrobial peptide genes. Proc. Natl. Acad. Sci. U.S.A. *106*, 9779–9784.

Frank, C.A., Kennedy, M.J., Goold, C.P., Marek, K.W., and Davis, G.W. (2006). Mechanisms underlying the rapid induction and sustained expression of synaptic homeostasis. Neuron *52*, 663–677.

Frank, C.A., Pielage, J., and Davis, G.W. (2009). A presynaptic homeostatic signaling system composed of the Eph receptor, ephexin, Cdc42, and CaV2.1 calcium channels. Neuron *61*, 556–569.

Gaviño, M.A., Ford, K.J., Archila, S., and Davis, G.W. (2015). Homeostatic synaptic depression is achieved through a regulated decrease in presynaptic calcium channel abundance. Elife *4*.

Genç, Ö., Kochubey, O., Toonen, R.F., Verhage, M., and Schneggenburger, R. (2014). Munc18-1 is a dynamically regulated PKC target during short-term enhancement of transmitter release. ELife Sciences *3*, e01715.

Gendrin, M., Zaidman-Rémy, A., Broderick, N.A., Paredes, J., Poidevin, M., Roussel, A., and Lemaitre, B. (2013). Functional analysis of PGRP-LA in Drosophila immunity. PLoS ONE *8*, e69742.

Georgel, P., Naitza, S., Kappler, C., Ferrandon, D., Zachary, D., Swimmer, C., Kopczynski, C., Duyk, G., Reichhart, J.M., and Hoffmann, J.A. (2001). Drosophila immune deficiency (IMD) is a death domain protein that activates antibacterial defense and can promote apoptosis. Dev. Cell *1*, 503–514.

Gottar, M., Gobert, V., Michel, T., Belvin, M., Duyk, G., Hoffmann, J.A., Ferrandon, D., and Royet, J. (2002). The Drosophila immune response against Gram-negative bacteria is mediated by a peptidoglycan recognition protein. Nature *416*, 640–644.

Gratz, S.J., Rubinstein, C.D., Harrison, M.M., Wildonger, J., and O'Connor-Giles, K.M. (2015). CRISPR-Cas9 Genome Editing in Drosophila. Curr Protoc Mol Biol *111*, 31.2.1-20.

Häcker, H., and Karin, M. (2006). Regulation and function of IKK and IKK-related kinases. Sci. STKE *2006*, re13.

Hallermann, S., Heckmann, M., and Kittel, R.J. (2010). Mechanisms of short-term plasticity at neuromuscular active zones of Drosophila. HFSP J *4*, 72–84.

Harris, N., Braiser, D.J., Dickman, D.K., Fetter, R.D., Tong, A., and Davis, G.W. (2015). The Innate Immune Receptor PGRP-LC Controls Presynaptic Homeostatic Plasticity. Neuron *88*, 1157–1164.

Hauswirth, A.G., Ford, K.J., Wang, T., Fetter, R.D., Tong, A., and Davis, G.W. (2018). A postsynaptic PI3K-cII dependent signaling controller for presynaptic homeostatic plasticity. Elife *7*.

Heckscher, E.S., Fetter, R.D., Marek, K.W., Albin, S.D., and Davis, G.W. (2007). NF-kappaB, IkappaB, and IRAK control glutamate receptor density at the Drosophila NMJ. Neuron *55*, 859–873.

Hedengren, M., Asling, B., Dushay, M.S., Ando, I., Ekengren, S., Wihlborg, M., and Hultmark, D. (1999). Relish, a central factor in the control of humoral but not cellular immunity in Drosophila. Mol. Cell *4*, 827–837.

Hengen, K.B., Lambo, M.E., Van Hooser, S.D., Katz, D.B., and Turrigiano, G.G. (2013). Firing rate homeostasis in visual cortex of freely behaving rodents. Neuron *80*, 335–342.

Hengen, K.B., Torrado Pacheco, A., McGregor, J.N., Van Hooser, S.D., and Turrigiano, G.G. (2016). Neuronal Firing Rate Homeostasis Is Inhibited by Sleep and Promoted by Wake. Cell *165*, 180–191.

Hoffmann, J.A., and Hoffmann, D. (1990). The inducible antibacterial peptides of dipteran insects. Res. Immunol. *141*, 910–918.

Hong, S., Beja-Glasser, V.F., Nfonoyim, B.M., Frouin, A., Li, S., Ramakrishnan, S., Merry, K.M., Shi, Q., Rosenthal, A., Barres, B.A., et al. (2016). Complement and microglia mediate early synapse loss in Alzheimer mouse models. Science *352*, 712–716.

Huh, G.S., Boulanger, L.M., Du, H., Riquelme, P.A., Brotz, T.M., and Shatz, C.J. (2000). Functional requirement for class I MHC in CNS development and plasticity. Science *290*, 2155–2159.

Ibata, K., Sun, Q., and Turrigiano, G.G. (2008). Rapid synaptic scaling induced by changes in postsynaptic firing. Neuron *57*, 819–826.

Imig, C., Min, S.-W., Krinner, S., Arancillo, M., Rosenmund, C., Südhof, T.C., Rhee, J., Brose, N., and Cooper, B.H. (2014). The morphological and molecular nature of synaptic vesicle priming at presynaptic active zones. Neuron *84*, 416–431.

Janeway, C.A., Travers, P., Walport, M., and Shlomchik, M.J. (2001). *Immunobiology*. Garland Science.

Jorquera, R.A., Huntwork-Rodriguez, S., Akbergenova, Y., Cho, R.W., and Littleton, J.T. (2012). Complexin controls spontaneous and evoked neurotransmitter release by regulating the timing and properties of synaptotagmin activity. J. Neurosci. *32*, 18234–18245.

Kaeser, P.S., and Regehr, W.G. (2017). The readily releasable pool of synaptic vesicles. Curr. Opin. Neurobiol. *43*, 63–70.

Kaneko, T., Yano, T., Aggarwal, K., Lim, J.-H., Ueda, K., Oshima, Y., Peach, C., Erturk-Hasdemir, D., Goldman, W.E., Oh, B.-H., et al. (2006). PGRP-LC and PGRP-LE have essential yet distinct functions in the drosophila immune response to monomeric DAP-type peptidoglycan. Nat. Immunol. *7*, 715–723.

Kazama, H., and Wilson, R.I. (2008). Homeostatic matching and nonlinear amplification at identified central synapses. Neuron *58*, 401–413.

Keller, L.C., Cheng, L., Locke, C.J., Müller, M., Fetter, R.D., and Davis, G.W. (2011). Glial-derived prodegenerative signaling in the Drosophila neuromuscular system. Neuron *72*, 760–775.

Kim, S.H., and Ryan, T.A. (2010). CDK5 serves as a major control point in neurotransmitter release. Neuron *67*, 797–809.

Kim, T., Yoon, J., Cho, H., Lee, W.-B., Kim, J., Song, Y.-H., Kim, S.N., Yoon, J.H., Kim-Ha, J., and Kim, Y.-J. (2005). Downregulation of lipopolysaccharide response in Drosophila by negative crosstalk between the AP1 and NF-kappaB signaling modules. Nat. Immunol. *6*, 211–218.

Kittel, R.J., Wichmann, C., Rasse, T.M., Fouquet, W., Schmidt, M., Schmid, A., Wagh, D.A., Pawlu, C., Kellner, R.R., Willig, K.I., et al. (2006). Bruchpilot promotes active zone assembly, Ca2+ channel clustering, and vesicle release. Science *312*, 1051–1054.

Kondo, S., and Ueda, R. (2013). Highly Improved Gene Targeting by Germline-Specific Cas9 Expression in Drosophila. Genetics *195*, 715–721.

König, H.-G., Schwamborn, R., Andresen, S., Kinsella, S., Watters, O., Fenner, B., and Prehn, J.H.M. (2017). NF-κB regulates neuronal ankyrin-G via a negative feedback loop. Sci Rep *7*, 42006.

Krahe, T.E., and Guido, W. (2011). Homeostatic plasticity in the visual thalamus by monocular deprivation. J. Neurosci. *31*, 6842–6849.

Kreutzberg, G.W. (1996). Microglia: a sensor for pathological events in the CNS. Trends Neurosci. *19*, 312–318.

Lampson, L.A., and Siegel, G. (1988). Defining the mechanisms that govern immune acceptance or rejection of neural tissue. Prog. Brain Res. *78*, 243–247.

Lee, H., Brott, B.K., Kirkby, L.A., Adelson, J.D., Cheng, S., Feller, M.B., Datwani, A., and Shatz, C.J. (2014). Synapse elimination and learning rules co-regulated by MHC class I H2-Db. Nature *509*, 195–200.

Lee, J.S., Ho, W.-K., Neher, E., and Lee, S.-H. (2013). Superpriming of synaptic vesicles after their recruitment to the readily releasable pool. Proc. Natl. Acad. Sci. U.S.A. *110*, 15079–15084.

Lemaitre, B., Kromer-Metzger, E., Michaut, L., Nicolas, E., Meister, M., Georgel, P., Reichhart, J.M., and Hoffmann, J.A. (1995). A recessive mutation, immune deficiency (imd), defines two distinct control pathways in the Drosophila host defense. Proc. Natl. Acad. Sci. U.S.A. *92*, 9465–9469.

Levin, R.S., Hertz, N.T., Burlingame, A.L., Shokat, K.M., and Mukherjee, S. (2016). Innate immunity kinase TAK1 phosphorylates Rab1 on a hotspot for posttranslational modifications by host and pathogen. Proc. Natl. Acad. Sci. U.S.A. *113*, E4776-4783.

Lewitus, G.M., Konefal, S.C., Greenhalgh, A.D., Pribiag, H., Augereau, K., and Stellwagen, D. (2016). Microglial TNF-α Suppresses Cocaine-Induced Plasticity and Behavioral Sensitization. Neuron *90*, 483–491.

Lou, X., Korogod, N., Brose, N., and Schneggenburger, R. (2008). Phorbol esters modulate spontaneous and Ca2+-evoked transmitter release via acting on both Munc13 and protein kinase C. J. Neurosci. *28*, 8257–8267.

Ma, Y., Haynes, R.L., Sidman, R.L., and Vartanian, T. (2007). TLR8: an innate immune receptor in brain, neurons and axons. Cell Cycle *6*, 2859–2868.

Mahoney, R.E., Rawson, J.M., and Eaton, B.A. (2014). An age-dependent change in the set point of synaptic homeostasis. J. Neurosci. *34*, 2111–2119.

Mahr, A., and Aberle, H. (2006). The expression pattern of the Drosophila vesicular glutamate transporter: a marker protein for motoneurons and glutamatergic centers in the brain. Gene Expr. Patterns *6*, 299–309.

Maillet, F., Bischoff, V., Vignal, C., Hoffmann, J., and Royet, J. (2008). The Drosophila peptidoglycan recognition protein PGRP-LF blocks PGRP-LC and IMD/JNK pathway activation. Cell Host Microbe *3*, 293–303.

Marder, E., and Prinz, A.A. (2002). Modeling stability in neuron and network function: the role of activity in homeostasis. Bioessays *24*, 1145–1154.

Marie, B., Sweeney, S.T., Poskanzer, K.E., Roos, J., Kelly, R.B., and Davis, G.W. (2004). Dap160/intersectin scaffolds the periactive zone to achieve high-fidelity endocytosis and normal synaptic growth. Neuron *43*, 207–219.

Marie, B., Pym, E., Bergquist, S., and Davis, G.W. (2010). Synaptic homeostasis is consolidated by the cell fate gene gooseberry, a Drosophila pax3/7 homolog. J. Neurosci. *30*, 8071–8082.

Markram, H., Toledo-Rodriguez, M., Wang, Y., Gupta, A., Silberberg, G., and Wu, C. (2004). Interneurons of the neocortical inhibitory system. Nature Reviews Neuroscience *5*, 793–807.

Meffert, M.K., Chang, J.M., Wiltgen, B.J., Fanselow, M.S., and Baltimore, D. (2003). NF-kappa B functions in synaptic signaling and behavior. Nat. Neurosci. *6*, 1072–1078.

Müller, M., Pym, E.C.G., Tong, A., and Davis, G.W. (2011). Rab3-GAP controls the progression of synaptic homeostasis at a late stage of vesicle release. Neuron *69*, 749–762.

Müller, M., and Davis, G.W. (2012). Transsynaptic control of presynaptic Ca^{2+} influx achieves homeostatic potentiation of neurotransmitter release. Curr. Biol. *22*, 1102–1108.

Müller, M., Liu, K.S.Y., Sigrist, S.J., and Davis, G.W. (2012). RIM controls homeostatic plasticity through modulation of the readily-releasable vesicle pool. J. Neurosci. *32*, 16574–16585.

Müller, M., Genç, Ö., and Davis, G.W. (2015). RIM-binding protein links synaptic homeostasis to the stabilization and replenishment of high release probability vesicles. Neuron *85*, 1056–1069.

Mullins, C., Fishell, G., and Tsien, R.W. (2016). Unifying Views of Autism Spectrum Disorders: A Consideration of Autoregulatory Feedback Loops. Neuron *89*, 1131–1156.

Myllymäki, H., Valanne, S., and Rämet, M. (2014). The Drosophila imd signaling pathway. J. Immunol. *192*, 3455–3462.

Neher, E., and Sakaba, T. (2008). Multiple roles of calcium ions in the regulation of neurotransmitter release. Neuron *59*, 861–872.

Neher, E. (2015). Merits and Limitations of Vesicle Pool Models in View of Heterogeneous Populations of Synaptic Vesicles. Neuron *87*, 1131–1142.

Nelson, S.B., and Valakh, V. (2015). Excitatory/Inhibitory Balance and Circuit Homeostasis in Autism Spectrum Disorders. Neuron *87*, 684–698.

Nerbonne, J.M., Gerber, B.R., Norris, A., and Burkhalter, A. (2008). Electrical remodelling maintains firing properties in cortical pyramidal neurons lacking KCND2-encoded A-type K+ currents. J. Physiol. (Lond.) *586*, 1565–1579.

Okun, E., Griffioen, K.J., and Mattson, M.P. (2011). Toll-like receptor signaling in neural plasticity and disease. Trends Neurosci. *34*, 269–281.

Orr, B.O., Gorczyca, D., Younger, M.A., Jan, L.Y., Jan, Y.-N., and Davis, G.W. (2017). Composition and Control of a Deg/ENaC Channel during Presynaptic Homeostatic Plasticity. Cell Rep *20*, 1855–1866.

Orr, B.O., Fetter, R.D., and Davis, G.W. (2017). Retrograde semaphorin-plexin signalling drives homeostatic synaptic plasticity. Nature *550*, 109–113.

Paredes, J.C., Welchman, D.P., Poidevin, M., and Lemaitre, B. (2011). Negative regulation by amidase PGRPs shapes the Drosophila antibacterial response and protects the fly from innocuous infection. Immunity *35*, 770–779.

Park, J.M., Brady, H., Ruocco, M.G., Sun, H., Williams, D., Lee, S.J., Kato, T., Richards, N., Chan, K., Mercurio, F., et al. (2004). Targeting of TAK1 by the NF-kappa B protein Relish regulates the JNK-mediated immune response in Drosophila. Genes Dev. *18*, 584–594.

Parrish, J.Z., Kim, C.C., Tang, L., Bergquist, S., Wang, T., Derisi, J.L., Jan, L.Y., Jan, Y.N., and Davis, G.W. (2014). Krüppel mediates the selective rebalancing of ion channel expression. Neuron *82*, 537–544.

Peixoto, R.T., Kunz, P.A., Kwon, H., Mabb, A.M., Sabatini, B.L., Philpot, B.D., and Ehlers, M.D. (2012). Transsynaptic signaling by activity-dependent cleavage of neuroligin-1. Neuron *76*, 396–409.

Penney, J., Tsurudome, K., Liao, E.H., Elazzouzi, F., Livingstone, M., Gonzalez, M., Sonenberg, N., and Haghighi, A.P. (2012). TOR is required for the retrograde regulation of synaptic homeostasis at the Drosophila neuromuscular junction. Neuron *74*, 166–178.

Petersen, S.A., Fetter, R.D., Noordermeer, J.N., Goodman, C.S., and DiAntonio, A. (1997). Genetic analysis of glutamate receptors in Drosophila reveals a retrograde signal regulating presynaptic transmitter release. Neuron *19*, 1237–1248.

Plomp, J.J., van Kempen, G.T., and Molenaar, P.C. (1992). Adaptation of quantal content to decreased postsynaptic sensitivity at single endplates in alpha-bungarotoxin-treated rats. J. Physiol. (Lond.) *458*, 487–499.

Polley, S., Huang, D.-B., Hauenstein, A.V., Fusco, A.J., Zhong, X., Vu, D., Schröfelbauer, B., Kim, Y., Hoffmann, A., Verma, I.M., et al. (2013). A structural basis for IκB kinase 2 activation via oligomerization-dependent trans auto-phosphorylation. PLoS Biol. *11*, e1001581.

Pratt, K.G., and Aizenman, C.D. (2007). Homeostatic regulation of intrinsic excitability and synaptic transmission in a developing visual circuit. J. Neurosci. *27*, 8268–8277.

Rivera-Quiñones, C., McGavern, D., Schmelzer, J.D., Hunter, S.F., Low, P.A., and Rodriguez, M. (1998). Absence of neurological deficits following extensive demyelination in a class I-deficient murine model of multiple sclerosis. Nat. Med. *4*, 187–193.

Ramocki, M.B., and Zoghbi, H.Y. (2008). Failure of neuronal homeostasis results in common neuropsychiatric phenotypes. Nature *455*, 912–918.

Rothwarf, D.M., and Karin, M. (1999). The NF-kappa B activation pathway: a paradigm in information transfer from membrane to nucleus. Sci. STKE *1999*, RE1.

Royet, J., and Dziarski, R. (2007). Peptidoglycan recognition proteins: pleiotropic sensors and effectors of antimicrobial defences. Nat. Rev. Microbiol. *5*, 264–277.

Saha, S., Qi, J., Wang, S., Wang, M., Li, X., Kim, Y.-G., Núñez, G., Gupta, D., and Dziarski, R. (2009). PGLYRP-2 and Nod2 are both required for peptidoglycan-induced arthritis and local inflammation. Cell Host Microbe *5*, 137–150.

Sakaba, T., and Neher, E. (2001). Calmodulin mediates rapid recruitment of fast-releasing synaptic vesicles at a calyx-type synapse. Neuron *32*, 1119–1131.

Sakaba, T., and Neher, E. (2003). Involvement of actin polymerization in vesicle recruitment at the calyx of Held synapse. J. Neurosci. *23*, 837–846.

Samad, T.A., Moore, K.A., Sapirstein, A., Billet, S., Allchorne, A., Poole, S., Bonventre, J.V., and Woolf, C.J. (2001). Interleukin-1β-mediated induction of Cox-2 in the CNS contributes to inflammatory pain hypersensitivity. Nature *410*, 471–475.

Sato, S., Sanjo, H., Takeda, K., Ninomiya-Tsuji, J., Yamamoto, M., Kawai, T., Matsumoto, K., Takeuchi, O., and Akira, S. (2005). Essential function for the kinase TAK1 in innate and adaptive immune responses. Nat. Immunol. *6*, 1087–1095.

Schafer, D.P., and Stevens, B. (2015). Microglia Function in Central Nervous System Development and Plasticity. Cold Spring Harb Perspect Biol *7*, a020545.

Schafer, D.P., Lehrman, E.K., Kautzman, A.G., Koyama, R., Mardinly, A.R., Yamasaki, R., Ransohoff, R.M., Greenberg, M.E., Barres, B.A., and Stevens, B. (2012). Microglia sculpt postnatal neural circuits in an activity and complement-dependent manner. Neuron *74*, 691–705.

Schneggenburger, R., Meyer, A.C., and Neher, E. (1999). Released fraction and total size of a pool of immediately available transmitter quanta at a calyx synapse. Neuron *23*, 399–409.

Shepherd, J.D., Rumbaugh, G., Wu, J., Chowdhury, S., Plath, N., Kuhl, D., Huganir, R.L., and Worley, P.F. (2006). Arc/Arg3.1 mediates homeostatic synaptic scaling of AMPA receptors. Neuron *52*, 475–484.

Shim, J.-H., Xiao, C., Paschal, A.E., Bailey, S.T., Rao, P., Hayden, M.S., Lee, K.-Y., Bussey, C., Steckel, M., Tanaka, N., et al. (2005). TAK1, but not TAB1 or TAB2, plays an essential role in multiple signaling pathways in vivo. Genes Dev. *19*, 2668–2681.

Silverman, N., Zhou, R., Stöven, S., Pandey, N., Hultmark, D., and Maniatis, T. (2000). A Drosophila IkappaB kinase complex required for Relish cleavage and antibacterial immunity. Genes Dev. *14*, 2461–2471.

Steiner, H. (2004). Peptidoglycan recognition proteins: on and off switches for innate immunity. Immunol. Rev. *198*, 83–96.

Steinmetz, C.C., and Turrigiano, G.G. (2010). Tumor necrosis factor-α signaling maintains the ability of cortical synapses to express synaptic scaling. J. Neurosci. *30*, 14685–14690.

Stellwagen, D., and Malenka, R.C. (2006). Synaptic scaling mediated by glial TNF-alpha. Nature *440*, 1054–1059.

Stevens, B., Allen, N.J., Vazquez, L.E., Howell, G.R., Christopherson, K.S., Nouri, N., Micheva, K.D., Mehalow, A.K., Huberman, A.D., Stafford, B., et al. (2007). The classical complement cascade mediates CNS synapse elimination. Cell *131*, 1164–1178.

Stöven, S., Ando, I., Kadalayil, L., Engström, Y., and Hultmark, D. (2000). Activation of the Drosophila NF-kappaB factor Relish by rapid endoproteolytic cleavage. EMBO Rep. *1*, 347–352.

Takatsu, Y., Nakamura, M., Stapleton, M., Danos, M.C., Matsumoto, K., O'Connor, M.B., Shibuya, H., and Ueno, N. (2000). TAK1 participates in c-Jun N-terminal kinase signaling during Drosophila development. Mol. Cell. Biol. *20*, 3015–3026.

Takehana, A., Yano, T., Mita, S., Kotani, A., Oshima, Y., and Kurata, S. (2004). Peptidoglycan recognition protein (PGRP)-LE and PGRP-LC act synergistically in Drosophila immunity. EMBO J. *23*, 4690–4700.

Tang, A.-H., Chen, H., Li, T.P., Metzbower, S.R., MacGillavry, H.D., and Blanpied, T.A. (2016). A trans-synaptic nanocolumn aligns neurotransmitter release to receptors. Nature *536*, 210–214.

Terman, J.R., and Kashina, A. (2013). Post-translational Modification and Regulation of Actin. Curr Opin Cell Biol *25*, 30–38.

Thanawala, M.S., and Regehr, W.G. (2013). Presynaptic calcium influx controls neurotransmitter release in part by regulating the effective size of the readily releasable pool. J. Neurosci. *33*, 4625–4633.

Thiagarajan, T.C., Lindskog, M., and Tsien, R.W. (2005). Adaptation to synaptic inactivity in hippocampal neurons. Neuron *47*, 725–737.

Turrigiano, G.G., Leslie, K.R., Desai, N.S., Rutherford, L.C., and Nelson, S.B. (1998). Activity-dependent scaling of quantal amplitude in neocortical neurons. Nature *391*, 892–896.

Turrigiano, G.G. (2008). The self-tuning neuron: synaptic scaling of excitatory synapses. Cell *135*, 422–435.

Valanne, S., Wang, J.-H., and Rämet, M. (2011). The Drosophila Toll signaling pathway. J. Immunol. *186*, 649–656.

Verhage, M., Maia, A.S., Plomp, J.J., Brussaard, A.B., Heeroma, J.H., Vermeer, H., Toonen, R.F., Hammer, R.E., Den, T.K. van, Berg, et al. (2000). Synaptic Assembly of the Brain in the Absence of Neurotransmitter Secretion. Science *287*, 864–869.

Vezzani, A., and Granata, T. (2005). Brain Inflammation in Epilepsy: Experimental and Clinical Evidence. Epilepsia *46*, 1724–1743.

Vidal, S., Khush, R.S., Leulier, F., Tzou, P., Nakamura, M., and Lemaitre, B. (2001). Mutations in the Drosophila dTAK1 gene reveal a conserved function for MAPKKKs in the control of rel/NF-kappaB-dependent innate immune responses. Genes Dev. *15*, 1900–1912.

Voineagu, I., Wang, X., Johnston, P., Lowe, J.K., Tian, Y., Horvath, S., Mill, J., Cantor, R.M., Blencowe, B.J., and Geschwind, D.H. (2011). Transcriptomic analysis of autistic brain reveals convergent molecular pathology. Nature *474*, 380–384.

Wang, T., Hauswirth, A.G., Tong, A., Dickman, D.K., and Davis, G.W. (2014). Endostatin is a trans-synaptic signal for homeostatic synaptic plasticity. Neuron *83*, 616–629.

Wang, T., Jones, R.T., Whippen, J.M., and Davis, G.W. (2016). α2δ-3 Is Required for Rapid Transsynaptic Homeostatic Signaling. Cell Rep *16*, 2875–2888.

Wang, Y., Okamoto, M., Schmitz, F., Hofmann, K., and Südhof, T.C. (1997). Rim is a putative Rab3 effector in regulating synaptic-vesicle fusion. Nature *388*, 593–598.

Weimer, R.M., Richmond, J.E., Davis, W.S., Hadwiger, G., Nonet, M.L., and Jorgensen, E.M. (2003). Defects in synaptic vesicle docking in unc-18 mutants. Nat. Neurosci. *6*, 1023–1030.

Wellmann, H., Kaltschmidt, B., and Kaltschmidt, C. (2001). Retrograde transport of transcription factor NF-kappa B in living neurons. J. Biol. Chem. *276*, 11821–11829.

Wolfram, V., Southall, T.D., Brand, A.H., and Baines, R.A. (2012). The LIM-homeodomain protein islet dictates motor neuron electrical properties by regulating K(+) channel expression. Neuron *75*, 663–674.

Wu, L.-G., Westenbroek, R.E., Borst, J.G.G., Catterall, W.A., and Sakmann, B. (1999). Calcium Channel Types with Distinct Presynaptic Localization Couple Differentially to Transmitter Release in Single Calyx-Type Synapses. J. Neurosci. *19*, 726–736.

Wu, M.N., Fergestad, T., Lloyd, T.E., He, Y., Broadie, K., and Bellen, H.J. (1999). Syntaxin 1A interacts with multiple exocytic proteins to regulate neurotransmitter release in vivo. Neuron *23*, 593–605.

Wu, Z.-H., Wong, E.T., Shi, Y., Niu, J., Chen, Z., Miyamoto, S., and Tergaonkar, V. (2010). ATM- and NEMO-dependent ELKS ubiquitination coordinates TAK1-mediated IKK activation in response to genotoxic stress. Mol. Cell *40*, 75–86.

Yeates, C.J., Zwiefelhofer, D.J., and Frank, C.A. (2017). The Maintenance of Synaptic Homeostasis at the Drosophila Neuromuscular Junction Is Reversible and Sensitive to High Temperature. ENeuro *4*.

Younger, M.A., Müller, M., Tong, A., Pym, E.C., and Davis, G.W. (2013). A presynaptic ENaC channel drives homeostatic plasticity. Neuron *79*, 1183–1196.

Publishing Agreement

It is the policy of the University to encourage the distribution of all theses, dissertations, and manuscripts. Copies of all UCSF theses, dissertations, and manuscripts will be routed to the library via the Graduate Division. The library will make all theses, dissertations, and manuscripts accessible to the public and will preserve these to the best of their abilities, in perpetuity.

I hereby grant permission to the Graduate Division of the University of California, San Francisco to release copies of my thesis, dissertation, or manuscript to the Campus Library to provide access and preservation, in whole or in part, in perpetuity.

Author Signature _____ Date 4/26/18